Nicolás Francisco Lori

From Deep Learning in Imaging Neuroscience to Nuclear Physics in Quantum Computing

University of Minho

University of Aveiro

U.PORTO

Fevereiro 2020

From Deep Learning in Imaging Neuroscience to Nuclear Physics in Quantum Computing

Nicolás F. Lori

UMinho2020

REPÚBLICA PORTUGUESA

POCH

UNIÃO EUROPEIA
Fundo Social Europeu

FCT Fundação para a Ciência e a Tecnologia

Universidade do Minho

Escola de Engenharia

Nicolás Francisco Lori

From Deep Learning in Imaging Neuroscience to Nuclear Physics in Quantum Computing

Programa de Doutoramento em Informática
das Universidades do Minho, de Aveiro e do Porto

Universidade do Minho

Universidade de Aveiro

U.PORTO

Trabalho realizado sob a orientação do

Professor Doutor Victor Manuel Rodrigues Alves

e do

Professor Doutor Nuno J. Carvalho de Sousa

Fevereiro 2020

Acknowledgments

Foremost, I would like to thank Eduarda Sousa for her support.

I am extremely indebted to my wife, Sandra Calado Lori, for her loving presence and help, and to all the help by the other family members and friends.

This thesis would have been impossible to finish without the untiring support of my two thesis advisors, Victor Alves and Nuno Sousa, thus my thankfulness to both is profound.

My colleagues have been extremely generous with their time, and thoroughly patient in tolerating my mistakes, impatience, and lack of temperance. For all that, I am extremely thankful.

Also, a very special word of appreciation for José Neves, which was among the first to see the value to Computer Science of my efforts in advanced mathematical Physics.

The publications associated to this Thesis were supported by ERASMUS scholarship, QREN, FEDER, COMPETE: POCI-01-0145-FEDER-007043, and by FCT (Fundação para a Ciência e a Tecnologia): UID/CEC/00319/2013, Investigador FCT, Ciencia 2007, PTDC/SAU-BEB/100147/2008, MEDPERSYST - POCI-01-0145-FEDER-016428, REP - PTDC/SOC-SOC/29207/2017, INESC-ID multi-annual funding from the PIDDAC program (UID/CEC/50021/2019).

Data collection for this work was in part from ”Human Connectome Project” (HCP; Principal Investigators: Bruce Rosen, M.D., Ph.D., Arthur W. Toga, Ph.D., Van J. Weeden, MD). HCP funding was provided by the National Institute of Dental and Craniofacial Research (NIDCR), the National Institute of Mental Health (NIMH), and the National Institute of Neurological Disorders and Stroke (NINDS). HCP data are disseminated by the Laboratory of Neuro Imaging at the University of Southern California. This data is referred to as “HCP data”.

Data collection for this work was in part from SWITCHBOX Consortium project (http://www.switchbox-online.eu/) realized in the “Life and Health Sciences Research Institute” (ICVS) and acquired using a Siemens Magnetom Avanto 1.5 T MRI scanner. This data is referred to as “In-House data”.

No non-human animal data was obtained or used for this thesis.

The human Magnetic Resonance Imaging (MRI) used in this thesis was obtained from publicly available published data, with the published data stating that the data had been approved by the corresponding ethical committees.

Statement of Integrity

I hereby declare having conducted this academic work with integrity. I confirm that I have not used plagiarism or any form of undue use of information or falsification of results along the process leading to its elaboration.

I further declare that I have fully acknowledged the Code of Ethical Conduct of the University of Minho.

Resumo

Do Deep Learning em Neurociência de Imagem à Física Nuclear em Computação Quântica

Esta tese mostra como as descobertas da Ciência da Computação e da Computação Quântica, que se desenvolveram em alguns aspectos do Deep Learning em Neurociência de Imagem à Física Nuclear em Computação Quântica, podem levar a uma drástica e inovadora fundação no campo da Ciência da Computação. De facto, abrem-se oportunidades para melhorar temas aplicados e teóricos nessas disciplinas. Em particular, descobrimos que os avanços na Tecnologia da Informação dependem mais do "Deep Learning em Neurociência de Imagem" do que da "Física Nuclear em Computação Quântica". A razão para isso é que o foco é mais nos paralelos à computação da informação em sistemas biológicos do que na miniaturização, o que se concentraria nos paralelos à Física Nuclear. Inegavelmente, uma consequência importante desta tese é que a Ciência da Computação representa uma disciplina que pode ser interpretada como base para as outras tecnologias de inferência causal, ou seja, a Ciência da Computação denota não apenas uma coleção de ferramentas para Matemática, Física, Neurociências e Economia, mas também pode ser entendida como um valor agregado de tais disciplinas à ComputaçãoQuântica.

Palavras-Chave: Computação Quântica, Deep Learning, Filosofia da Informação, Neurociência de Imagem.

Abstract

From Deep Learning in Imaging Neuroscience to Nuclear Physics in Quantum Computing

This thesis shows how findings from Computer Science (CS) and Quantum Computing, which developed in some aspects from Deep Learning in Imaging Neuroscience to Nuclear Physics in Quantum Computing, can lead to severe and groundbreaking foundation in the field of CS. Indeed, opportunities open up to improve both applied and theoretical topics in these disciplines. In particular, we found that advances in Information Technology depends more on "Deep Learning in Imaging Neuroscience" than on "Nuclear Physics in Quantum Computing". The reason for this is that the focus is more on the parallels to information computation in biological systems than on miniaturization, which would focus on the parallels to Nuclear Physics. Undeniably, an important consequence of this thesis is that CS stands for a discipline that can be interpreted as the basis for the other causal inference technologies, i.e., CS denotes not just a collection of tools for Mathematics, Physics, Neurosciences and Economics, but can also be understood as an added value from such disciplines to Quantum Computing.

Keywords: Deep Learning, Imaging Neuroscience, Philosophy of Information, Quantum Computing.

Contents

List of Figures ix

List of Tables xi

Acronyms xiii

1. Introduction 1

1.1 Computer Science´s Present and Future 3

1.2 Relating the publications with Computer Science 5

2. Computer Science’s Present 10

2.1 Distributed Computing “Wormholes” approach 10

2.1.1. Wormhole approach to distributed systems 11

2.1.2. Quantum Darwinism approach to Quantum Mechanics 14

2.1.3. Relation of Wormhole approach to Computer Science’s future 20

2.2 Monte-Carlo simulations improve Diffusion MRI data-processing 23

2.2.1. White Matter tractography using Imaging Neuroscience data 25

2.2.2. Monte-Carlo approach to Imaging Neuroscience data 30

2.3 Deep Learning pipeline improves functional MRI data processing 35

2.3.1. Building a Functional Connectivity Table 37

2.3.2. Deep Learning in Functional Connectivity Table 41

2.4 Application of partial Information approaches to Management 51

3. Computer Science’s Future 59

3.1. Axiomatic formalization of human mental health 59

3.1.1. Mental state objectivity using an axiomatic system 61

3.1.2. Mental state free-will using an axiomatic system 69

3.1.3. Integrating objectivity and free-will using 3-axes approach 75

3.1.4. Experimental evidences for 3-axes approach 82

3.2. Quantum computing at sub-atomic scales and Moore’s law future 90

3.2.1. Quantum fields and the future Computing Power 92

3.2.2. From miniaturization to lateralization 97

4. Conclusion and Discussion 104

4.1. Conclusion of Thesis 104

4.2. Discussion of Work In-Progress 108

5. References 117

List of Figures

1.1.1 Contemporary Computer Science within human knowledge: **a)** Relation between CS and the other sciences with their corresponding scales from ref. (Wikipedia, 2019); **b)** Interaction between CS and the more closely related fields from ref. (UALT, 2019). 3

1.1.2 CS's future roles: **a)** Development of societal improvement from ref. (Adpakkala, 2017); **b)** Branch of physical sciences from ref. (Eigenfactor.org, 2004). 3

1.2.1 Contemporary CS perspectives: Theoretical and Applied Computation from ref. (Connectedreams.com, 2016). 5

1.2.2 Contemporary and future CS covered in Thesis: Theoretical and Applied Computation types are from ref. (Connectedreams.com, 2016). 9

2.1.1 The Wormhole model, with Wormholes in green and payloads in yellow: **a)** Local Wormholes; **b)** Distributed Wormholes (from (Verissimo, 2006)). (Lori, 2017) 12

2.1.2 **a)** When the probability of a favorable swap is the same before and after the swap, then the states are equivalent (≈). **b)** In classical Physics, because of its objective perspective, the states before and after swap are equivalent (≈) but not equal (≠). **c)** In QD, the swapping of ♠ and ♥ in the system *S* is possible to compensate by the swapping of ♦ and ♣ in the environment *E*, thus obtaining a state that is equal (=) to the original state. (from (Zurek, 2005) [©2005 The American Physical Society]) 16

2.2.1 Examples of human brain dMRI data processing, shown are Sagittal slices of tractography final images. **a)** DTI-based spaghetti of lines, **b)** DTI-based connection probabilities with seed region in corpus callosum. (Lori, 2016) 25

2.2.2 Example of DSI connections from one seed with colors depend on orientation. The lines are 1-axis connections ($k=1$), planes are 2-axis connections ($k=2$), and crossing planes are 3-axis connections ($k=3$). (Lori, 2016) 26

2.2.3 Experimental (blue line) and theoretical signals (green line) along the corresponding q-vector number. The example voxel is on the position pointed by the green arrow near the ventricles (black triangular shapes) in the brain image overlaid by the isotropic fractions (yellow-red scale). (Lori, 2016) 28

2.2.4 Example of results using HCP DSI human data overlaid on HCP anatomical MRI. (Lori, 2016) 31

2.2.5 Comparison of Ξ_{iso} calculated with all the voxels (straight line ± 1 SEM) versus Ξ_{iso} calculated with a Monte Carlo fraction of the voxels (y-axis) as a function of the fraction of the Monte Carlo-selected voxels (x-axis): **a)** *k=1* , **b)** *k=2* , **c)** *k=3*. (Lori, 2016) 32

2.2.6 Calculation using Monte Carlo method of the fraction of voxels with Ξ_{iso} within ±1 SEM of the Ξ_{iso} calculated with all the voxels (y-axis) as a function of the fraction of the Monte Carlo-selected voxels (x-axis): **a)** *k=1* , **b)** *k=2* , **c)** *k=3*. (Lori, 2016) 32

2.3.1 A correlation matrix for 50 nodes parcellation (and using 93 brain regions) with the values of the static FC of the label 1. (Lori, 2018) 41

2.3.2 Schema of the materials and methods used. (Lori, 2018) 43

2.3.3 Development environment schema with the support technology used in the development of the different methods, the method itself and their respective Python files created. (Lori, 2018) 44

2.3.4 The best result of one of 3 tests for Leaky Relu with alpha equal to 0.8. (Lori, 2018) 47

2.4.1 An assessment of the attained energy with respect to a single worker answer to *CSEQ-6*. (Neves, 2019) 55

3.1.1 Relation between the axiomatic system from Alphabet to Output, and the extra structure of the connection relating the information-based axiomatic system to the Consciousness Types 0-1-2 described in refs. (Shea, 2016)(Kahneman, 2011) and Consciousness Type 3 proposed in ref. (Lori, 2019). 71

3.1.2 Relation between axiomatic system (from Alphabet to Output), and the structure of the connection relating Information-based axiomatic system to Consciousness Type. (Lori, 2019) 75

3.1.3 Simplified relation between brain 3-axes approach and brain function. On the left is a view from above (® Sandra Lori), and on the right a view from the left side (® Sandra Lori). 77

3.1.4 Cortical Word Map obtained by fMRI correlations. (Huth, 2016) 86

List of Tables

2.2.1 The parameters used in our search (Lori, 2016). 28

2.2.2 Experimental (blue line) and theoretical signals (green line) along the corresponding q-vector number. The example voxel is on the position pointed by the green arrow near the ventricles (black triangular shapes) in the brain image overlaid by the isotropic fractions (yellow-red scale). (Lori, 2016) 32

2.3.1 Table of atlases with number of total nodes in descending order. 39

2.3.2 Features of the correlation matrices by each brain parcellation. 40

2.3.3 Resume of the values obtained by the approach from ref. (Finn, 2015) using the In-House dataset for "Predict session 1" and "Predict session 2", for the different brain parcellations. (Lori, 2018) 45

2.3.4 Mean, Standard Deviation, Max and Min of the correlation values in the correct and incorrect classifications, and respective difference for the In-House data. (Lori, 2018) 45

2.3.5 Average validation accuracy and cost values of 3 tests for different alpha rates in the Leaky Relu activation function for 50 nodes parcellation. (Lori, 2018) 47

2.4.1 *CSEQ – 6* single worker answer. (Neves, 2019) 54

2.4.2 Best Case vs. Worst Case scenario calculations. (Neves, 2019) 55

3.1.1 Structure of information-based axiomatic system, and its relation to Psychology. (Lori, 2019) 65

3.1.2 Comparison of the axiomatic axes system with other axes systems. (Lori, 2019) 79

3.1.3 Relationship between the Eating-Choosing-Hunting axes, and feelings. (Lori, 2019) 82

3.1.4 Relation between Shakespeare, Freud, and Damasio Consciousness levels. (Lori, 2019) 85

3.1.5 Relation between axiomatic systems in Mathematics and CS, narrative structure in Psychology, and the characteristics occurring in schizophrenia (from normal to pathological levels). 88

4.1.1 Relation between works and causal inferences: The types of causal inference existing in contemporary technology can be divided into three types; viz.; Deterministic, 106

Statistical, Quantum. In contemporary CS these three types of inferences are implemented, whereas future CS will develop novel approaches to causal inference.

4.2.1 Description of how CS relates value with Beauty. 112

Acronyms

A

AI – Artificial Intelligence

AD - Alzheimer's Disease

ANN - Artificial Neural Networks

B

BOLD - Blood Oxygenation Level-Dependent

C

CA - Connectomic Analysis

CC - Classical Computer

CS – Computer Science

CSE - Collective Self-Esteem

CSEQ - Collective Self-Esteem Questionnaire

CSF - Cerebrospinal-Fluid

CUDA - Compute Unified Device Architecture

CMIPR - Contemporary Maximum Information Processing Rate

CMPs - Continuous Markov processes

CNS - Central Nervous System

CPA – Complete Physics-cells Approach

CPU - Central Processing Unit

D

DAS - Darwinian Axiomatic System

DICOM - Digital Imaging and Communications in Medicine

DL - Deep Learning

dMRI – Diffusion Magnetic Resonance Imaging

DNN - Deep Neuronal Networks

DOF - Degrees of Freedom

DSI- Diffusion Spectrum Imaging

DTI - Diffusion Tensor Imaging

E

EPI - Echo-Planar Imaging

ECS - Emotional-Competent-Stimulus

EPR - Einstein-Podolsky-Rosen

EU – European Union

F

FAS - Formal Axiomatic Systems

FC - Functional Connectivity

FDs - Failure detectors

fMRI – Functional Magnetic Resonance Imaging

FMRIB - fMRI of the Brain

FSL - FMRIB Software Library

FWP - Free-Will Perception

G

GM - Gray Matter

GPUs - Graphical Processing Units

GR - General Relativity

GRA – Gratitude

GUT - Grand Unified Theory

H

HARDI - High Angular Resolution Diffusion Imaging

HCP - Human Connectome Project

HCT - Hammersley-Clifford Theorem

I

ICA - Independent Component Analysis

IDE - Integrated Development Environment

i.i.d. - Independent Identically Distributed

IPython - Interactive Console of Python

ITER - International Thermonuclear Experimental Reactor

K

KEMs - Key-Encapsulation Mechanisms

KRR - Knowledge Representation and Reasoning

M

MIPR - Maximum Information Processing Rate

ML - Machine Learning

MRI – Magnetic Resonance Imaging

N

NAS - Newtonian Axiomatic Systems

O

ODF - Orientation Distribution Function

OE - Organizational Efficiency

P

PA - Physics-cells Approach

PC - Principal Components

PCA - Principal Component Analysis

PC-MIPR - Physics-cell Maximum Information Processing Rate

PDF - Probability Distribution Function

PKC - Public-Key Cryptography

PQ - Prosocialness Questionnaire

PQC - Post-Quantum Cryptography

PRO - Prosocialness

PSTHs - Postsynaptic Time Histograms

Q

QC - Quantum Computer

QCD - Quantum Chromodynamics

QD - Quantum Darwinism

QE - Quantum Existentialism

QM - Quantum Mechanics

QF - Quantum Field

R

R-LWE - Ring Learning with Errors

ROIs - Regions of Interest

rs-fMRI - Resting-State functional Magnetic Resonance Imaging

RSNs - Resting State Networks

S

SBA - Seed-Based Analysis

SD - Spherical Decomposition

SEM - Standard Error of the Mean

SMP - Standard Model of Physics

SU(n) - Special Unitary n-dimensional

W

WG - Wormhole Gateways

WM - White Matter

Chapter 1

Introduction

1.1. Computer Science's Present and Future

Key points:

- Explains that the focus of the Thesis is what the future of Computer Science (CS) is likely to be given what is known in the present about the usage of CS.
- The major comparison being between "Deep Learning in Imaging Neuroscience" and "Nuclear Physics in Quantum Computing".

The term Computer Science (CS) was first defined in the 1950's and it has always been applied and interdisciplinary in nature, but despite its name, a lot of CS does not involve the study of computers themselves, but rather its focus is mostly about software, specifically about the theory, design, development, and application of software. The CS departments can be divided in two major types, the Mathematics-based and the Engineering-based types; with the first being focused in "theory and design", whereas the second focuses in "development and application". Usually, each CS scientist focuses in one of these two types, but this CS Ph.D. Thesis will consider both types. The Chapter 2 is mostly about "development and application" within CS's present, whereas Chapter 3 is also about the appropriate "theory and design" for CS's future.

The most common description of contemporary CS in comparison with other sciences is to describe it as a branch of Mathematics (Fig. 1.1.1), whereas we propose that the future CS will be itself the source of the models generating the causality approaches that are the basis of the approaches used in different Technologies (e.g. Physics, Biology, Economics) (Fig. 1.1.2), moreover CS has been affirming itself as a form of theoretical Computer Engineering and as a branch of applied statistics (e.g. Fig. 1.2.1).

The four published works that serve as basis for the four sections of Chapter 2 are respectively in Theoretical CS, Applied Statistics, Applied CS, and in a CS application to Economics/Management:

2.1. Distributed Computing "Wormholes" approach [PUBLISHED]

Lori, N. F., Alves, V. (2017). Wormhole approach to control in distributed computing has direct relation to physics. CONTROLO 2016. Proceedings of the 12th Portuguese Conference on Automatic Control. Lecture Notes in Electrical Engineering (LNEE), volume 402. Springer-Verlag. pp. 105-117.

2.2. Monte-Carlo simulations improve Diffusion MRI data-processing [PUBLISHED]

Lori, N. F., Ibañez, A., Lavrador, R.; Fonseca, L., Santos, C; Travasso, R., Pereira, A., Rossetti, R., Sousa, N., Alves, V. (2016). Processing Time Reduction: an application in living human high-resolution diffusion magnetic resonance imaging data. Journal of Medical Systems. 40(11), 243.

2.3. Deep Learning pipeline improves functional MRI data processing [PUBLISHED]

Lori, N. F., Ramalhosa, I., Marques, P., Alves, V. (2018). Deep Learning Based Pipeline for Fingerprinting Using Brain Functional MRI Connectivity Data. Procedia CS. Volume 141, pp. 539-544.

2.4. Application of partial information approaches to Management [PUBLISHED]

Neves, J., Maia, N., Marreiros, G., Neves, M., Fernandes, A., Ribeiro, J., Araújo, I., Araújo, N., Ávidos, L., Ferraz, F., Capita, A., **Lori, N.**, Alves, V., Vicente, H. (2019). Entropy and Organizational Performance. In: Pérez García H., Sánchez González L., Castejón Limas M., Quintián Pardo H., Corchado Rodríguez E. (eds) Hybrid Artificial Intelligent Systems. HAIS 2019. Lecture Notes in CS, vol 11734. Springer, Cham.

a) b)

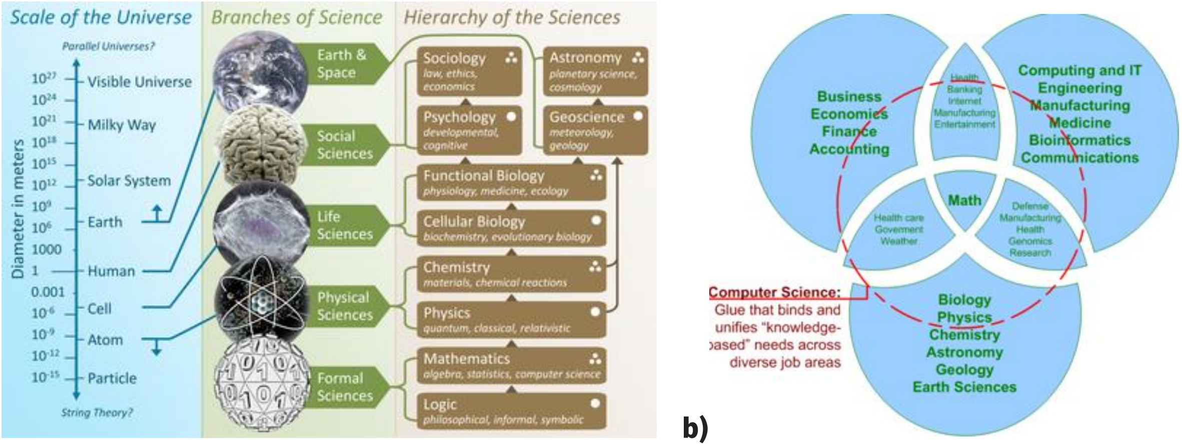

Figure 1.1.1. Contemporary Computer Science within human knowledge: **a)** Relation between CS and the other sciences with their corresponding scales from ref. (Wikipedia, 2019); **b)** Interaction between CS and the more closely related fields from ref. (UALT, 2019).

The trend in Future CS described in Chapter 3 implies that CS is becoming the source of the causal inference model, rather than simply being a vehicle for causal inferences assumed by science.

a) b)

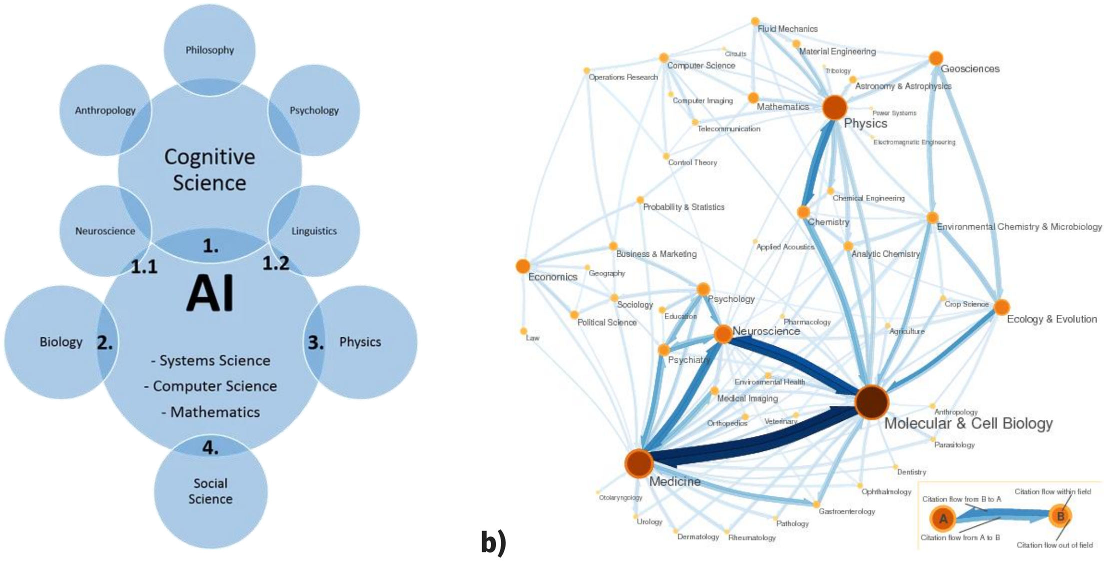

Figure 1.1.2. CS's future roles: **a)** Development of societal improvement from ref. (Adpakkala, 2017); **b)** Branch of physical sciences from ref. (Eigenfactor.org, 2004).

The two published works that serve as basis for the two Sections of Chapter 3 are respectively in Neuroscience where it was proposed an axiomatic formalism-based description of the causal inferences associated to human mental health (Fig. 1.1.2a), and in how the different role causal inference has in quantum computers (QCs) will not be able to overcome the incapacity of classical computers (CCs) in continuing to uphold Moore's law (Fig. 1.1.2b):

3.1. Axiomatic Formalization of Human Mental Health [PUBLISHED]

Lori NF, Samit E, Picciochi G, Jesus P. (2019). Free-will Perception in Human Mental Health: an Axiomatic Formalization. IN: Automata's inner movie: Science and Philosophy of Mind. Vernon Press.

3.2. Quantum computing at sub-atomic scales and Moore's law future [PUBLISHED]

Lori NF, Neves J, Alves, V. (2020). Some considerations on quantum computing at sub-atomic scales and its impact in the future of Moore's law. Quantum Information & Computation. Vol. 20, No. 1&2. pp. 1-13.

Plus, there were three published works in "Imaging Neuroscience" associated to this Thesis:

1. Ibañez, A., Zimerman, M., Sedeño, L, **Lori, N.**, Rapacioli, M., Cardona, J., Suarez, D., Herrera, E., García, A., Manes, F. (2018). Early bilateral and massive compromise of the frontal lobes. NeuroImage: Clinical. Volume 18, pp. 543-552.

2. Sedeño, L., Piguet, O., Abrevaya, S. G., Garcia-Cordero, I., Baez, S., de la Fuente, L. A., Reyes, P., Tu, S., Mogilner, S., **Lori, N.**, Landin-Romero, R., Matallana, D., Slachevsky, A., Torralva, T., Chialvo, D., Kumfor, F., Garcia, A. M,. Manes, F., Hodges, J., Ibañez, A. (2017). Tackling variability: A multicenter study to provide a gold-standard network approach for frontotemporal dementia. Human Brain Mapping. 38(8), Aug, pp. 3804-3822.

3. Yoris, A., Abrevaya, S., Esteves, S., Salamone, P., **Lori, N.**, Martorell, M., Legaz, A., Alifano, F., Petroni, A., Sánchez, R., Sedeño, L., García, A. M., Ibáñez, A. (2017). Multilevel convergence of interoceptive impairments in hypertension: New evidence of disrupted body-brain interactions. Human Brain Mapping, 39(4), Apr; pp. 1563-1581.

1.2. Relating the publications with Computer Science

Key points:

- Both Chapter 2 and Chapter 3 are based in published studies, hence the content of this Thesis is fully based in publications.
- Both the relation of the publications with CS, and the relation between publications are described here.

The relation of CS with the works of the four Sections of Chapter 2 and the two Sections of Chapter 3 are described in Fig. 1.2.1, where it is made clear which work was done in "Applied CS" or "Theoretical CS".

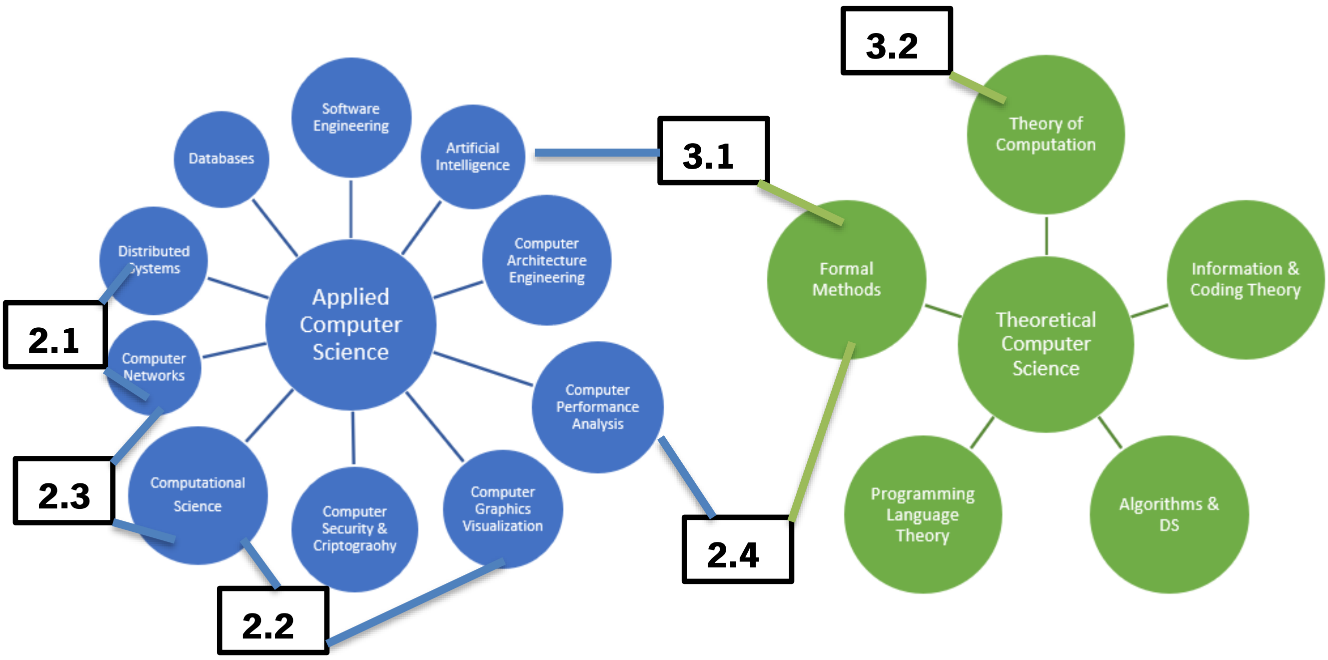

Figure 1.2.1. Contemporary CS perspectives: Theoretical and Applied Computation from ref. (Connectedreams.com, 2016).

To analyze contemporary CS, we focused in two aspects of science where Applied and Theoretical CS have been used, "Imaging Neuroscience" and "Quantum Computing". The goal of this Thesis is to assess whether the future of CS will be more based in the "Deep Learning in Imaging Neuroscience" or in the "Nuclear Physics in Quantum Computing", hence we started by analyzing distributed computing using Nuclear Physics concepts (see Section 2.1) and by analyzing how Monte-Carlo processing helped reduce the processing time of "Imaging Neuroscience" data (see Section 2.2.).

In Section 2.1, the topic of Wormholes in distributed computing is described as creating two different realms with different characteristics, the synchronous Wormholes and the asynchronous payload with the goal of using the Wormholes to control the synchronism of the payload processes. We describe the characteristics of Wormholes in distributed computing, and relate them to issues in Physics, specifically, Wormholes in general relativity (GR) and entanglement in quantum mechanics (QM). The entanglement in QM is about the existence of fixed relations between different physical systems as if they were still the same system. The entanglement is made evident by the occurrence of decoherence, which transform the multiple outcome possibilities of quantum systems into a single outcome "classical Physics"-like objective reality. It is here presented the similarity between the decoherence process in quantum Physics and the consensus problem in distributed computing. The approach to QM used is quantum Darwinism (QD), a Darwinian approach to decoherence where the environment controls the outcome of a measurement. It is here proposed that wormhole systems can be used to implement environment-based control of distributed computing systems.

In Section 2.2., we analyze High Angular Resolution Diffusion Imaging (HARDI) which is a type of diffusion Magnetic Resonance Imaging (dMRI) "Imaging Neuroscience" data that requires a very large amount of data, and if many subjects are considered then it amounts to a big data framework, for example, the human connectome project (HCP) has 20 Terabytes bytes of data. HARDI is also becoming increasingly relevant for clinical settings, for example, in the early detection of cerebral ischemic changes in acute stroke and in pre-clinical assessments of white matter (WM) anatomy using tractography. Thus, use of very large amounts of data are becoming a routine occurrence in clinical settings. In such settings, the computation time is critical, and hence finding forms of reducing the processing time in high computation processes such as Diffusion Spectrum Imaging (DSI) which is a form of HARDI data, it is thus very useful to find forms of increasing the data-processing speed. Here, we analyze a method for reducing the computation time of the dMRI-based axonal orientation distribution function h by using Monte Carlo sampling-based methods for voxel selection. Results evidenced a robust reduction in required data sampling of about 50% without losing signal's quality. Moreover, we show that the convergence to the correct value in this type of Monte Carlo HARDI/DSI data-processing has a linear improvement in data-processing speed of the Orientation Distribution

Function (ODF) determination. Although further improvements are needed, these results represent a promissory step for future processing time reduction in big data.

To further reach the goal of the thesis, we assess the CS application of "Deep Learning in Imaging Neuroscience" (see Section 2.3), and we assess the CS application of how the worker's behaviors and feelings affect a system's performance (see section 2.4). Both Section 2.3 and Section 2.4 are very important for the future of CS as is described in Section 3.1, and Section 3.1 helps strengthen the validity of Section 3.2.

The Section 2.3 aims at describing an appropriate pipeline for using Deep Learning (DL) as a form of improving the functional connectivity-based fingerprinting process which is based in functional Magnetic Resonance Imaging (fMRI) data. This approach is mostly intended for image-processing computer scientists, imaging neuroscientists, and biomedical engineers. This Section looks for an easy form of using fMRI-based DL in identifying people, for identifying drastic brain alterations in those same people, or for identifying pathologic consequences to people's brains. There were specific data-processing improvements made in using the here-proposed pipeline.

In Section 2.4, we analyze the impact of the workers' behavior in terms of their emotions and feelings in system`s performance, i.e., we look at issues concerned with Organizational Sustainability. Indeed, our aim in this section is to define a process that motivates and inspires managers and personnel to act upon the limit, i.e., to achieve the organizational goals through an effective and efficient implementation of operational and behavioral strategies. The focus being in the importance of specific psychosocial variables that may affect collective pro-organizational attitudes. The data obtained is increasing exponentially, and to prevent it from becoming out of control, we assessed how this information can be processed in a realistic situation.

An analysis of the future of CS is presented in Chapter 3. In Section 3.1, the focus is in "Imaging Neuroscience"; whereas in Section 3.2, the focus is in "Quantum Computing". In Section 3.1, we will analyze how using "Imaging Neuroscience" and other approaches it is possible to define objective human mental health by using mathematical representations of computational processes represented by use of axiomatic systems. Finally, we reach the Section 3.2 that is the convergence and resolution of the other Sections, in this section we obtain what is the result of the comparison between the "Deep Learning in Imaging Neuroscience" and the "Nuclear Physics in Quantum Computing".

In Section 3.1, we analyze the importance of free-will perception to objective human mental health. Hence, we first define how to represent mental states in an objective manner. Then, we describe how it is possible to represent free-will in the objective representation of mental states. Finally, we will explain how the convergence of the objective and free-will aspects of the mental states allows for an objective definition of human mental health. We will then present computational, literary, historical, religious, dMRI, and fMRI evidence for the approach proposed here. We thus obtain a CS-like interpretation of human mental health where a decrease in human mental health can be perceived as a reduction in computation efficiency. This perspective of the relation between computation efficiency and mental health is in very good agreement with the relation between computational efficiency and productivity described in Section 2.4.

In section 3.2, we describe how the contemporary development of QCs has opened new possibilities for computation improvements over CCs, whereas the limits of Moore's law validity are starting to show. We then analyze the possibility that miniaturization will continue to be the source of Moore's law validity in the near future, and our conclusion is that miniaturization is no longer a reliable answer for the future development of CS, but instead we suggest that lateralization is the correct approach. By lateralization, we mean the use of a Biology-based approach as the correct format for the implementation of ubiquitous computerized systems, a format that might in many circumstances eschew miniaturization as an overly expensive useless advantage, whereas in other cases miniaturization might play a key role.

The description of how the different sections cover different aspects of CS, and how some sections serve as the basis for latter sections is described in Fig. 1.2.2, where the key highlight is how much of CS has been covered when all the Sections are taken into account. Hence, this Thesis successfully analyzes several areas of contemporary CS, and describes future CS in keys areas, specifically "Deep Learning in Imaging Neuroscience" and "Nuclear Physics in Quantum Computing", using a format that is short enough to have the format of a Thesis, but with all aspects of the Thesis being strengthened by successfully being published in peer-review publications.

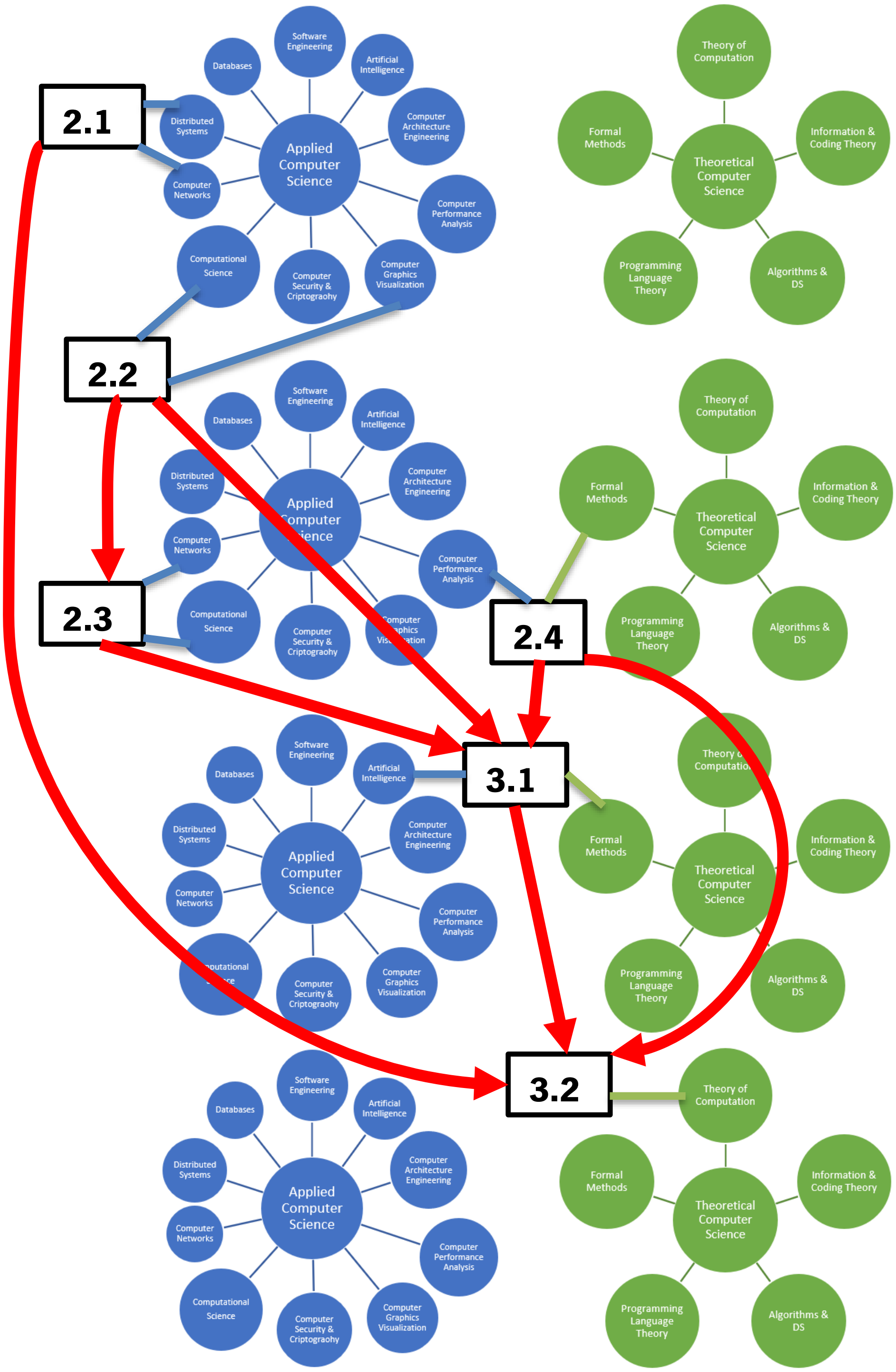

Figure 1.2.2. Contemporary and future CS covered in Thesis: Theoretical and Applied Computation types (blue and green circles) are those of Fig. 1.2.1 (Connectedreams.com, 2016).

Chapter 2

Computer Science's Present

2.1 Distributed Computing "Wormholes" approach

Key points:

- To reach the goal of analyzing the future of CS in using "Nuclear Physics in Quantum Computing" as described in Section 3.2, we start here by assessing the usefulness of using "Nuclear Physics" concepts in distributed computing.
- We obtained that it is useful, and some of the results obtained here are used in Section 3.1 and Section 3.2.

To assess the role of contemporary CS in establishing a comparison between the "Deep Learning in Imaging Neuroscience" and the "nuclear Physics in quantum Computing" we start by analyzing the relation between distributed computing, something neurons are considered to do in biological systems (Lori, 2019), and Information-processing in quantum Physics, something considered to be important for QCs (Arute, 2019)(Lori, 2019). The relation between Information-transport (in this Thesis, Information always means Shannon Information) and QM is known to exist for a long time (e.g. (Zurek, 2005)(Zurek, 2007)(Zurek, 2009)), but the challenge of reconciling uncertainty with predictability required by the simultaneous pressure of both the need to increase the applications' quality of service and the necessary degrading of the assurance given by the infrastructure, implies that also in distributed computing the Information-transport will play a key role (Verissimo, 2006). In the Wormhole paradigm of distributed computing (Verissimo, 2006), it is proposed the use of hybrid (vs. homogeneous) models as a key to overcoming some of the difficulties faced when asynchronous models (with associated uncertainty) occur simultaneously with timing specifications (which require predictability), whereas in ref. (Lori, 2017) it is obtained a relation between the QM perspective about system's entanglement (Sakurai, 1994), meaning the connection and/or interaction between systems, and the Wormholes approach to distributed computing.

The approach described here allows for a bridge between distributed computing and quantum Physics, and this bridge might open new perspectives about the internal structure of QCs. We first build the parallel between the Wormhole approach to distributed computing and fundamental Physics, and then at the end of this Section we describe a possible distributed computing effect at a fundamental Physics level that has been experimentally detected. (Lori, 2017)

2.1.1. Wormhole approach to distributed systems

There are two aspects to the difficulty of reconciling uncertainty with predictability in distributed computing: i. Time, the asynchronous computing model is not capable of making timed requirements, which is a major drawback as today there are very few useful applications where Time is absent from; ii. Security, the crash fault model is not a realist form of constructing systems that are secure enough for being successful in the Security world market. Finally, the arbitrary (a.k.a. Byzantine fault model) is an over-pessimistic abstraction for safety-critical applications subject to independent accidental faults, because both of its lack of independence and its stochastic search of malicious faults. The intention of the Wormhole approach is to partially solve both the Time and Security issues (Verissimo, 2006). (Lori, 2017)

The hybrid models in distributed computing have the positive relevant characteristics that they are expressive models with sound theoretical basis, and they are supported by hybrid architectures which allow for the development of new algorithms. They are expressive models because they mimic reasonably realistic systems when those systems are partially synchronous in the time dimension, and because they generally have components that have different degrees of synchronism which homogeneous models cannot take advantage from, since such homogeneous models are confined to using the worst-case values (which ultimately implies asynchrony). The hybrid models have sound theoretical basis, since by using a hybrid model the properties of the different loci of the system (the space dimension) are heterogeneous, and thus correctness assertions about each of the loci of the system can be made, which implies that it is possible to establish interfaces between loci without needing to make unrealistic homogeneous timing assumptions (Verissimo, 2006). (Lori, 2017)

In the Wormholes distributed systems model (see Fig. 2.1.1) (Verissimo, 2006)(Lori, 2017) there is a payload system S_p, and a S_w Wormhole sub-system. The payload system is where algorithms and applications are normally executed, and it is composed of N_p payload processes p_i that communicate by messages passing through payload channels. The payload system S_p follows a set of fault and synchrony assumptions H_p (which are normally weak such as asynchronous processing and communication, plus having the faulty behavior be Byzantine). The Wormhole subsystem is composed of N_w Wormhole processes w_i. The Wormhole processes may or not communicate amongst themselves, but if they communicate then they do so by having messages pass through Wormhole channels. The Wormhole subsystem S_w follows a set of fault and synchrony assumptions H_w which are normally stronger than the payload synchrony assumptions because, for example, in the Wormhole subsystem the processing and communication are synchronous and have faulty behavior crashes. The only way for payload processes to communicate with Wormhole processes is through Wormhole gateways (WG) with well-defined interfaces.

Nevertheless, there are several things that the Wormhole model does not specify: interface specificity; relative number of payload vs. Wormhole processes; and degree of knowledge the payload processes have about the Wormhole processes, and vice-versa. Thus, for payload processes the properties offered by any Wormhole are defined and expressed at a Wormhole gateway. In fact, maybe not all payload processes access Wormholes in certain algorithms, or maybe in other algorithms more than one payload process can access the same Wormhole.

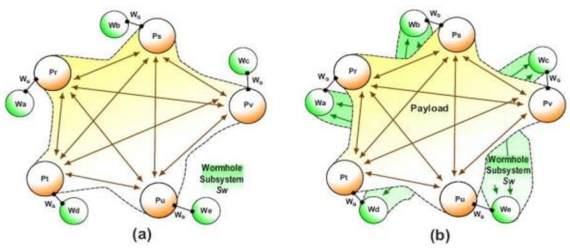

Figure 2.1.1. The Wormhole model, with Wormholes in green and payloads in yellow: **a)** Local Wormholes; **b)** Distributed Wormholes (from (Verissimo, 2006)). (Lori, 2017)

It is common in science-fiction the use of space-time Wormholes for faster than-light travel and/or the use of quantum tunneling for teleportation (e.g. Star Trek). Thus, it is fair to ask if the use of Wormholes in distributed computing accomplishes what it sets out to achieve in the real world, or if it is a sort of CS equivalent to science-fiction. This is especially relevant as QCs have recently become a reality (Arute, 2019), even though there are still some doubts about its actual impact (Lori, 2020) as we will describe in Section 3.2. Thus, this question about the Wormhole approach being practical, or just sci-fi phantasy, is a relevant question (Lori, 2017) that can be translated into two specific questions:

1. Is it feasible to construct Wormhole distributed systems?
2. Are distributed systems with Wormholes useful?

For the first question, in the Wormhole approach (Verissimo, 2006) the architectural hybridization was proposed as a new paradigm. This implies that systems may have zones (a.k.a. realms) with different nonfunctional properties, such as synchronism, faulty behavior, and quality-of-service. This implies that the properties of each zone/realm are obtained by construction of the subsystem(s) therein, and that these subsystems have well-defined encapsulation and interface approaches through which these former properties become manifested. The Timely Computing Base (TCB) allows for the obtaining of timely actions in systems that can be asynchronous; which means that the TCB distributed Wormhole gateway provides very helpful services such as: timely execution, duration measurement, and timing failure detection. Through the TCB, it is possible (Verissimo, 2006) to make an asynchronous system perform timely (synchronous) actions or detect the failure thereof. So, the answer to the first question is yes, it is feasible to construct Wormhole distributed systems. (Lori, 2017)

For the second question, it is relevant to consider that the most important implications of the use of hybrid distributed network models are: quantification of the assumptions' substance rather than just considering what the assumptions are, difference to partial synchrony models, a new approach to the FLP impossibility (Fischer, 1985) result; and the existence of failure detectors (FDs). The substance of these assumptions is important because it is the "assumption+coverage" pair that measures the weakness or strength of the distributed network model, and because the use of architectural hybridization can possibly improve the building of hybrid fault-tolerance approaches. The Wormhole approaches are different from the partial synchrony approaches in that the first are heterogeneous, whereas the second are homogeneous. Moreover, the Wormholes can circumvent the FLP impossibility result because a form of avoiding the FLP impossibility is by using synchronism (Chandra, 1996). (Lori, 2017)

The avoidance of the FLP impossibility in Wormholes approaches occurs using FDs. The FDs in asynchronous systems are difficult, but the consensus in the payload systems agrees with FDs in the Wormhole realm, which implies that functionality in a Wormhole is not confined to FDs, thus opening towards other, more generic, approaches. The Wormhole approach clarifies borderline situations where homogeneous asynchronous systems fail, and when asynchronous models must be complemented with timing assumptions to address timeliness specifications; thus, there is no alternative to Wormholes for correct specification of such settings (Verissimo, 2006). So, the answer to the second question is yes, it is useful to construct Wormhole distributed systems. (Lori, 2017)

The Wormholes approach allows extending partial synchrony to the space dimension, meaning that, regardless of the asynchronism of the whole system, some parts of the system exhibit a well-defined (perpetual if desired) time-domain behavior. The parallel to QM is, for example, that before a measurement in QM (Zurek, 2005)(Zurek, 2005)(Zurek, 2007) the quantum states behave as if they were the asynchronous components of the payload system, but as the quantum states interact (and thus become measured) they start behaving more as synchronous Wormholes. To better describe that parallel, we describe QM in the next section. (Lori, 2017)

2.1.2. Quantum Darwinism approach to Quantum Mechanics

Contemporary Physics is based on two approaches that have not yet been reconciled, quantum fields (QFs) (Sakurai, 1994) and GR (Wald, 1984). In stable conditions, meaning when the creation and destruction of fermions (e.g. electrons, protons, and neutrons) is small, the QFs can be represented by QM (Sakurai, 1994). While GR is deterministic (implying that there are no fundamental uncertainties associated with physical variables), QM has intrinsic fundamental uncertainty which is dissipated by the interaction with the environment. It can be said that the uncertainty in QM is kept alive at long distances through the occurrence of entanglement along quantum tunnels, and some recent work has indicated that the existence of quantum tunneling might be based on the occurrence of extremely tiny Wormholes (Sonner, 2013)(MIT, 2013), and following this possibility it becomes possible that although Physics' Wormholes (a.k.a. Einstein-Rosen bridges (Einstein, 1935)) are a solution to the GR equations, they can still have strong structural similarities to a QM process called entanglement, a process by which the uncertainty associated to pairs of quantum systems can remain connected even if the systems are very far apart. Whereby for the entangled pair of quantum systems, the resolving of the uncertainty about one of the quantum systems faster-than-light resolves the uncertainty on the other quantum system, no matter how far apart each pair element is from the other pair element. It is as if there was a Wormhole joining the pair of quantum systems. Thus, Wormholes in distributed computing can be associated to both the Physics of GR's Wormholes and/or the entanglement of QM. In both QM and GR, the physical representation of a state is always about two realms, specifically, the system and the environment (Lori, 2017). The system is what we aim to represent, and the environment is everything else that influences the system, which in extreme cases means the rest of the universe. (Lori, 2017)

There are different approaches to QM, we will follow the QD (Zurek, 2005)(Zurek, 2007)(Zurek, 2009) approach, which is an approach to QM that is strongly based in the Information-transport and thus is very relevant for the analysis of QCs (Arute, 2019)(Lori, 2020) as will be described in Section 3.2. Moreover, in Section 3.1 we assess the role of distributed networks in determining objective mental health (Lori, 2019), and so it it is useful to define the axioms of QD in a format that is more general, and so applies not only to QM but also to other situations of Information-transport (e.g. in distributed networks). Thus, we move away from the QM interpretation of these postulates, but stay with their mathematical structure, which is given in terms of vector spaces. For instance, where one reads quantum system in the QD formalism, we write system, with the understanding that the characteristic property of such a system is to be individually accessible to measurements; likewise, the quantum state is replaced by a vector in a multidimensional vector space; and so on. (Lori, 2017)

In Fig. 2.1.2 instead of the → used in the vector states of the rest of the article, the |> symbol will be used; and we use suits because that is a representation used in ref. (Zurek, 2005). In Fig. 2.1.2 is described how the principle of indifference, the basis of statistics, has a different meaning in quantum versus classical Physics. In Fig. 2.1.2a, the principle of indifference is described, and it states that a card player who knows one of the two cards is ♠ but does not see their faces, does not care—is indifferent—when cards get swapped. So, when the probability of a favorable swap is the same before and after the swap, then the states are equivalent (≈). In Fig. 2.1.2b it is described how in classical Physics, because of its objective perspective, the states before and after the swap are equivalent but not equal. In Fig. 2.1.2c it is described how in the QD perspective of QM if the system *S* and the environment *E* interact (a.k.a. entangle), then the definition of the system *S* only exists in relation to the environment *E*, and so does not exist by itself, meaning that the states before and after the swap are equal. This means that the swapping of ♠ and ♥ in the system *S* is possible to compensate by the swapping of ♦ and ♣ in the environment *E*. (Zurek, 2005). (Lori, 2017)

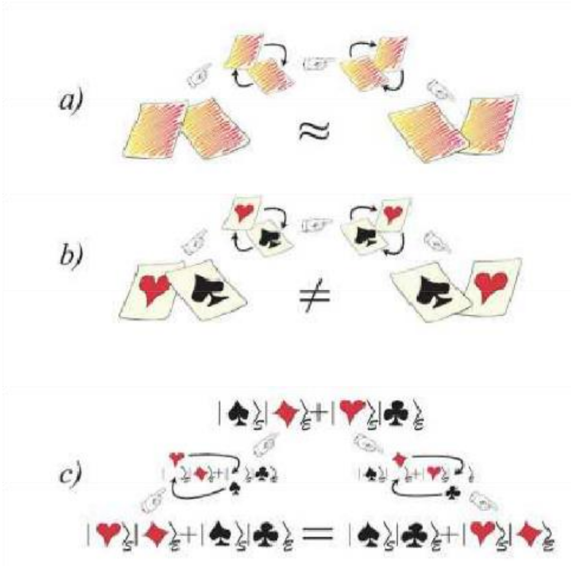

Figure 2.1.2. **a)** When the probability of a favorable swap is the same before and after the swap, then the states are equivalent (≈). **b)** In classical Physics, because of its objective perspective, the states before and after swap are equivalent (≈) but not equal (≠). **c)** In QD, the swapping of ♠ and ♥ in the system *S* is possible to compensate by the swapping of ♦ and ♣ in the environment *E*, thus obtaining a state that is equal (=) to the original state. (from (Zurek, 2005) [©2005 The American Physical Society])

The use of this new notation makes the QD axioms have the following aspect (Lori, 2017):

o. The universe consists of systems individually accessible to observations.

i. The state of a system is represented by a vector in a multidimensional vector space, and all converging series of vectors of the vector space converge to a vector of that same vector-space. To each vector is associated a dual vector. The inner product between a dual vector and a vector is a scalar.

ii. The time-evolution of a vector is such that the inner product of a vector is preserved.

iii. If the outside of a system (the environment) remains unchanged, then the observation of the system remains unchanged across time.

According to QD axiom iii, there must be a set of states of the system that remains unaltered by the interaction with the environment, call it vector state set S_k. So, there must be an alteration of the environment leading to the environment being now represented by the vector state set E_k. (Lori, 2017)

Let's consider that the possible states of the system S are $\spadesuit$ and $\heartsuit$, and that the possible states of the environment *E* are $\diamondsuit$ and $\clubsuit$. In that case, due to QD axioms *o* and *i*, the state of the system can be represented by (α and β are scalars) (Lori, 2017):

$$\vec{S} = \propto \overrightarrow{\heartsuit} + \beta \overrightarrow{\spadesuit} \qquad (2.1.1)$$

Consider that the environment *E* can make one-to-one measurements of *S*, such that before interacting with *S* the environment *E* is represented by the vector state (Lori, 2017):

$$\overrightarrow{E_0} = \propto \overrightarrow{\diamondsuit_0} + \beta \overrightarrow{\clubsuit_0} \qquad (2.1.2)$$

Consider that after *S* and *E* start interacting, the state vector of *E* is then (Lori, 2017):

$$\vec{E} = \propto \vec{\diamondsuit} + \beta \vec{\clubsuit} \tag{2.1.3}$$

Implying that before *S* and *E* start interacting, the state of "*S+E*" is (Lori, 2017):

$$\overrightarrow{SE} = \left(\propto \vec{\heartsuit} + \beta \vec{\spadesuit}\right) \otimes \left(\overrightarrow{\diamondsuit_0} + \overrightarrow{\clubsuit_0}\right) \tag{2.1.4}$$

After *S* and *E* start interacting, for postulate iii to be valid it is necessary that the state of "*S+E*" is (Lori, 2017):

$$\overrightarrow{SE} = \left(\propto \vec{\heartsuit} \otimes \vec{\diamondsuit} + \beta \vec{\spadesuit} \otimes \vec{\clubsuit}\right) \tag{2.1.5}$$

Due to QD axiom *ii*, the evolution of the "*S+E*" state must preserve the inner product, and thus also preserve the amplitude of the vector representing the state. Thus, the joining of QD axioms *o*, *i*, and *ii* implies that the evolution of the state of "*S+E*" during a measurement must be such that it is capable of going from a state of *S* and *E* being not-linked (Eq. 2.1.4), to a state of *S* and *E* being linked (Eq. 2.1.5), without altering the amplitude of the vector representing the state. If the square amplitude of the "*S+E*" vector is the same before (Eq. 2.1.4) and after *S* and *E* start interacting (Eq. 2.1.5), then (Lori, 2017):

$$\propto \beta \left(\vec{\heartsuit} \bullet \vec{\spadesuit}\right) \left(\left\| \overrightarrow{\diamondsuit_0} + \overrightarrow{\clubsuit_0} \right\|^2 - \vec{\diamondsuit} \bullet \vec{\clubsuit}\right) = 0 \tag{2.1.6}$$

Due to QD axiom *iii*, the above equation should continue being valid long after *S* and *E* start interacting. Since this result must be valid for any value of α and β, there are only two possibilities (Lori, 2017):

$$\begin{cases} \left\| \overrightarrow{\blacklozenge_0} + \overrightarrow{\clubsuit_0} \right\|^2 = \overrightarrow{\blacklozenge} \bullet \overrightarrow{\clubsuit} \\ \overrightarrow{\heartsuit} \bullet \overrightarrow{\spadesuit} = 0 \end{cases} \quad (2.1.7)$$

The upper line of the previous equation implies that the system has no influence in the environment, whereas the lower line implies that the system states are orthogonal. The joint consequence of both lines is that (Zurek, 2005)(Lori, 2010a)(Lori, 2017): "the vector states of the system capable of leaving a print in the environment, no matter how small the print, will necessarily be orthogonal vector states".

The Darwinian aspect of QD is that states of the system that fail to print themselves into the environment cease to exist (Zurek, 2005)(Zurek, 2007)(Zurek, 2009), meaning they become extinct. This aspect of QD is called Quantum Existentialism (QE) because the states only survive by their capacity for printing Information about themselves in the environment (Zurek, 2005)(Zurek, 2007)(Zurek, 2009). (Lori, 2017)

The preservation in the environment, after the measurement, of the Information about the measurement in large enough quantities on the environment so as to be read by multiple observers creates the illusion of the state's "objective reality". The "objective reality" of the vector states of the system is given by their capacity to transmit Information into the vector states of the environment. The successful transmission of Information is the printing of the Information about the system in the environment states, such that the environment states become themselves orthogonal. When that occurs, then the system and the environment become entangled. (Lori, 2017)

An entangled combination of system and environment can be described by a vector state where each component of the vector state is the product of a system output state S_k with its corresponding environment output state E_k. The coefficient associated to that product of states is called the Schmidt coefficient, which is a complex number of amplitude one (Ekert, 1995). This implies that for an entangled "system+environment" state an action on the system causes an angle shift on the Schmidt coefficient phase θ_k, and that angle shift can be compensated by an action on the environment. This implies that in the presence of entanglement it is possible to describe a type of invariance where the system is altered by an action on the system, but that alteration of the system can be totally compensated by an action on the environment without the occurrence of any further action on the system (see Fig. 2.1.2c). This type of invariance is called an environment-assisted invariance, which in short form is called *envariance* (Zurek, 2005). This analysis of the effect of Information-transport is the representation of a system is made in the Section based on ref. (Lori, 2017), in Section 3.1 based on (Lori, 2019), and in Section 3.2 based on ref. (Lori, 2020).

2.1.3. Relation of Wormhole approach to Computer Science's future

The Wormholes approach allows for different processes of the payload to communicate "immediately" through the synchronism of the Wormholes, the Wormholes thus play the same role as the entanglement in QD by assuring that there can be "immediate" connection between different components of the payload. This form of control of the payload by the Wormholes is especially useful in representing distributed quantum computing control as the Wormholes in the Wormhole model can accurately represent the role of the environment in quantum entanglement.

To represent QD using the Wormholes model it should be noted that because the Wormholes are becoming synchronous within themselves, they then could be used to eliminate the time-evolution of the payload processes that are not in agreement with the Wormhole synchronization, so forcing the payload processes to become synchronous with the Wormholes or stop. So, it is possible to consider QD as a Wormhole control system occurring in quantum reality.

The parallels between distributed computing, Wormholes and Physics (Lori, 2017) as described in this work might be useful a describer of QC performance within distributed quantum computing (e.g. ref. (Arute, 2019) and ref. (Lori, 2020), see Section 3.2), and for clarifying what are the computations associated to the occurrence of Consciousness in humans (Lori, 2019) which is very relevant for the issue of objective human mental health (Lori, 2019) as described in Section 3.1.

For correctly understanding the relation between the Wormhole approach and QM it is relevant to describe that in the Laboratory for Attosecond Physics it was possible to generate visible flashes of light in attosecond dimensions (Hassan, 2016). At that laboratory, they dispatched light-flashes to the electrons in krypton atoms, and they were thus able to obtain that the electrons, which are stimulated by the flashes, needed roughly 100 attoseconds to respond to the incident light. Until then it was assumed that particles respond to incident light without delay. These experimental results might be directly related to the Wormhole approach proposed here. The 100 attosecond of light traveling in vacuum corresponds to a travel distance of about 300 Angstroms, implying that this cannot be the size of the electron or any fundamental particle.

If it is considered that electrons have a finite computation capacity, as proposed in ref. (Lori, 2017); then electrons would need to take 100 attoseconds to process the corresponding Feynman diagrams, or the physical equivalent of the mathematical object that the Feynman diagrams are, before the electron could compute the outputted light. To check if this perspective makes mathematical sense, we can check if the "lifetime of the excited state" described in ref (Hassan, 2016) can be the computation time of the Planck volumes associated to the volume of the electron. If the lifetime is *T* and the particle is a sphere with volume *V*, then if each Planck cube (a cube with sides equal to Planck length) is a processor that takes a Planck time to process the input Information into output Information, and A is the Planck area (a square with sides equal to Planck length) and *c* is the speed of light in vacuum, then the radius *R* of the electron would relate to *T* by the relation (Lori, 2017):

$$R = \sqrt[3]{\frac{3}{4\pi} c\, A\, T} \tag{2.1.8}$$

The above equation implies that the electron has a radius of about $25*10^{-28}$ meters. It is usually assumed that "a search for a contact interaction at the LEP storage ring probes for electron structure at the 10 TeV energy scale in which case R < 2 x 10^{-20} m." (Bourilkov, 2001). Which is in total compatibility with the result obtained in Eq. 2.1.8. (Lori, 2017)

This Section aimed at the goals of establishing a bridge between Information-transport in distributed computing and the decoherence processes in QM, which is relevant for Section 3.2; plus a bridge between Information-transport in distributed networks of biological neurons and the axioms of QD, which is relevant for Section 3.1. Thus, both goals were achieved, but before going on to Section 3.1 and Section 3.2, several intermediary steps need to be achieved. Specifically, we need to: assess if the required Information-processing power necessary to high-density "Imaging Neuroscience" is too demanding for CCs, or if good-enough CS-based shortcuts can be used to achieve good-enough "Imaging Neuroscience" while still using CCs, and this is done in Section 2.2; assess if "Deep Learning in Imaging Neuroscience" can be achieved in a good enough form using contemporary CCs and this is done in Section 2.3; and assess if the qualification of the Information-transport is useful for describing human mental health by analyzing the productivity within a company, and this is done in Section 2.4.

2.2 Monte-Carlo simulations improve Diffusion MRI data-processing

Key points:

- To reach the goal of analyzing the future of CS in using "Deep Learning in Imaging Neuroscience" described in Section 3.1, we start here by assessing the usefulness of using CS concepts in "Imaging Neuroscience".
- We obtained that it is useful, and its increased usefulness in "Imaging Neuroscience" large datasets agrees well with the importance of such datasets for the approach described in Section 3.1.

In Section 2.3, we will assess the capacity for contemporary CCs for doing "Deep Learning in Imaging Neuroscience" data, but we will first asses in this Section the potential advantages of using the Monte-Carlo approach to reduce the amount of data-processing necessary for assessing "Imaging Neuroscience" data. The brain is one of the most complex structures in the universe given that each neuron is connected with hundreds or thousands of other neurons, not only in the neuron's vicinity but also by constituting large-scale physiologic neuronal networks (Lichtman, 2014). Structural connections provide crucial Information for healthy, psychiatric and neurological signatures of brain organization (Barkhof, 2014)(Worbe, 2015)(Zhou, 2014)(Sharp, 2014), and later in Section 3.1 we will assess the possibility of objectively identifying psychiatric states. Recent technological developments have allowed for big data connectome resources, open science sharing of large amounts of scans, and massive clinical assessment (Lichtman, 2014)(Craddock, 2015)(Marder, 2015). Nevertheless, the processing speed requirements for these analyses have been presenting a challenge (Lichtman, 2014)(Marder, 2015), thus increasing computational power and time. Urgent time-reduction methods without loss of quality are required for practical use (Lichtman, 2014)(Craddock, 2015)(Marder, 2015)(Boubela, 2015), especially for multicenter studies and clinical settings. (Lori, 2016)

We establish here, an example of how much the use of the Monte Carlo method can increase the speed of complex and large numerical data-processing. Specifically, we will consider the determination of the white matter (WM) neural circuitry in humans by the dMRI data-processing, which is often done using the Diffusion Tensor Imaging (DTI) approach (Conturo, 1999)(Lori, 2002). Despite the development of improved dMRI WM fiber tracking techniques (Tuch, 2004)(Behrens, 2007)(Wedeen, 2008)(Raffelt, 2012)(Wedeen, 2012), results are still behind those obtained using in-vitro data (Dani, 2010); or in-vitro microscopic studies (Hawrylycz, 2012). Thus, to improve WM anatomical representation more gradient orientations and higher gradient intensities have been used which have steadily increased the dMRI`s data size and data-processing complexity. (Lori, 2016)

The DTI approach represents the diffusion of water molecules in WM by a 3x3 symmetric matrix, the diffusion tensor, which completely represents that diffusion if the WM is constituted by straight WM fibers all pointing in the same orientation. In this case, the ellipsoid represented by the diffusion tensor has its biggest axis pointing in the orientation of the WM fibers. Different WM fiber tracking techniques have different capacities to accurately represent the anisotropic component of the axonal orientation distribution function (ODF). The bigger the amount of different diffusion-sensitizing parameters the data acquisition has, the more Information can be obtained (Tuch, 2003)(Hill, 2012)(Wang, 2007)(Assaf, 2008), but this increases the size of the data set and the corresponding data processing time. (Lori, 2016)

A typical example of advanced dMRI data acquisition and processing is DSI (Wang, 2007); while for DTI it suffices to have 6 orientations all with the same gradient amplitude, DSI requires hundreds of different gradient orientations and amplitudes. The end-result of the advanced dMRI data processing is often tractography, which consists on showing the WM connections more likely to exist. The final images of the tractography are typically a spaghetti of lines, Fig. 2.2.1a (e.g. Ref. (Behrens, 2007)); and/or a colored anatomical image of connection probabilities, Fig. 2.2.1.b (e.g. Ref. (Wedeen, 2008)). We describe here the dMRI data processing for extracting the WM axonal ODF, *h*, with an improved estimation of its isotropic and anisotropic fractions. We then calculate how much the use of the Monte Carlo method can reduce the data size required to be within ±1 standard error of mean (SEM) from the value obtained using the full data set. (Lori, 2016)

a) 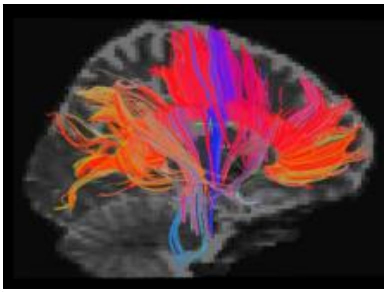 b) 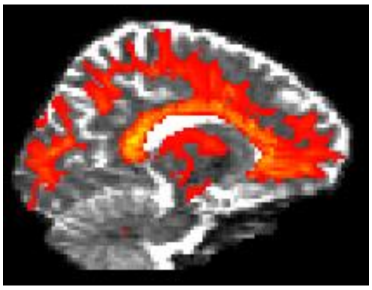

Figure 2.2.1. Examples of human brain dMRI data processing, shown are Sagittal slices of tractography final images. **a)** DTI-based spaghetti of lines, **b)** DTI-based connection probabilities with seed region in corpus callosum. (Lori, 2016)

2.2.1. White Matter tractography using Imaging Neuroscience data

To obtain the axonal ODF, h, it is necessary that the experimental dMRI signal is modeled by axons having a certain orientation, and those axons need to have physiologically reasonable properties so that the recovered axonal ODF accurately represents the physiological ODF. Using our model, we determine the parameters which give the best fit of the calculated theoretical dMRI signal to the experimental signal.

From the best fit, we obtain the experimental axonal ODF, h_{fit}. The experimental axonal ODF can then be separated into an isotropic and an anisotropic component. We proceed to calculate for each voxel the isotropic fraction and the integer k number of WM axes. Then, the number of WM axes in each voxel that are parallel to the WM axes of neighboring voxels is determined by a procedure we developed, which calculates in automatic fashion the WM axes obtained in ref. (Wedeen, 2012). Comparing these axis numbers between neighboring voxels, we can quantify the existent number of equally oriented axes in neighboring voxels. This allows us to distinguish between 1-axis connections ($k=1$), which are lines identical to those obtained in DTI tractography; 2-axes connections ($k=2$), which occur when 2 fiber-axes at a voxel are compatible with 2 fiber-axes at a neighboring voxel; and 3 axes connections ($k=3$), which occur when 3 fiber-axes at a voxel are compatible with 3 fiber-axes at a neighboring voxel, similar to ref. (Wedeen, 2012) (see Fig. 2.2.2).

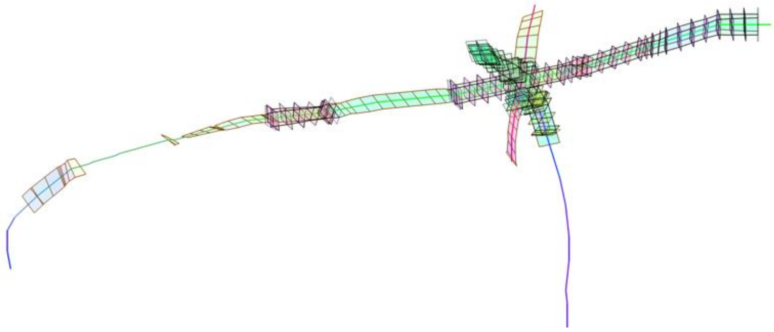

Figure 2.2.2. Example of DSI connections from one seed with colors depend on orientation. The lines are 1-axis connections (*k=1*), planes are 2-axis connections (*k=2*), and crossing planes are 3-axis connections (*k=3*). (Lori, 2016)

Using the multi-exponential representation of the dMRI signal in ref. (Milne, 2009), a parameter search is done (see Table 2.2.1) where D_F denotes the diffusion tensor of apparent fast diffusion and D_S denotes the diffusion tensor of the apparent slow diffusion orthogonal to the direction of fast diffusion. If the highest eigenvalue of the diffusion tensor for a single axon is $\lambda_{//}$, and the two smaller eigenvalues are both equal to $\lambda_{\perp}$, then based on ref. (Milne, 2009) the D_F and D_S for an axon with a $\hat{r}(\theta,\varphi)$ orientation expressed in spherical coordinates (θ,φ), and where *I* is the identity matrix, are (Lori, 2016):

$$D_F(\theta,\varphi) = [\hat{r}\,(\theta,\varphi)\,\hat{r}(\theta,\varphi)^T]\lambda_{||} \tag{2.2.1}$$

$$D_S(\theta,\varphi) = [I - \hat{r}\,(\theta,\varphi)\,\hat{r}(\theta,\varphi)^T\,]\lambda_{\perp} \tag{2.2.2}$$

The $\lambda_{//}$ corresponds to diffusion parallel to the axon, and $\lambda_{\perp}$ to diffusion perpendicular to the axon, and they were both collected from Table 1 in ref. (Raffelt, 2012); corresponding, respectively, to the D_F and D_S experimental averages in the table of ref. (Milne, 2009). If we consider $\vec{q}$ as the q-vector given by the product of the proton gyromagnetic ratio γ, with the diffusion-sensitizing gradient duration δ, and the magnetic field gradient vector $\vec{g}$ (Tuch, 2003), $\hat{q}$ as the unit-size q-vector, τ as the regularized diffusion-time, and ζ as a scalar between 0 and 1 (from Table 1 in ref. (Raffelt, 2012)), then the dMRI signal reduction for an orientation *(θ,φ)* is:

$$S(\theta,\varphi)_{\hat{q}} = \zeta e^{-|\vec{q}|^2 \tau \hat{q}^T D_S(\theta,\varphi)\hat{q}} + (1-\zeta)e^{-|\vec{q}|^2 \tau \hat{q}^T D_F(\theta,\varphi)\hat{q}} \quad . \qquad (2.2.3)$$

The q-vector has units of one over length, and that length expresses the diffusion spatial length scale-order the dMRI signal is probing. We model this dMRI signal reduction starting from the ODF of the WM fiber orientations, $h(\theta,\varphi)$. The WM fiber orientation ODF, h, is expressed as the sum of an isotropic and an anisotropic component, the first of which is given by a sphere of radius R, and the second by a number k of Gaussian-like peaks indexed by j and with standard deviation σ_j. The theoretical dMRI signal equation E_T is obtained using both Eq. 2.2.1 and Eq. 2.2.2 on Eq. 2.2.3 to define S, and then using the defined h to obtain (Lori, 2016):

$$E_T(\vec{q}) = \frac{\int_0^{2\pi}\int_0^{\pi} h(\theta,\varphi)S(\theta,\varphi)_{\hat{q}} \sin\theta d\theta d\varphi}{\int_0^{2\pi}\int_0^{\pi} h(\theta,\varphi)\sin\theta d\theta d\varphi} \qquad (2.2.4)$$

If the experimentally obtained dMRI signal intensity is E_{exp}, then the difference G_{DSI} between the experimental and theoretical dMRI signal for DSI is obtained by the sum, over all the $\vec{q}$ used in DSI, of the squared differences between E_{exp}, and E_T. The E_T was compared to E_{exp}, and the parameters that give the best approximation were selected by choosing the R, L_j, and σ_j parameters that minimize the difference between E_T and E_{exp} for the used data acquisition method, and they so define the h_{fit} for that acquisition method. The parameter combinations are described in Table 2.2.1 and are based on diffusion parameters from ref. (Milne, 2009), all parameter combinations were assessed for each voxel (Fig. 2.2.3 is the example for one voxel). (Lori, 2016)

Table 2.2.1. The parameters used in our search (Lori, 2016).

Parameters	R	L_1	L_2	L_3	σ_1	σ_2	σ_3	$\lambda_{//}$	$\lambda_{\perp}$	Z
Values	1	0:50: 300	0:50: 300	0:50: 300	0:0.1: 0.5	0:0.1: 0.5	0:0.1: 0.5	1.69 $x10^{-9}$	0.36 $x10^{-9}$	20.91 $x10^{-2}$

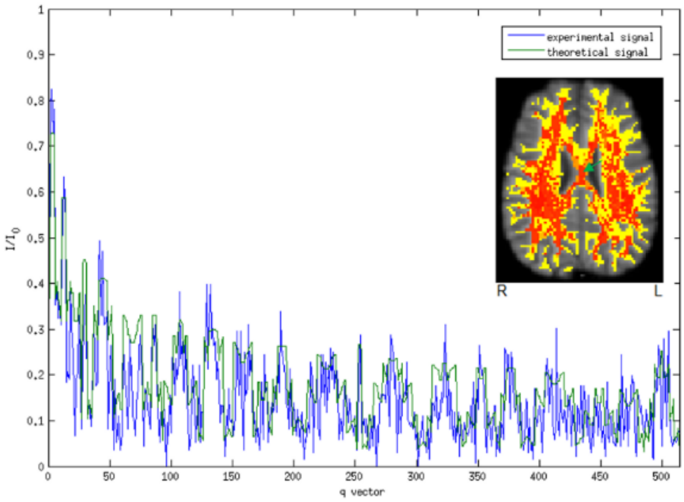

Figure 2.2.3. Experimental (blue line) and theoretical signals (green line) along the corresponding q-vector number. The example voxel is on the position pointed by the green arrow near the ventricles (black triangular shapes) in the brain image overlaid by the isotropic fractions (yellow-red scale). (Lori, 2016)

The isotropic and anisotropic fractions were obtained from the volume obtained from the h_{fit}. The total volume is calculated by:

$$V_{total} = \int_0^{2\pi} \int_0^{\pi} h_{fit}(\theta,\varphi) \sin\theta d\theta d\varphi \qquad (2.2.5)$$

The isotropic volume corresponds to the volume of the sphere with radius equal to the minimum value of $h_{fit}(\theta,\varphi)$; therefore $h_{fit}(\theta,\varphi)$ in Eq. 2.2.5 is replaced by the minimum of h_{fit} (Lori, 2016):

$$V_{iso} = \int_0^{2\pi} \int_0^{\pi} min(h_{fit}) sin\theta d\theta d\varphi \quad (2.2.6)$$

The anisotropic volume is the difference between total volume and isotropic volume: $V_{aniso} = V_{total} - V_{iso}$ The ratio between the anisotropic fraction of WM fibers, and the total amount of WM fibers is: $\Xi_{aniso} = \frac{V_{aniso}}{V_{total}}$. The ratio for the isotropic fractions (only calculated for WM voxels) is thus (Lori, 2016):

$$\Xi_{iso} = \frac{V_{iso}}{V_{total}} \quad (2.2.7)$$

The Ξ_{iso} of each voxel was correlated with the k values obtained using the approach described in the next section. The study was performed on high quality DSI dMRI data from the Human Connectome Project (HCP). Henceforth, we will refer to these data as "HCP data". The HCP data used in the preparation of this work were obtained from the database of the MGH-UCLA section of the HCP (all the HCP data has been approved by the corresponding ethical committees and internal review boards) (UCLA, 2012), the HCP data includes an anatomical T1-weigthed volume. The anatomical data, and segmented maps were coregistered to diffusion space using "fMRI of the brain Software Library" (FSL). Furthermore, we also used anatomical labeling provided by FSL; so that WM can be distinguished from gray matter (GM), from cerebro-spinal-fluid (CSF), and from everything else that is not WM. The anatomical image had its intensity inhomogeneity corrected, contrast adjusted, voxel re-sampled, and co-registered to the dMRI data. The values of TR and TE differed depending on which gradient orientation and amplitude is considered (Lori, 2016).

The HCP DSI data was acquired in Siemens 3T scanners in a cubic q-space grid format, with 514 gradient directions, 2 mm isovoxels, an image size of 104x104, and 55 transversal slices. There were available only 2 subjects with data suitable for our analysis, for our analysis required data which was acquired using the maximum gradient strength and that could be processed using DSI approach.

The subject 1, was acquired using a maximum gradient of 300 mT/m, b maximum of 15000 s/mm^2; whereas subject 2 was acquired at a maximum gradient of 90 mT/m and b-value maximum of 10000 s/mm^2. The segmentation of the WM was performed in HCP data using FSL (Zhang, 2001). The anatomical data, and segmented maps were coregistered to diffusion space using FSL. (Lori, 2016)

2.2.2. Monte-Carlo approach to Imaging Neuroscience data

The Diffusion Toolkit/TrackVis software (Wedeen, 2008) was used to obtain a 181 points ODF surface (not the axonal ODF). The obtained ODF data contains ODF peaks, which are the orientations for which the ODF is higher. The ODF peaks data binary data takes the value of 1 if the value of the ODF is a local maximum, and zero otherwise. For each peak, there is a peak pointing in the opposite direction with almost equal amplitude. If the ODF contains more than 3 pairs of opposing peaks, only the 3 highest ODF pairs of opposing peaks will be used. In this Section, we call the orientation of a pair of ODF opposing peaks, an axis. In an axis, a connection to a neighboring voxel can be made by either advancing or retreating along that axis. We developed an automatic approach method based on previous works (Wedeen, 2012), which is a WM axis extension approach where for each WM point it is determined the number of axes parallel to the axis of another WM point. The obtained topological structure is a 3-plane crossing grid, such as occurs in Fig. 2.2.2 (Lori, 2016).

The number of coincident axes between two neighboring points is denoted by a non-negative integer *k*, implying that in the same voxel there can be different *k* values depending on which neighboring WM points are considered. The value of *k* between two neighboring points defines the number of parallel fiber axes between the two sets of 3 axes, one set per point. The axes extension and parallelism detection are only performed for WM voxels, Fig. 2.2.4.

The isotropic fractions are higher near the vicinity of GM, as it is expected, since the fibers theoretically become less organized and with a less defined main direction. The regions with lower Ξ_{iso} are mostly located in the corpus callosum, superior longitudinal fasciculus, and corticospinal tracts (Fig. 2.2.4). The regions with lower isotropic fraction are in agreement with bigger *k* values from the tractography method. It is apparent that high *k* values correspond to low values of Ξ_{iso}. This was confirmed by calculating the mean values of the Ξ_{iso} for each group of voxels with a given *k* value, Table

2.2.2. To assess the required amount of data needed to get the correct results without needing to deal with the multiple comparison problems, we used the Monte Carlo permutation test. The data were randomly sampled without replacement, so as to guarantee that the same data point is not sampled twice, This also limited the number of possible samples to the maximum number of data points existing with the feature of the population being sampled (e.g. k=1). One of the advantages of the Monte-Carlo method is that the sampling ordering is random, which reduces the systematic errors caused by sequential sampling. (Lori, 2016)

The relation between the percentage of voxels used (x-axis) and the value of Ξ_{iso} represented as a fraction of the Ξ_{iso} obtained when all voxels are used (y-axis) appears in Fig. 2.2.5. We obtain the relations between the percentage of voxels used (x-axis) and the percentage of sub-partitions whose averages are within ±1 standard error of the mean (SEM) of the true average (y-axis) (Fig. 2.2.6), the needed percentage of used voxels being defined when the percentage of means within ±1 SEM is 68%, as it should be. These results were obtained for each of the three axis connections possibilities, specifically, *k=1*, *k=2*, and *k=3*. For both Fig. 2.2.5 and Fig. 2.2.6 the voxels are randomly sampled without replacement using a Monte Carlo method. (Lori, 2016)

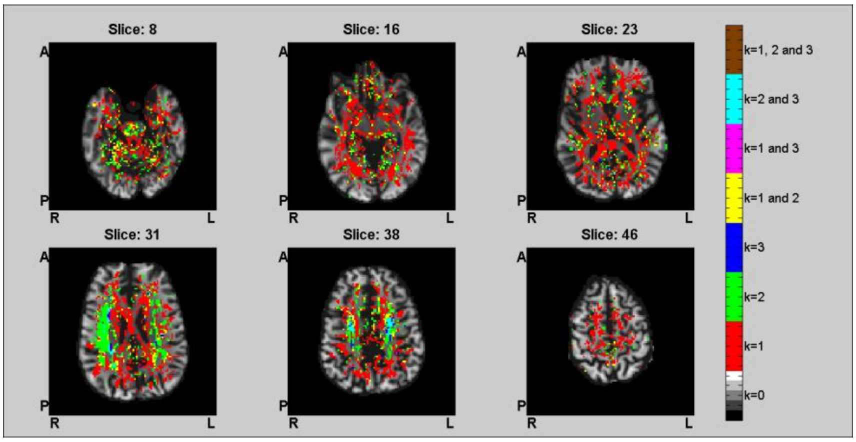

Figure 2.2.4. Example of results using HCP DSI human data overlaid on HCP anatomical MRI. (Lori, 2016)

Table 2.2.2. Isotropic fractions' Ξ_{iso} relation to *k* values for two subjects. Only *k* values with more than 5 voxels were considered statistically significant. (Lori, 2016)

		k=1	k=2	k=3	k=1 V 2	k=1 V 3	k=2 V 3	k=1 V 2 V 3
Subject 1	$\langle \Xi_{iso} \rangle \pm SEM$	63.1±0.5	41.3±0.8	38.7±1.8	43.0±1.4	53.7±6.2	35.9±2.4	N/A
	Number of voxels	5777	2322	247	708	27	124	4
Subject 2	$\langle \Xi_{iso} \rangle \pm SEM$	53.6±0.4	37.4±0.7	38.4±2.0	38.8±1.3	46.0±7.0	33.0±2.4	47.1±9.8
	Number of voxels	8251	3342	280	867	29	146	12

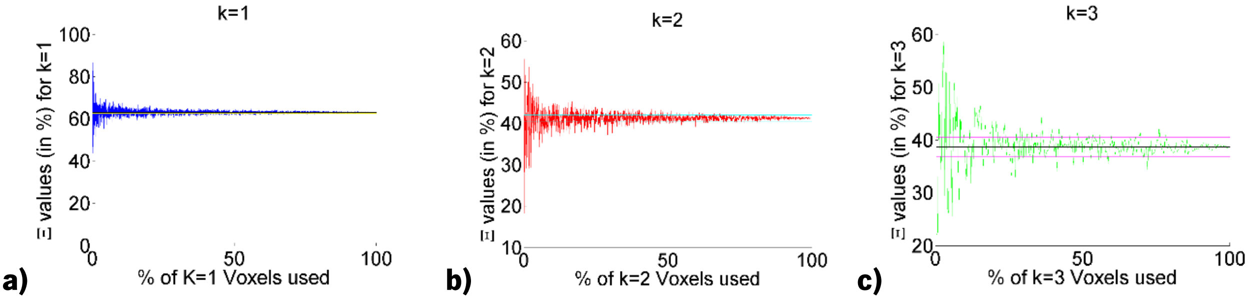

Figure 2.2.5. Comparison of Ξ_{iso} calculated with all the voxels (straight line ± 1 SEM) versus Ξ_{iso} calculated with a Monte Carlo fraction of the voxels (y-axis) as a function of the fraction of the Monte Carlo-selected voxels (x-axis): **a)** *k=1* , **b)** *k=2* , **c)** *k=3*. (Lori, 2016)

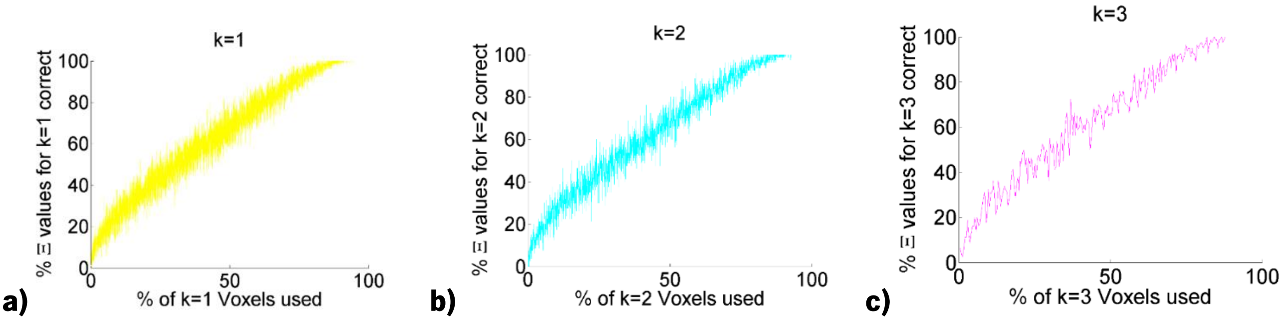

Figure 2.2.6. Calculation using Monte Carlo method of the fraction of voxels with Ξ_{iso} within ±1 SEM of the Ξ_{iso} calculated with all the voxels (y-axis) as a function of the fraction of the Monte Carlo-selected voxels (x-axis): **a)** *k=1* , **b)** *k=2* , **c)** *k=3*. (Lori, 2016)

We show that the use of Monte Carlo voxel sampling obtained the correct result within ±1 standard (SEM) 68% of the times using only about 50% of the data, which is what allows us to say that the Monte Carlo method is capable of reducing the computation time by about 50% without loss in result quality. Plus, we found that the regions with higher k values correspond to regions with lower Ξ_{iso}. An arrangement $k=3$ between voxels suggests a lower isotropic fraction, which means that the 3-axis arrangement of the axons is a good representation of the majority of the axons' distribution, in agreement with the results of ref. (Wedeen, 2012) used in Section 3.1. The simpler the arrangement, respectively $k=2$ and $k=1$, the higher the isotropic component of axonal distribution. (Lori, 2016)

The neuroscience of big data has challenged the processing speed requirements, especially in the field of connectomics (Lichtman, 2014)(Marder, 2015). Recent developments of new brain network technologies will soon allow for scalable data analysis. In dMRI data, high image resolutions are needed to accurately reconstruct connections, making the size of the input set very large (Lichtman, 2014); and we describe in Section 3.1 how these types of "Imaging Neuroscience" data will allow for the clarification of what objectively is human mental health. To make assessment like those proposed in Section 3.1 using contemporary CCs, it is likely that an improvement in "Imaging Neuroscience" data-processing speed will have an exponential effect in big data platforms (Lichtman, 2014)(Craddock, 2015)(Marder, 2015)(Boubela, 2015), especially in the context of current collaborative multicenter studies (Sedeño, 2017) and also in clinical settings (Ibañez, 2018). Hence, the brain structural connections among regions and their mapping to clinical and individual differences in healthy, psychiatric and neurological domains will have a critical growing with future big data connectome, open science resources, and massive clinical assessment (Craddock, 2015). (Lori, 2016)

As will be described in Section 3.1, the alteration of brain connectivity is observed across a large range of psychiatric and neurological disorders. In fact, most of them have some degree of aberrant connectivity (Barkhof, 2014)(Worbe, 2015)(Zhou, 2014)(Sharp, 2014). This knowledge will soon have direct applications for both clarification of the biology of these diseases as well as in drug discovery process. In the future, it is very likely that connectomics will become part of the routine clinical assessment. In these settings, short time windows between recordings and evaluation became crucial. Hence, although the approach provided here needs to be replicated in larger samples, in different recordings, with dissimilar scan qualities, and in diverse neuropsychiatric conditions, approaches such as those proposed here will likely be useful in application to "Neuroscience Imaging" big data.

2.3 Deep Learning pipeline improves functional MRI data processing

Key points:

- To reach the goal of analyzing the future of CS in using "Deep Learning in Imaging Neuroscience" as described in Section 3.1, we start here by assessing its use in the present of CS.
- The results obtained here increase the applicability of the new forms of using CS described in Section 3.1, and it is the joining of Section 2.2, Section 2.3, Section 2.4, and Section 3.1 that allow for some of the perspectives proposed in Section 3.2.

A major goal of this thesis is the use of "Deep Learning in Imaging Neuroscience" and in this Section we will directly assess this topic. Neuroimaging has a major clinical application of serving as medical support in the field of Neurology, and even more so for the case of diagnosis. Nevertheless, the use of "Imaging Neuroscience" has been growing in other fields, e.g. in Psychiatry as a mean of a better understanding psychiatric disorders (Lori, 2019) (see Section 3.1). Moreover, a new dimension called brain-body medicine focuses in the study and understanding of the interactions between the brain, peripheral pathways and bodily organs (e.g. (Yoris, 2017)). These new advances give three new approaches to "Imaging Neuroscience" research (Lori, 2018): mind-body connections, psychosomatic behavior, and integrative medicine (Lane, 2009)(Horowitz, 2009). These three new approaches are used in Section 3.1 to objectively define what is human mental health (Lori, 2019), but in this Section we will focus in how to use DL in this type of "Imaging Neuroscience" data.

In "Imaging Neuroscience", the study of brain structure (e.g. by dMRI) is not enough, as it doesn't give relevant Information for the diagnosis of pathologies when structural alterations are not anatomically detected. Thus, it was necessary to find an appropriate method to assess brain function, which led to the development of fMRI, a technique that monitors hemodynamic events related to changes in neuronal activation in the brain, relying on the Blood Oxygenation Level-Dependent (BOLD) contrast (FMRI, 2009)(Ogawa, 1990). This use of fMRI has countless advantages such as non-invasiveness, relative easiness of implementation, and high spatial resolution. Moreover, the resulting signal is robust, it is easily reproducible and highly consistent. (Horowitz, 2009). The fMRI is typically used in the context of a given task, performed within the magnetic resonance equipment (a.k.a. scanner), so as to identify brain regions associated with the neuronal processes involved in the performance of that task. However, this precludes the analysis of the default interactions between different brain regions (i.e. default brain connectivity). Nowadays the neuroimaging community is changing emphasis from functional specialization towards functional integration (Smith, 2012). Functional Connectivity (FC) is based on the temporal correlation between spatially remote neurophysiological events in the brain (Friston, 1994)(Biswal, 1995). The FC can be measured using a variety of different techniques, but the most used is the resting-state fMRI (rs-fMRI) (Gusnard, 2001). The use of fMRI together with the dMRI technology described in Section 2.2. has been used for a long time (e.g. (Conturo, 1999)(Ibañez, 2018)) and is the basis for the HCP which was already describe in Section 2.2; and the perspective described in Section 3.1 which is partially based (Lori, 2019) in the results of the HCP.

There are three main methods used by the "Imaging Neuroscience" community to analyze and evaluate FC: Seed-Based Analysis (SBA), Independent Component Analysis (ICA), and Connectomic Analysis (CA). All these methods have the same final goal which is the attainment of brain connectivity networks. In this section, we will use the CA method. The CA analyzes the interactions between every possible pair of brain regions. The CA method uses the fMRI time-series extracted for each region belonging to a given atlas, or for every voxel in the dataset. Then, the correlations between the time-series of all pair of regions are calculated. Thus, this results in a correlation for each pair, quantifying the FC between pairs of regions. The CA data is typically represented as a connectivity matrix (see an example in Fig. 2.3.1). The connectivity matrix is the schematization in matrix form of the values of the correlation between all pairs of regions. So, its size is N x N, where N is the number of regions or nodes resulting from the brain parcellation. The Information obtained in the connectivity matrices has shown a lot of applications (e.g. (Sedeño, 2017)), such as the study of changes in brain functionality due to Alzheimer's Disease (AD) (Dennis, 2009) or Autism (Maximo, 2014). Another application is the study of the main networks in the connectome responsible for a specific psychological trait (Jung, 2016) or some mental capacity (Yoris, 2017)(Lori, 2019). Moreover, these matrices are used for classification recurring to Machine Learning (ML) or statistical methods (Lori, 2018).

In some publications (Ball, 2016), those FC matrices have been able to discriminate preterm infants at term - equivalent age and healthy term – with born controls with 80% accuracy using a ML method. Plus, their approach was used to distinguish between healthy controls and depressed patients with accuracy values of 85.85% and 70.75%, respectively for patients with treatment resistant depression and patients with non-treatment resistant depression (Byun, 2014). Furthermore, this connectivity matrices have shown to be reliable fingerprints, making possible to identify accurately a specific subject from a large group. The research made in Functional Connectome Fingerprinting which identified individuals using FC patterns (Finn, 2015) demonstrated that when applied to resting-states, these methods can predict and identify an individual, respectively, with 92.5% and 94.4% accuracy. For fMRI acquisition in task conditions, they also obtained results that presented a great accuracy, with rates of about 87.3%. Relatively to classifications using train and test data with different fMRI conditions (resting or task), for each one, the final accuracy values achieved were lower, with maximum rates of 50.4%. (Lori, 2018)

The approach to FC used here is based in techniques of ML, and hence there is always a learning process in order to obtain accurate representation of data and prior knowledge (Suzuki, 2012). In "Imaging Neuroscience", ML can be used as both a supporting tool to studies of FC and as a form for solving the need for classification models. A novelty of the approach used here (Lori, 2018) being the use of Deep Neuronal Networks (DNN) to make the analysis of the rs-fMRI-based FC data so as to achieve a classification model for each person. The DL allows for the modelling of higher-level data-structure abstraction using Artificial Neural Networks (ANN), and thus improves the predictions by providing a better classification (LeCun, 2015). The DL is a technique that has seen its usage expand quickly and has allowed for the creation of a lot of applications such as new approaches to object recognition. Since the FC values are saved in large dimension connectivity matrices completed with a lot of features, they allow these features' granularity to be diversified, where the unit in study can be a voxel, or a brain region obtained from brain parcellation (Wang, 2016)(Greenspan, 2016). (Lori, 2018)

2.3.1. Building a Functional Connectivity Table

Using the FC technique, several spatially distributed patterns were observed across subjects and presented a strong similarity between them (Friston, 1994)(Biswal, 1995). These patterns were denominated as the Resting State Networks (RSNs) (Biswal, 1995)(Gusnard, 2001) because they use rs-fMRI data. The fMRI is also used to determine the effective connectivity (Friston, 1994). The effective connectivity establishes which brain regions are mainly active during action, perception and cognition, plus the causal relations between those regions. (Lori, 2018)

The data used as features for the models in this Section were the FC matrices extracted from rs-fMRI data obtained from different subjects. The learning process of the models is based in the supervised learning, hence we used some Information of the subjects, such as: identity, gender or age. There was also the necessity to use atlases so that FC data can be associated to specific brain regions. Part of the work developed in this Section is related to the results and work performed by ref. (Shen, 2013), wherein the FC provided from rs-fMRI is used as the subjects' fingerprint. Therefore, the approach followed in this work aims at a comparison with ref. (Shen, 2013) in order to find a better approach. The ref. (Shen, 2013) work used two different sessions of rs-fMRI acquired in different days as the subjects' set. Plus, each correlation matrix with FC data for each session was correlated by Pearson's correlation with all the other FC matrices in the other session. (Lori, 2018)

The different atlases have different number of Regions of Interest (ROIs), and different creation processes by use of different MRI data types (Table 2.3.1). The name of the atlas in ref. (Shen, 2013) don't coincide with the total number of anatomical regions because the name is associated to the number of "seeds" used in each cerebral hemisphere during the atlas application process. The rs-fMRI data used in this Section was obtained from the SWITCHBOX Consortium project (http://www.switchbox-online.eu/) realized in the "Life and Health Sciences Research Institute" (ICVS) and we call it the "In-House data" (Magalhães, 2015), and moreover we chose to use this In-House data as it is a 1.5T clinical scanner similar to the clinical scanners more commonly used worldwide (Rentz, 2012). The In-House data used in this work are volumes with the temporal data saved from rs-fMRI. Initially, the data is a set of "Digital Imaging and Communications in Medicine" (DICOM) brain images of different temporal points of the acquisition which are converted into a single volume file. Then they undergo a pre-processing pipeline to obtain a file with the values of the correlation of intensities between each pair of brain regions, for each of the 76 subjects (39 male and 37 female). The scanner used was a Siemens Magnetom Avanto 1.5 T MRI scanner with a 12-channel receive-only head-coil. The rs-fMRI was obtained using BOLD sensitive Echo-Planar Imaging (EPI) sequence with these parameters: 30 axial slices; TR/TE = 2000 ms/30 ms; flip angle = 90°; slice thickness = 3.5 mm; slice gap = 0.48 mm; voxel size = 3.5 x 3 x 3.5 mm^2; FoV = 1.344 mm. The final outcome of the standard FSL data processing of the rs-fMRI data is a file with 355 lines, one for each of the volumes of the acquisition with the mean BOLD signal for each region of the brain. (Lori, 2018)

Table 2.3.1. Table of atlases with number of total nodes in descending order.

Parcellation Name	**Total regions**	**MRI data type**
150 nodes	278	Functional
268 nodes	268	Functional
100 nodes	184	Functional
Freesurfer	160	Anatomical
AAL	116	Anatomical
50 nodes	93	Functional

The datasets of this Section are constituted by two major parts: FC data, and respective subject's labels. The labels are a class that saves some Information about the subject which can be categorical, ordinal, integer-valued or real-valued. These labels can be the identity Information of the subject, the gender, the state in a disease, the blood type, and others. The label is the Information that will be used in the supervised learning for training, validation and testing of the DL models. The FC was analyzed through the correlation matrix (a.k.a. ROIs FC analysis method). The FC features were produced in matrix form from the different volumes produced after the brain parcellation step. Each FC input file has one line for each volume in the acquisition and one column for each region of the atlas used in the parcellation process (e.g. the average value for each volume and region). Therefore, the FC input file size is related to the parcellation used, which in turn affects the number of the total values present in the matrix (Table 2.3.2). There are two different approaches to extract FC maps: static, and dynamic. In this Section, we focus in the static approach. (Lori, 2018)

Table 2.3.2. Features of the correlation matrices by each brain parcellation.

Atlas applied	Matrix Size	Number of values	Features
150 nodes	278 x 278	77284	38503
268 nodes	268 x 268	71284	35778
100 nodes	184 x 184	33856	16836
Freesurfer	160 x 160	25600	12720
AAL	116 x 116	14456	6670
50 nodes	93 x 93	8649	4278

The static FC was computed through the Pearson's correlation between the full time-series of each pair of brain regions, resulting in the symmetric matrix with the Pearson's coefficients expressed in one adjacency matrix per subject (Biswal, 1995)(Al-Rfou, 2016). The Pearson correlation coefficient between two series X and Y, both of size N, is given by Eq. 2.3.1. This FC static approach is widely used in the Neuroscience field, and it allows us to infer the strength of the FC by estimating the linear correlation coefficient between two temporal signals. If the regions have the same behavior, they are activated and deactivated at the same time, the Pearson's value will then be high showing that it is probable that the regions have a strong functional connection, and hence a positive high FC. Then a Fisher's r-to-Z transformation was applied to each correlation matrix to improve the normality of the correlation coefficients. An example of a matrix with static FC is showed in Figure 2.3.1. (Lori, 2018)

$$\rho_{X,Y} = \frac{\sum_{n=1}^{N}(X_n - \bar{X})(X_n - \bar{Y})}{\sqrt{\sum_{n=1}^{N}(X_n - \bar{X})^2}\sqrt{\sum_{n=1}^{N}(X_n - \bar{Y})^2}} \qquad (2.3.1)$$

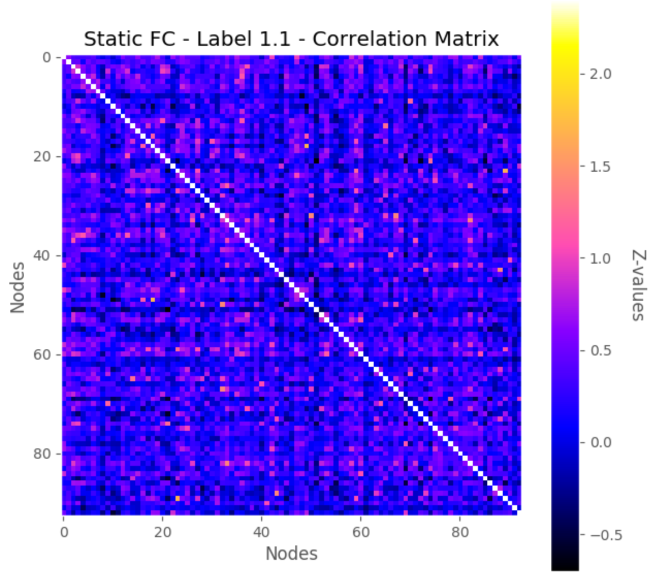

Figure 2.3.1. A correlation matrix for 50 nodes parcellation (and using 93 brain regions) with the values of the static FC of the label 1. (Lori, 2018)

2.3.2. Deep Learning in Functional Connectivity Table

In CS, the development environment is an essential part of the development of computer programs and can be described as a set of specific aspects: processes, programming, and technologies. The development environment used in this Section (Lori, 2018) is represented by the work architecture of Figure 2.3.2. The DL module obtains the best models and their respective results. Thus, the use of the DL module allows for a better automation of the processes, an easier and more efficient data management, and plus the creation of a workflow which deals with the FC Information and uses it as features for the construction of DL models that allow for an improvement in subject's classification. This processing is a reliable method for obtaining reliable FC from rs-fMRI data, in which we used a recent library Nipy (Gorgolewski, 2011) that is based in the Python programming language (Van Rossum, 2006). The datasets creation; which includes the analysis of the values by dataset and subject or class of the dataset; is then prepared for use in the training, validation and test of DL models. Finally, the major objective, the DL application over the FC data to improve the subject's classification tasks includes the fine-tuning of the models, the selection of the best models, the analysis of the results, and the management of the different results. (Lori, 2018)

The work in this Section was based in the Python programming language (Van Rossum, 2006); downloaded and managed using Anaconda; a free and open-source distribution of Python (Continuum, 2016); and we used it mostly because Python has been developed in order to improve data processing, predictive analysis and scientific computing applications. Moreover, to support the development of the different parts of the work (Lori, 2018), we used PyDev which is a Python Integrated Development Environment (IDE) for Eclipse developed to support the development of Java; whereas most of the work was developed and tested by using either the bash console or the interactive console of Python (iPython). Finally, to increase computation velocity, we used the Compute Unified Device Architecture (CUDA), a parallel computing platform and a programming model developed by NVIDIA (NVIDIA, 2017) which uses graphical processing units (GPUs) in different computation tasks. The use of CUDA permits the use of GPUs as the computation unit of the DL application (Lori, 2018) with all the software for this Section being ran in a Ubuntu operating system (see Figure 2.3.3).

In this Section, we find optimal architectures and hyperparameters using DL, so that the FC data can be used to obtain good performances in subject's classification tasks. This is relevant for the "Deep Learning in Imaging Neuroscience" aspect of this Thesis as the possibility for identifying individual subject's characteristics is relevant for the mental health model proposed in Section 3.1, which is then a key argument for the comparison made in Section 3.2 of the expected relative importance for the future of CS of "Deep Learning in Imaging Neuroscience" vs. "Nuclear Physics in Quantum Computing". Thus, two different DL models were tested in this Section, with each one being based in one of two different types of layers: fully connected layers, and convolutional layers. For each of the two types of layers, we then tested architectures with different depths. Moreover, we also searched for the hyperparameters that best fit the models created. The fine-tuning of these parameters is fundamental for the learning process to evolve and achieving models with good generalization, a major objective of this Section. Hence, it was essential (Lori, 2018) for us to create a way to study, compare, and obtain feedback from the developed models; so as to make the right decisions towards systematically improving the performance of the models.

To obtain such a systematic improvement, we designed a small DL framework (part G of Figure 2.3.2) (Lori, 2018) working alongside other methods, as part of a bigger framework, so that this small framework could deal with the FC matrices extracted from the rs-fMRI data. The small DL framework was divided in two major parts (see part G of Fig. 2.3.2)(Lori, 2018): models fine-tuning, and final models. The fine-tuning part is responsible for the continuous adjustment of the model, wherein the model is approved to pass to the final phase. In the final phase, the more extensive tests are done, with increasing number of repetitions, and where the model and the model's performance values are saved for future uses. The validation of each model is made manually, after analysis of the performance measurements.

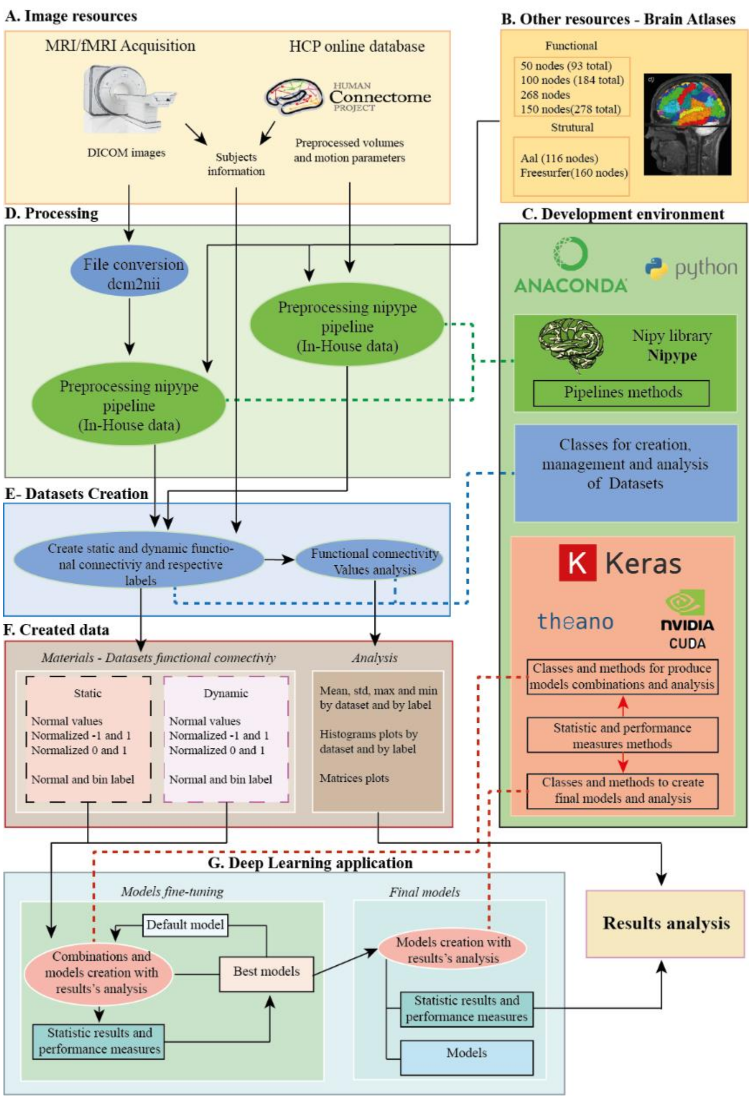

Figure 2.3.2. Schema of the materials and methods used. (Lori, 2018)

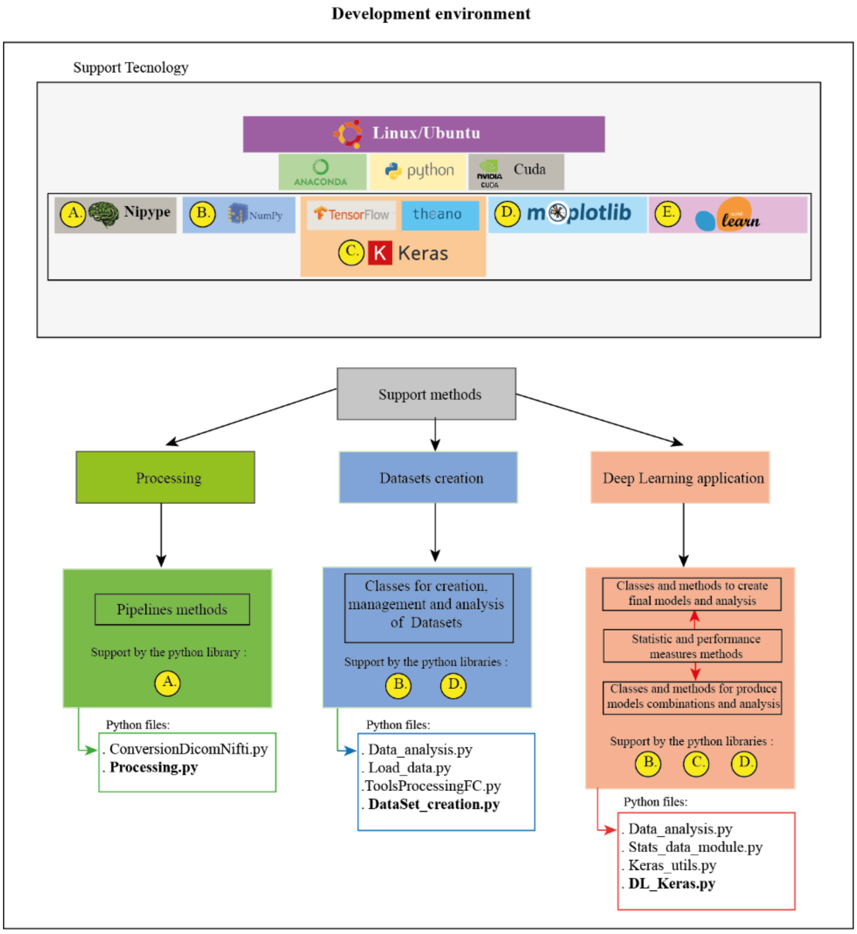

Figure 2.3.3. Development environment schema with the support technology used in the development of the different methods, the method itself and their respective Python files created. (Lori, 2018)

In ref. (Finn, 2015), the process applied to compare the FC matrices was the similarity based on Pearson's correlation (see Eq. 2.3.1). During that process, for each subject, it is made a Pearson's correlation between that subject's FC matrix of an experimental session (the target matrix), with each of the other existent FC matrices obtained in different experimental sessions which constitute the database matrices. After that, we only choose the database FC matrix with the maximum correlation value, which defines the chosen matrix. If the chosen matrix and the target matrix are of the same subject, then the classification is correct and so the classification score obtained is 1. If it is not the same subject, then the classification is incorrect, and the obtained classification score is 0. To test the approach, we used the In-

House data, with static FC for the set of atlases used in this Section, and the obtained values are presented in Table 2.3.3. These values in Table 2.3.3 are the objective values to be outperformed by the DL approach described in this Section (Lori, 2018). Analyzing the average correlations values for correct and incorrect classifications, it was verified that the correlation value affects positively the classification result. Implying that the difference between the two situations was significant, thus, the amount of correlation value is also correlated with the average accuracy over the dataset (see Table 2.3.) (Lori, 2018).

Table 2.3.3. Resume of the values obtained by the approach from ref. (Finn, 2015) using the In-House dataset for "Predict session 1" and "Predict session 2", for the different brain parcellations. (Lori, 2018)

Predict session 1			*Predict session 2*		
Parcellation	**Value**	**Difference**	**Parcellation**	**Value**	**Difference**
150 nodes	0.342	0.000	*150 nodes*	0.342	0.0000
100 nodes	0.316	0.026	*268 nodes*	0.303	0.0395
268 nodes	0.316	0.026	*100 nodes*	0.289	0.0526
Freesurfer	0.263	0.079	*AAL*	0.276	0.0658
AAL	0.250	0.092	*Freesurfer*	0.250	0.0921
50 nodes	0.237	0.105	*50 nodes*	0.237	0.1053

Table 2.3.4. Mean, Standard Deviation, Max and Min of the correlation values in the correct and incorrect classifications, and respective difference for the In-House data. (Lori, 2018)

	Correct classification	**Incorrect classification**	**Difference**
Average value	0.464	0.394	0.070
Standard Deviation	0.082	0.089	-0.006
Maximum	0.650	0.625	0.025
Minimum	0.271	0.190	0.081

The search for the best set of hyperparameters started with a simple model, followed by the adding of both depth and convolutional networks. Using the best set of hyperparameters, the models can be extended for other parcellations having new features and values by simply making some adjustments to the model's architecture. The In-House dataset has 76 subjects (Lori, 2018), hence the probability of correct classification by a random process is 1/76≈0.01316. The selection process of the best set of hyperparameters is started by using the 50 nodes atlas, which has the fewer number of features and the worst results, and so it will have a greater interval for improvement with a lesser number of parameters and thus less features to learn (Lori, 2018). The first set of hyperparameters wasn't selected randomly but by use of refs. (Ball, 2016)(Finn, 2015)(Fischl, 2004)(Byun, 2014), and tests were made before testing the models. The Tested i-iii and Fixed iv-vii model parameters were (Lori, 2018):

i. Learning rate: {0.5; 0.3; 0.1; 0.05; 0.01; 0.005; 0.001; 0.0005; 0.0001},
ii. Loss function set: {Categorical cross-entropy, hinge and squared hinge},
iii. Activation functions set: {Relu, Leaky Relu, Sigmoid, Prelu and tanh function};
iv. Epochs: 2000,
v. Optimizer: SGD,
vi. Bias initializer: Truncated Normal class with standard deviation equal to 1,
vii. Weights initializer: Variance Scalling class, with the average of the inputs and outputs.

The models described above amount to a total of 135 models, and for each model we made 10 tests, with each test having a different set of alpha rates used for the activation function Leaky relu (Table 2.3.5), where: alpha rates= {0.1; 0.2; 0.3; 0.4; 0.5; 0.6; 0.7; 0.8; 0.9}. The values obtained (Lori, 2018) demonstrated that the best alpha is 0.8 which implies that the models give some importance (near to 1.0) to the negatives values in the dataset so as to obtain better classifications results (see Figure 2.3.4)(Lori, 2018). The probability of the improvement with the increase of epochs is very likely as the training accuracy continually increases as the epochs increase, and so does the learning process. Plus, for these tests, we only intended to get a comparison between the results for different tests, and hence we were not yet aiming for the best model. (Lori, 2018)

Table 2.3.5. Average validation accuracy and cost values of 3 tests for different alpha rates in the Leaky Relu activation function for 50 nodes parcellation. (Lori, 2018)

Alpha	Validation accuracy average	Validation cost mean
0.1	0.08553 ± 0.02648	0.99918 ± 0.00015
0.2	0.08421 ± 0.01785	0.99926 ± 0.00014
0.3	0.08289 ± 0.02568	0.99919 ± 0.00015
0.4	0.08816 ± 0.02825	0.99914 ± 0.00016
0.5	0.08947 ± 0.02186	0.99917 ± 0.00016
0.6	0.08684 ± 0.03540	0.99913 ± 0.00032
0.7	0.06711 ± 0.02528	0.99931 ± 0.00014
0.8	0.09737 ± 0.02510	0.99912 ± 0.00020
0.9	0.07763 ± 0.02387	0.99918 ± 0.00019

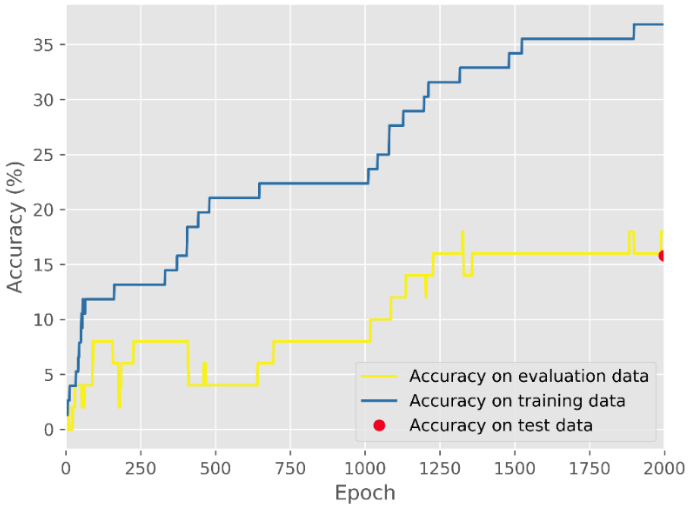

Figure 2.3.4. The best result of one of 3 tests for Leaky Relu with alpha equal to 0.8. (Lori, 2018)

As the number of combinations in analysis for the i-viii Tested and Fix model parameters are 135, wherein 15 models with different loss and activation function were tested for 9 learning rates; thus, after analyzing the 15 different models for different parameters, it was obtained that the best model for a 50 Nodes parcellation, for both accuracy and cost, was the model with the following parameters (Lori, 2018):

Loss function = Categorical cross-entropy

Activation function = Tanh

Learning rate = 0.01

Batch Size: 1

Kernel Initializer: Glorot Uniform

Bias Initializer: Random Uniform

Hidden Layers: 1

Nodes per hidden layer:200

Learning Rate: adjustable

Initial Learning Rate: 0.001

Best Learning Rate: 0.0001

fMRI Data Temporal Filtering: none

This best model (Lori, 2018) obtained an average accuracy of 0.3132 ± 0.0129 and an average validation cost of 3.1422 ± 0.0668, which clearly outperformed the published Pearson correlation approach performance with a 50 Nodes parcellation (Finn, 2015), which had a validation accuracy of 0.237. The parameters of the best model were (Lori, 2018):

Loss function = Categorical cross-entropy

Activation function = Tanh

Initial Learning rate = 0.01 (the number of epochs recommended are 1000 or more)

Batch Size = 1

Kernel Initializer = Glorot uniform

Bias Initializer = Random uniform

Optimizer = RMSprop

For the comparison between the different models; we used a set of metrics to assess the behavior of the model in both training and validation, such as, accuracy and loss. In addition, during the training we also calculated other values, such as, the maximum accuracy in validation with corresponding epoch occurrence, and the differences between the different data (e.g. training vs. validation). The cross-validation approach is the most correct form of validation; however, it was not possible to use that approach for this Section, as for the static FC there were too few cases for each label. Thus, we chose instead to divide the FC data of each acquisition session into two equal parts, one part being used as the validation data and the other as the test data. Hence, by joining all the different aspects of this Section, it was possible to create an architecture framework which uses rs-fMRI in raw format (e.g., DICOM images) combined with DL models to improve FC-based classifications tasks. (Lori, 2018)

In this Section, we describe a complete "Deep Learning in Imaging Neuroscience" approach that comprehends the pre-processing of the raw data, the creation of datasets with different FC Information, and the creation of a DL module which helps fine-tune the different DL models before getting the best model which is then used to make the final analysis. This description is a good description of what "Deep Learning in Imaging Neuroscience" can be done using CS's present capacities by use of CCs, but to obtain a hint of what CS's future entails for "Deep Learning in Imaging Neuroscience" it is necessary to go through the descriptions presented in Section 3.1., whereas to fully understand the potential economic impact of Section 3.1 it is first necessary to go through Section 2.4, where an analysis is made of how a perspective of CS based in Information-transport (Neves, 2019) can help improve the economic performance of a company.

2.4 Application of partial Information approaches to Management

Key points:

- To show how findings from Computer Science (CS) and Quantum Computing, which developed in some aspects from Deep Learning in Imaging Neuroscience to Nuclear Physics in Quantum Computing, can lead to severe and groundbreaking foundation in the field of CS; in particular, it was developed a partial Information system to healthcare management that coincides well with the partial Information perspective of objective human mental health as described in Sections 2.1, 3.1 and 3.2.
- Undeniably, an important consequence of this thesis is that CS stands for a discipline that can be interpreted as the basis for the other causal inference technologies, i.e., CS denotes not just a collection of tools for Mathematics, Physics, Neurosciences and Economics, but can also be understood as an added value from such disciplines to Quantum Computing.

The use of partial Information in CS to improve management performance is relevant (Neves, 2019), but for this thesis its applicability lies in certain aspects of the present approach, in particular the use of either Information-transport in CS or the use of partial Information as a key aspect in the attribution of economic value to a management act. The former is most important for section 3.2, while the latter is chief for section 3.1. Section 3.1 is critical because it shows how neuronal dynamics have strong parallels with economic systems (Montague, 2002), and by what means social interactions (including the attribution of economic value to a management act) play a role in the described model of mental health (Lori , 2019) (in Section 3.1.)

In this Section, efficiency refers to understanding the phenomenon of improving organizational sustainability, in view of the inputs used and the achievable results. When the focus is on the process of improving work effectiveness, one of the dimensions that influence the process depends on the interaction between people and their behavior in the organizational environment, as well as their impact on the process of achieving improved results. It is often assumed that people act as the engine for increasing efficiency at the organizational level to support the sustainability of the corporation. While in 1973 David McClelland questioned this assumption in his article "Testing for Competence Instead of Intelligence" (McClelland, 1973), pleading that individual academic aptitude and literacy are not compatible with a person's good performance in a corporation. He argued that there were a number of skills that played an important role in the organizational environment, and focused on a number of skills that supported professional performance for success, such as empathy, self-discipline, and initiative (Neves, 2019).

These factors, empathy, self-discipline and initiative were good predictors of leader performance in leading their teams. A characteristic of these people was the ability to read, interpret and influence other people's feelings and emotions. The analysis of this attitude was the goal of ref. (Neves, 2019), being the objective of this Section to provide a brief overview of how much of it has been achieved through the use of Logic Programming for Knowledge Representation and Reasoning (KRR), and how the evolution of their induced scenarios can be understood as a process of energy devaluation (Wenterodt, 2014) (Neves, 1984). In addition, a case study on organizational efficiency was presented and as in ref. (Neves, 2019), considering the emotions and feelings of the workforce. A diverse mix of features was used that indicate the level of collective confidence, gratitude, and pro-sociality, i.e. how employees respond to certain questionnaires that, when translated into logical programs and viewed in isolation, form the organization's knowledge base (Neves 2019).

All KRR practices can be understood as a process of energy devaluation (Wenterodt, 2014). A data element is understood to be at a certain point in time, at a given entropic state as untainted energy, ranging in the interval from 0 to 1, that, according to the First Law of Thermodynamics is a quantity well-preserved that cannot be consumed in the sense of destruction, but may be consumed in the sense of devaluation. It can be introduced by dividing a certain amount of energy by the following three parameters (Neves, 2019), viz.

- Exergy, sometimes called available energy or more precisely available work, is the part of the energy which can be arbitrarily used after a transfer operation or, in other words, its entropic counterpart;

- Vagueness, the corresponding energy values that may or may not have been transferred and consumed; and

- Anergy, that stands for an energetic potential that was not yet transferred and consumed, being therefore available, i.e., all of energy that is not Exergy.

These three terms refer to all possible energy operations as pure energy transmission and consumption practices. In order to make the process traceable, it is shown graphically. An example of the types of questions that are asked is the group of 6 (six) questions that make up the Collective Self-Esteem Questionnaire-Six-Item (CSEQ – 6) (Luhtanen, 1992)(Neves, 2019), viz.

Q1 – I am a worthy member of the social groups I belong to;

Q2 – Overall, my social groups are considered good by others;

Q3 – The social groups I belong to are an important reflection of who I am;

Q4 – I am a cooperative participant in the social groups I belong to;

Q5 – In general, others respect the social groups that I am a member of;

Q6 – In general, belonging to social groups is an important part of my self-image.

This questionnaire is designed to assess the workers' general feelings about their corporation, on the assumption that high collective self-esteem will cause positive outcomes and benefits. The scale used was made based upon these terms (Rosenberg, 1965)(Baumeister, 2003), viz.

strongly agree (4), agree (3), disagree (2), strongly disagree (1), disagree (2), agree (3), strongly agree (4)

Moreover, it is included a neutral term, *neither agree nor disagree*, which stands for *uncertain* or *vague*. The reason for the individual's answers is in relation to the query (Neves, 2019), viz.

On the other hand, as an individual, how much would you agree with each one of CSEQ – 6 referred to above?

Once the questions have been answered, the results can be summarized in structures like Table 2.4.1 and Figure 2.4.1. After multiple calculations we get results like those in Table 2.4.2. The input for Q1 means that he/she *strongly agrees (4)* but does not rule out that he/she will *agree (3)* in certain situations. The inputs are to be read from left to right, from *strongly agree (4)* to *strongly disagree (1)* (with increasing entropy), or from *strongly disagree (1)* to *strongly agree (4)* (with decreasing entropy), i.e., the markers on the axis correspond to any of the possible scale options, which may be used from bottom → top (from *strongly agree (4)* to *strongly disagree (1)*), indicating that the performance of the system decreases as entropy increases, or is used from top → bottom (from *strongly disagree (1)* to *strongly agree (4)*), indicating that the performance of the system increases as entropy decreases (Neves, 2019).

Table 2.4.1. *CSEQ – 6* single worker answer. (Neves, 2019)

Questions	*Scale*							
	(4)	(3)	(2)	(1)	(2)	(3)	(4)	*vagueness*
Q1	×	×						
Q2					×	×		
Q3					×		×	
Q4								×
Q5		×						
Q6						×		

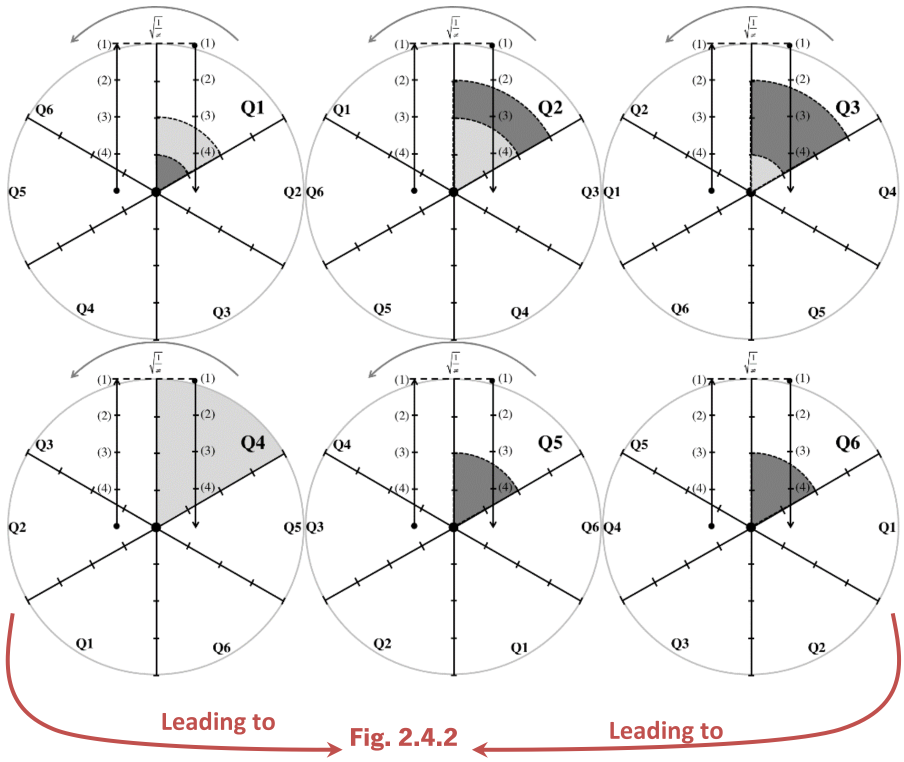

Figure 2.4.1. An assessment of the attained energy with respect to a single worker answer to *CSEQ-6*. (Neves, 2019)

Table 2.4.2. Best Case vs. Worst Case scenario calculations. (Neves, 2019)

Best Case Scenario	*Worst Case Scenario*
$exergy_{Q1} = \frac{1}{6}\pi r^2\Big]_0^{\frac{1}{4}\sqrt{\frac{1}{\pi}}} = \frac{1}{6}\pi\left(\frac{1}{4}\sqrt{\frac{1}{\pi}}\right)^2 - 0 = 0.01$	$exergy_{Q1} = \frac{1}{6}\pi r^2\Big]_0^{\frac{2}{4}\sqrt{\frac{1}{\pi}}} = 0.04$
$vagueness_{Q1} = \frac{1}{6}\pi r^2\Big]_{\frac{1}{4}\sqrt{\frac{1}{\pi}}}^{\frac{2}{4}\sqrt{\frac{1}{\pi}}} = 0.03$	$vagueness_{Q1} = \frac{1}{6}\pi r^2\Big]_{\frac{2}{4}\sqrt{\frac{1}{\pi}}}^{\frac{2}{4}\sqrt{\frac{1}{\pi}}} = 0$
$anergy_{Q1} = \frac{1}{6}\pi r^2\Big]_{\frac{1}{4}\sqrt{\frac{1}{\pi}}}^{\sqrt{\frac{1}{\pi}}} = 0.16$	$anergy_{Q1} = \frac{1}{6}\pi r^2\Big]_{\frac{2}{4}\sqrt{\frac{1}{\pi}}}^{\sqrt{\frac{1}{\pi}}} = 0.13$

Moreover, the concept of Organizational Efficiency (OE) is a complex theme, and so multiple other questions and calculations need to be performed, where in order to evaluate it, it is necessary to introduce a system analysis where technology, organizing methods and people interact in order to perform with the maximum efficiency. In this process, the inter-relational interactions between people have an important role in system performance (Haslam, 2004). For this purpose, it was necessary for us to look at principles that govern the Emotional development that underlies this process and particularly empathy, as a way to develop people involvement and participation in organizational challenges, all this supported by the dynamics of social relations. (Neves, 2019)

The social relations described in this Section support involvement and participation, and they denote a collective dimension. The former one is associated with the ability to include compromise and involve members of a particular group; the last one is linked with the ability to inform, to transmit, to communicate, and to share. The principles that govern this dimension that support the relationship between peers are associated with the phenomenon of Identity (Haslam, 2004)(Tajfel, 1981). It is the Identity that creates the common vision among people as members of a working group. This psychological process associated with Social Identity (Luhtanen, 1992)(Tajfel, 1981)(Tajfel, 1986)(Hogg, 1998) is in itself responsible for generating group behavior, in which solidarity among members and conformity to norms form the basis of behaviors and attitudes (Tajfel, 1981), and was addressed in ref. (Neves, 2019) in terms of the extensions of predicates Collective Self-Esteem (CSE), GRAtitude (GRA) and PROsocialness (PRO) (Neves, 2019).

This analysis of social relations is assessed in greater detail in Section 3.1, but the analysis made here points to the same major conclusion as that Section. Mainly that, the triplet of empathy-self-discipline-initiative is essential for assessing value-creation in a organization (Neves, 2019), and is in total agreement with the 3-axes perspective (Lori, 2019) of Section 3.1, as each of the axis corresponds to one of the three aspects of Leibnitz's causal approach (Chaitin, 2006) which have elsewhere been referred to as *Message-Alternative-Enablement* (Lori, 2010a) and *Eating-Choosing-Hunting* (Lori, 2019) (see Table 3.1.2 and Table 3.1.3). The clear connections between these two triplets are described in Section 3.2 and Section 4.2.

Moreover, by integrating all the different aspects of the assessment being done (Neves, 2019), we obtain a Mathematical Logic program that, through insights that are subject to formal proof (i.e., through the use of theorem proofs), allows us to understand and even adapt the actions and attitudes of individuals or groups, and hence make the organization adapt as a whole, viz.

Assessing Organizational Performance for the Worst-case Scenario

$$\neg\, cse(EX, VA, SP, QoI) \leftarrow not\ cse(EX, VA, SP, QoI),$$

$$not\ exception_{cse}(EX, VA, SP, QoI).$$

$$cse(0.47, 0, 0.88, 1).$$

$$\neg\, gra(EX, VA, SP, QoI) \leftarrow not\ gra(EX, VA, SP, QoI),$$

$$not\ exception_{gra}(EX, VA, SP, QoI).$$

$$gra(0.69,0,0.72,1).$$

$$\neg\, pro(EX, VA, SP, QoI) \leftarrow not\ pro(EX, VA, SP, QoI),$$

$$not\ exception_{pro}(EX, VA, SP, QoI).$$

$$pro(0.86,0,0.51,1).$$

Program 2. The make-up of the company's knowledge base for a single worker (Neves, 2019).

This is an evolutionary knowledge base that can be at the heart of symbolic Artificial Intelligence (AI). A knowledge-based system that decides how to act by running formal reasoning procedures over a body of explicitly represented knowledge. A system that is not programmed for specific tasks; rather, it is told what it needs to know and is expected to infer the rest. It showed how perceptions of Psychology, Management, CS and Mathematical Logic may be used to promote sustainable decisions and behaviors, i.e., a new interdisciplinary field of research and practice aimed at investigating and solving complex computer problems that are unique in scope, impact and complexity; and that exist in very dynamic and uncertain environments (see Section 4.2). An example of such an approach (Neves, 2019) is described in this Section, and its applicability to a diverse workforce is made clearer by what is described in Section 3.1.

Chapter 3

Computer Science's Future

3.1 Axiomatic formalization of human mental health

Key points:

- We provide here an axiomatic formalization of human mental health which because of its axiomatization is easier to harmonize with CS.
- This axiomatization helps integrate the consequences of Section 2.2 and Section 2.3 with the approach of Section 2.4, and it also supports the conclusions of Section 3.2.
- A major conclusion of this Section is that Information transport in the brain is likely to be key for the establishment of human mental health and thus Information representation is likely to be transferrable between the genetic and the mental levels, which helps justify some of the conclusions of Section 3.2.

In the last decade, a new perspective is being proposed of how the brain works, and thus how humans relate to their environment (Soon, 2008). This hypothesis (a.k.a, Predictive Processing Paradigm) sustains that the brain can respond appropriately to its environment by being able to anticipate the stimulation input coming from the environment, and in this Section we describe how this implies that the brain can recreate an emergent virtual scene which allows the brain to compensate for the stimuli processing time through the estimation of the environment's future events. In this paradigm, the brain generates its own version of the world by using a model of future events so that we can know where we are in real-time (e.g. the description by ref. (Andersen, 2011)). This approach thus proposes the human brain as being a statistical estimator of the appropriateness of a simulation, and so puts the human brain straight into a CS perspective. The Predictive Processing Paradigm approach to cognitive and computational Neuroscience has a long history and can be "more appropriately understood as the latest incarnation of an approach to perception and cognition initiated by Kant and refined by Helmholtz" (Swanson, 2016). (Lori, 2019)

The motor reactions to what is around a person occurs before the person's senses can appropriately locate the person in the environment (Brovelli, 2004). This neuronal "time-leap", allows a person to react with greater speed and control. Neuroscience has been able to locate brain areas very relevant to where this time-leap occurs, e.g. the posterior parietal cortex, and if decision-making occurs, then the pre-frontal cortex is also involved (Salazar, 2012). This time-leap has been experimentally observed not only in sensory processes, but also in self-perception processes, with the latter putting into question the very existence and meaning of conscious will (Wegner, 2002). According to Wolfang Prinz (Prinz, 1996), it seems as if the action-decision occurs before the conscious action-decision. If this is so, then the conscious decision cannot be the cause of the action, but rather the action will be based in sub-conscious processes. In Philosophy, free-will can be seen from different perspectives, but the root issue is that of Control (Stanford, 2010a)[1], and following that root issue we will focus in the more traditional way (Stanford, 2010a)[2] of defining free-will, where the existence of free-will assumes that the free-will is exerted by a free act of a self-conscious will (Stanford, 2010a)[3]. (Lori, 2019)

For this more traditional perspective of free-will, Dennett (Dennett, 2003) concluded that free-will does not exist, mostly because the large-scale of the human body makes the only relevant Physics being completely deterministic. But, by using Dennett's concept of structural-causality, and by changing the requirement of self-conscious will by that of a self-possessed will; it is possible to consider that the "existence of free-will" simply assumes that the will is an act which cannot be defined solely through the evolution of systems predating the organism having that will (Lori, 2009). This approach to the "existence of free-will" has the advantage that it implies that the "existence of free-will" becomes a measurable quantity, with the first calculations indicating that free-will exists (Lori, 2009). Moreover, free-will exists more strongly in humans than in other species (Lori, 2010a). (Lori, 2019)

[1] Free-Will is a "philosophical term of art for a particular sort of capacity of rational agents to choose a course of action from among various alternatives".
[2] " Many ... maintain the traditional view that the sort of freedom required for moral responsibility does indeed require that the agent could have acted differently".
[3] As Aristotle put it, ...'when the origin of the actions is in him, it is also up to him to do them or not to do them'.

3.1.1. Mental state objectivity using an axiomatic system

There has been a lot of work questioning the existence or non-existence of free-will (Stanford, 2010b)[4], and such work can be extended to fields in the border of what constitutes Philosophy (Dennett, 2003)(Lori, 2009)(Lori, 2010a)(Damasio, 2010), but the goal of this Section is not related to that specific search. The goal here is to analyze the role of Free-Will Perception (FWP) in the possibility of mental health. FWP is a term, defined elsewhere (Lori, 2019) and used here, as the perception of agency and self-ownership, in the sense that one perceives consciously the influence of one's own decision-making guiding one's conduct. The basis for the FWP definition is the definition of free-will used in Damasio's analysis of the relation between Spinoza and contemporary Neuroscience (Damasio, 2003). (Lori, 2019)

Some authors claim that FWP is a false perception, or delusional belief, because its conscious aspect turns out to be objectively false (Wegner, 2002)(Dennett, 2003); whereas others contend that FWP can be considered factually true-enough (Lori, 2009)(Lori, 2010a) as it only requires that conscious elaborations have an effect in decision-making, not necessarily an immediate or all-controlling effect in decision-making (Damasio, 2010). In short, Physics, Chemistry, and Neuroscience seem to indicate that FWP is a valid-enough perception of objective reality to not be dismissed as a fairy-tale. Thus, FWP can play a role in structuring mental health without the risk of its collapsing when confronted with objective reality (Lori, 2019). An issue we plan to address in this Section is if the FWP plays any role in structuring human mental health, and how important or significant that role might be in the possibility of objectively identifying mental health. Moreover, by using an axiomatic approach to represent mental processes, we are helping CS in its ability to represent mental processes, which would increase its capacity for achieving the goals outlined in Section 2.4.

The origin, structure, and function of the claustrum, a small bilateral structure of the brain, has been unclear since its discovery in the 17th century (Crick, 2005). With the contemporary use of dMRI it has been shown that the claustrum has the greatest connectivity per volume in the human brain (Torgerson, 2015), and a possible reason is that the claustrum is in the human Central Nervous System

[4] "philosophers have debated this question for over two millennia, and just about every major philosopher has had something to say about it".

(CNS) to serve as the gate-keeper for the Information flow necessary for self-consciousness or metacognitive processes. Recently (Reardon, 2017), it has been discovered an extremely large neuronal connection emanating from the claustrum. This is very important because the claustrum is a region of the brain which is very connected to brain areas that are associated to advanced integration of sensory patterns, for example in language. This very large neuron might thus play an important role in the existence of conscious thoughts (Crick, 2005). (Lori, 2019)

Before events occur, before reality reaches our senses, the brain is already generating a virtual environment allowing it to anticipate what is about to happen (Baars, 2002). The prediction of the future is a statistical guess, and it can at times make mistakes, a lot of magic is based on the predictable occurrence of such mistakes. The capacity to accurately predict the future favors environmental adaptation, because having to wait for the Information to arrive and be processed might sometimes take too long to avoid danger, and so “living in the future” is a very relevant survival-skill. This virtual scenery is coherent with the situational environment the person is in, but this process is not conscious (Dehaene, 2004), as in this case there is no access to the working-memory which is essential for conscious future-planning (Bennett, 2007). Associated to this anticipatory visualization there might be an anticipatory perception if the perceivable phenomenon is strong-enough to become conscious. (Lori, 2019)

Initially, the concept of social perception referred to the influence of cultural and social factors in perception, but more recently that term is starting to include the perception about other people, the recognition of emotions in others, and the perception the individual has about its physical and social environment, which includes the mechanisms of causal attribution (Arias, 2006). There have also been suggestions by Salazar (Salazar, 1986), and others, that the concept of social perception is not appropriate for describing all these social aspects of the interaction, but rather, that such concept is an incomplete and ambiguous description often referred to as social cognition. Thus, because of the difficulty in defining what social cognition entails, in this Section we will assess objective human mental health only at an individual level. (Lori, 2019)

In Mathematics, the structure of a mathematical language is obtained from an axiomatic system also used in CS (Chaitin, 2006), and which is constituted by these components: alphabet, grammar, axioms, rules of inference, and proof-checking algorithms. The CS approach (Neves, 2019) described in Section 2.4 is a formal approach, and so it has direct connections to the approach proposed here (Lori, 2019), but the approach of this section has the advantage of detailing all the different components of the axiomatic system; and this detailing will be very relevant for the description at the end of this Section of what constitutes objective human mental health. The axioms of an axiomatic system are complete if all the phrases expressed in the axiomatic system can be logically evaluated given the logical value of the axiomatic system's axioms; and the axioms of an axiomatic system are consistent if for no phrase can both the phrase and its negation be proved from the axioms. For non-trivial axiomatic systems, the Information-based approach to Gödel's incompleteness theorems obtains that an axiomatic system having a finite amount of Information cannot be both complete and consistent. (Chaitin, 2006) We consider here that the proof-checking in the input is the proof-checking from the output of a preceding axiomatic system inference process. (Lori, 2019)

In Psychology, there are multiple definitions of what feelings are, but in general feelings are understood as being in part a result of negotiating with our historical and cultural community (Gonçalves, 2000). This negotiating process puts feelings into a narrative order, of which our memory is a subjective selection that is strongly influenced by which narratives we consider to be more realistic. The narrative grammar structure used in Psychology is defined as being constituted by: setting, initiating event, internal response, goal, actions, outcome, and ending. (Gonçalves, 2000) The setting is a set of probability distributions for words constructed using symbols of a certain set of symbols. For the grammar to exist there must be a stored knowledge of the symbols and the frequencies of those symbols, the frequencies then being used as estimators of the probabilities. An axiomatic system therefore needs a storage device to work properly. In the somatic marker hypothesis (Damasio, 2000)(Damasio, 2003)(Damasio, 2010), the initiating event of a feeling is either an emotion occurring in the body, or a re-enacted memory of a past emotion. (Lori, 2019)

As described in previous paragraphs, the approach chosen here for mathematically representing narratives is by use of axiomatic systems. Let S be the set of symbols of the alphabet, and w represent a symbol-cluster/word, then a grammar, in a practical sense, is the joint set of: probability distribution of words $P[w]$; plus the probability distribution of words for each structure j, $P[w_j]$; plus the probability distribution of words for structure location j given that certain word l are occurring for other structure locations that are not j, $P[<l_{\sim j}\,/\,w_j>]$, which would be the probability a phrase makes sense; plus the joint probabilities of consecutive phrases $P[<l_{\sim j}\,/\,w_j>]$ & $P[<l_{\sim f}\,/\,w_f>]$ & $\cdots$, which would amount to the probability of a paragraph making sense; and so on. The components of the axiomatic system, and the here-proposed relation to the Psychology's narrative structure is described in Table 3.1.1. (Lori, 2019)

In Mathematics, the axioms are typically considered to be consistent rather than complete. Previously, it has been proposed (Lori, 2010b) that when the axioms are complete, rather than consistent, then the axiomatic system should be a Darwinian Axiomatic System (DAS). The axiomatic system where the axioms are consistent will be called Newtonian Axiomatic Systems (NAS) to distinguish them from DAS. In short, Formal Axiomatic Systems (FAS) can be either based on consistent or complete sets of axioms, in the first case they will be NAS and in the second they will be DAS. In the NAS, the rules of inference generate only one statement from the axioms, and the proof-checking algorithm verifies the compatibility of that statement with the axioms. In the DAS, the rules of inference generate multiple statements from the axioms, and the proof-checking algorithm verifies the validity of the statements by making those statements compete with other statements (both internal and external), with the consequent extinction of the loosing statements. In most of Mathematics, the axiomatic system used is the Zermelo–Fraenkel set theory with the axiom of Choice (Ciesielski, 1997), usually shortened to the ZFC set theory, the axioms of ZFC are consistent, and the nomenclature FAS is used for what we call here the NAS. (Lori, 2019)

To describe the difference between NAS and DAS in a form that directly relates to Information transmission in CS, and in a more general sense to Information transmission in other fields of science such as Neuroscience and Physics, it is best to first describe the ubiquitousness of central limit theorem conclusions. The outcome of the collective effect of random independent forces acting in fluid-state molecules is Brownian motion in which deterministic behavior is obtained by the constraining effects of the environment where the molecules move (Bar, 2013), and the creation of Brownian motion from random independent forces is valid even if we consider quantum effects (Zurek, 2007). Plus, Darwinian evolution displays a pattern that can be very similar to Brownian motion (Hallotschek, 2011), the major difference between Darwinian and Brownian dynamics being that for Brownian dynamics the molecules/species cannot be destroyed, whereas in Darwinian dynamics they can (Fischer, 2011)(Smerlak, 2016).

Table 3.1.1. Structure of Information-based axiomatic system, and its relation to Psychology. (Lori, 2019)

Axiomatic System	**Psychology's Narrative**
Alphabet(S) + Grammar($P[w], P[w_j], P[<l_{\sim j} \mid w_j>], \ldots$)	Setting
Proof-checking algorithm input (internal vs. external)	Initiating event
Axioms (consistent vs. complete)	Internal response
Rules of inference (single-alternative vs. multi-alternatives)	Goal + Actions
Inferred statements	Outcome
Proof-checking algorithm output (internal vs. external)	Ending

Hence, Darwinian evolution is like Brownian motion because of all the "random" effects occurring to the species as it moves throughout its life, but while the friction aspect of Brownian motion simply makes molecules tend to have the velocity typical for gases/liquids at that temperature, the friction in Darwinian evolution makes species only continue existing up to what the environment around them can support. This implies that Brownian motion is an egalitarian stochastic process as all molecules have the same infinite survival capacity and eventually all molecules pass through the same situations, whereas Darwinian evolution is a non-egalitarian stochastic process where all species have finite and non-equal survival capacities.

The Brownian motion is deterministic for the characteristics of the system for which the central limit theorem makes it so (Bar, 2013), but that is not the case for Darwinian evolution because species extinction and sexual procreation destroy the independent identically distributed (i.i.d.) characteristic that is required for the central limit theorem to be valid (Rouzine, 2003). The link between Brownian motion and Darwinian dynamics has also been described in both Economics (Beinhocker, 2006) and Neuroscience (Montague, 2002), which allows for a link between this Section and both Section 2.4 and Section 2.3, respectively. (Lori, 2019)

The Darwinian dynamics are only partially predictable, being the predictable part the shape of the fitness Probability Distribution Function (PDF) as defined by the fitness of the most recent species (Smerlak, 2016). Looking at the fitness PDF as an index of validity, it is possible to relate NAS and DAS respectively with Brownian and Darwinian processes. The NAS is related to a stochastic process where fitness is identical for all elements, as it occurs in isotropic random walks; whereas DAS is like a Darwinian evolution, since validity is not identical for all axioms. The Brownian motion with unequal and molecule-destroying boundary conditions is the intermediary stage between Physics and Biology (Nowak, 2008)(Lori, 2010c). If isotropic random walks are considered, then there is no specialization, but for anisotropic random walks there can be specialization based on boundary conditions; so much so, that in extreme conditions the boundary conditions can allow for objective randomness to occur in axiomatic systems. (Lori, 2010a)(Lori, 2019) Moreover, the axiom-driven CS is similar to Physics whereas the environment-driven CS, e.g. DL, is similar to Biology, hence allowing CS to play an important role in integrating Physics, Biology, and Economics; as is described in Section 4.2.

The independence from the past as perceived by a system of representations is associated to the characteristics of that system, and this quality is what allows that system to be considered as having free-will (Lori, 2009). As we are searching for an axiomatic approach compatible with free-will (Lori, 2010a), the approach followed here is to use the same axioms as those used to prove the existence of objective randomness in QD, and which we then extend so as to be applicable to other situations. (Lori, 2010a). By doing so, we will start from an axiomatic system that is compatible with objective randomness, hence it is compatible with independence from the past, and thus by the same token it is compatible with free-will as its independence from the past allows for the most free-will (Lori, 2011) that can coexist with the known laws of nature. Those random-causality axioms are equivalent to the QD axioms in P. 18 of Section 2.1 and are as follows (Lori, 2019):

o. The considered universe consists of systems individually accessible to measurements.

i. The state of a system is represented by a vector in a multidimensional vector space with inner product, and in that vector space any vector infinitesimally close to a vector of that vector space will also belong to that vector space.

ii. The alteration of state vectors is such that the inner product between state vectors is preserved.

iii. If the environment remains unchanged, then the outcome obtained by the axioms remains unchanged.

The relation of the *o-iii* random-causality axioms above to the Darwinian evolution of species can be established using the relations (Lori, 2019):

o. Means that for any species, their fitness to the environment can be known by interacting the species with a large enough range of environments.

i. Means that for any two species with different fitness it is possible to conceive of a species with intermediate fitness.

ii. Means that evolution in time preserves the fitness amplitude norm.

iii. Means that if the environment is unchanged, then the fitness remains the same.

The relation of the *o-iii* random-causality axioms above with the structure of axiomatic systems described in Table 3.1.1 can be done using the relations (Lori, 2019):

o. Is like an alphabet definition for an axiomatic system.

i. Is like a grammar definition.

ii. Is like the rules of inference.

iii. Is like a proof-checking device.

It is widely accepted that neurons (or at least small ensembles of about 200 neurons) represent negative-minimum PDFs (Knill, 2004)(Anderson, 1994); it is thus not a problem for neuronal ensembles to represent grammars, axioms, and the other aspects of axiomatic systems. Using the Weyl-Wigner transforms (Weyl, 1927), it is possible to transform any PDF into a density matrix, which can then always be represented by a vector state with complex numbers as elements. So, mathematically, a PDF is a complex vector state. Thus, any negative-minimum PDF can be represented as a complex vector state. A vector state is different from a vector in the sense that a system's vector state is the full describer of that system. The velocity of a car is a vector associated to a car but is not the vector state of the car, as the velocity does not fully describe the car. For example, the velocity does not provide the color of the car. It is thus possible to consider that the state of a Topological Representation zone (a.k.a. association areas (Damasio, 2003)) is described by a complex vector state, with each component of that vector state associated to a certain element of a basis state. A Topological Representation consists in a representation that is invariant over an object's continuous deformations, by continuous transformations meaning in our case not only mathematical transformations such as translation, rotation, stretching, crumpling and bending, but also sensory transformations such as changes of color, sound, and smell (each to a certain extent). (Lori, 2019)

The random-causality axiom *o* establishes the existence of systems. Let us consider system ***S*** surrounded by a set of systems that surrounds ***S*** and that we call ***E***. Henceforth, ***S*** will be called "system" and ***E*** will be called "environment". As an example, it is possible to consider that a Topological Representation zone is the system ***S*** and that the other Topological Representation zones are the environment ***E***. Any considered universe can therefore be represented as "***S*** coexisting-with ***E***", meaning the combined occurrence of the system ***S*** and the environment ***E***. The random-causality axiom *i* establishes that both the system and the environment are represented by vectors in a multi-dimensional vector space and that such vector space has an inner product and contains all (finite and infinite) linear combinations of its vectors. Due to random-causality axioms *o* and *i*, the state of the system can be represented by a vector state $\vec{S}$ defined as the linear superposition of vectors of the system **S**, where the scalars in the linear superposition that multiply the vectors are complex numbers; whereas the state of the environment can be represented by a vector state $\vec{E}$ defined as the linear superposition of vectors of the environment ***E***. The complex numbers, such as $z = |z|e^{j\theta}$, are a combination of an amplitude $|z|$ (a positive real number) with a phase θ (a real number), with *j* the imaginary unit and *e=2.718281...* being the Euler number. (Lori, 2019)

Let's assume that a time evolution satisfying random-causality axiom *ii* can be defined. Then, for the time evolution of system ***S*** and environment ***E***, a sharp and deterministic evolution obeying random-causality axioms *o-iii* is almost impossible to find, except for situations where the force between the system ***S*** components is either independent or linearly dependent on the "distance" separating the states of the system ***S*** components (Klein, 2012), for when the force fails to obey these very sharp conditions, then the sharp deterministic evolutions only occur for durations shorter than a knowable amount (Lori, 2009). When not in these extraordinary circumstances, what is obtained, instead of sharp deterministic evolutions, are classical statistical dynamics which can often be approximated by a Brownian motion description (Lori, 2011). Thus, what are almost never obtained are the sharp deterministic evolutions assumed by Newton Physics. The form of the Hodgkin-Huxley equations (Hodgkin, 1952), describing the membrane potential in a neuron, has forces that are either independent or linearly dependent on the "distance" separating the states of the system, with time being proportional to the imaginary unit *i*. Thus, it is not surprising that this equation can represent a sharp action potential at the neuronal membrane moving deterministically along an axon. Whereas, in other models, such as the Galves-Löcherbach (Galves, 2013) model which takes the dendritic trees into account, the forces are neither independent nor linearly dependent on the "distance" separating the states of the system, and so sharp determinism is no longer to be expected, which agrees with the Galves-Löcherbach model being a stochastic model and not a sharp deterministic model (Galves, 2013). (Lori, 2019)

The successful transmission of Information is the printing of the Information about the system in the environment states. The vector states, prior to the choice of a system state occurring by the interaction with the environment, have a certain ontic aspect to them, as the vector states are all that the system is before the measurement (meaning that they are all that can be said about the system); and the vector states of the system after the measurement have a certain epistemic aspect to them, as the system does not completely adopt an objective existence, but only does so in as much as it is capable of leaving imprints about itself in the environment. These vector states can therefore be called *epiontic* (Zurek, 2007). (Lori, 2019)

3.1.2. Mental state free-will using an axiomatic system

In Table 3.1.1, the grammars are described by PDFs, and the axioms are subsets of the set of all possibly valid grammar statements. As noted in previous paragraphs, it is possible for neuronal ensembles to represent PDFs, and thus it is also possible for neuronal ensembles to represent grammars, axioms, and the other aspects of axiomatic systems. To relate Consciousness Types 0-1-2 (Shea, 2016)(Kahneman, 2011) with vector states, it is helpful to search for an axiomatic and thus computational, yet simple, representation of what the different Consciousness Types relate to. We propose that conscious narratives are correctly described using Psychology's narrative structure, and that the relation of such structure to the axiomatic systems is as presented in Table 3.1.1. (Lori, 2019)

In Fig. 3.1.1, it is proposed that Darwinian extinction can be associated to Consciousness Type 2 processes, and that Darwinian extinctions can be associated to DAS. The relation between Consciousness Types and axiomatic processes is for us, the structure represented in Fig. 3.1.1. There is a major difference between Fig. 3.1.1 and Table 3.1.1, in that a new Translation aspect in introduced. The reason for its non-inclusion in Table 3.1.1 is that in there it is assumed that the Translation is unique and universal, whereas in this Thesis we propose that a key characteristic of the different Types of Consciousness is that they use different types of Translations. In Fig. 3.1.1, the Translation location is represented by a filled-circle. The Translation is different for each of the Types of Consciousness. For the Type 0 the Translation is one-to-one, meaning that for each of the group of Axioms there corresponds a unique Rule of Inference. For the Type 1, the Translation filters the group of Axioms into a single Rule of Inference, thus the Translation is multiple-to-one. For the Type 2, the Translation filters multiple Grammars into multiple groups of Axioms, thus the Translation is multiple-to-multiple. (Lori, 2019)

For a decision to be felt as free, meaning a FWP is associated to that decision, there must be at least two different ways a neuronal system could be perceived as being able to go from the immediate past to the present, and those two different ways must be swappable in the sense that they can be inter-changed without needing to change anything in the infinite past (as much as can be perceived by the neuronal ensemble). It has been obtained by neuron modeling (Montague, 2002) that a successful outcome prediction in a neuron (or small ensemble of neurons) improves the access to nutrients of the neuron, therefore increasing the "state of pleasure of the neuron" (Damasio, 2000)(Damasio, 2003)(Damasio, 2010). Thus, the continuing survival of the neuron requires the successful broadcasting of the validity of the neuron's predictions. The ontic/existence of the neuron thus requires the success obtained by its epistemic/broadcasting aspect, meaning that the requirements for the neuron's survival are epiontic. (Lori, 2019)

There are also strong indications that neuronal dynamics are themselves Darwinian (Edelman, 1987). For example, the motor nerve cells' neurons struggle to control the muscle occurs by sending out multiple-branched fingers called axons; these branches contact many muscle fibers, which are also in contact with axons from other nerve cells, and these different nerve endings have synaptic activities that drive the "synaptic rearrangement in the vertebrate nervous system; indeed, this appears to be a main way in which experience shapes neural connectivity" (Buffelli, 2003). In short, branches from different nerve cells compete, until one of them wins and starves out the other branches. Thus, the neuronal dynamics can be represented accurately as DAS, and the transaction between conscious states and unconscious states can be perceived, from a neuronal perspective, as being objectively free if the conditions for uncaused axiomatic evolution are met. Based on this Section's random-causality axioms *o-iii* for the uncaused axiomatic evolution, and because neuronal ensembles agree with those random-causality axioms *o-iii*, from the perspective of the neuronal ensemble the access to conscious decision-making appears as an act of objectively free will, a FWP. (Lori, 2019)

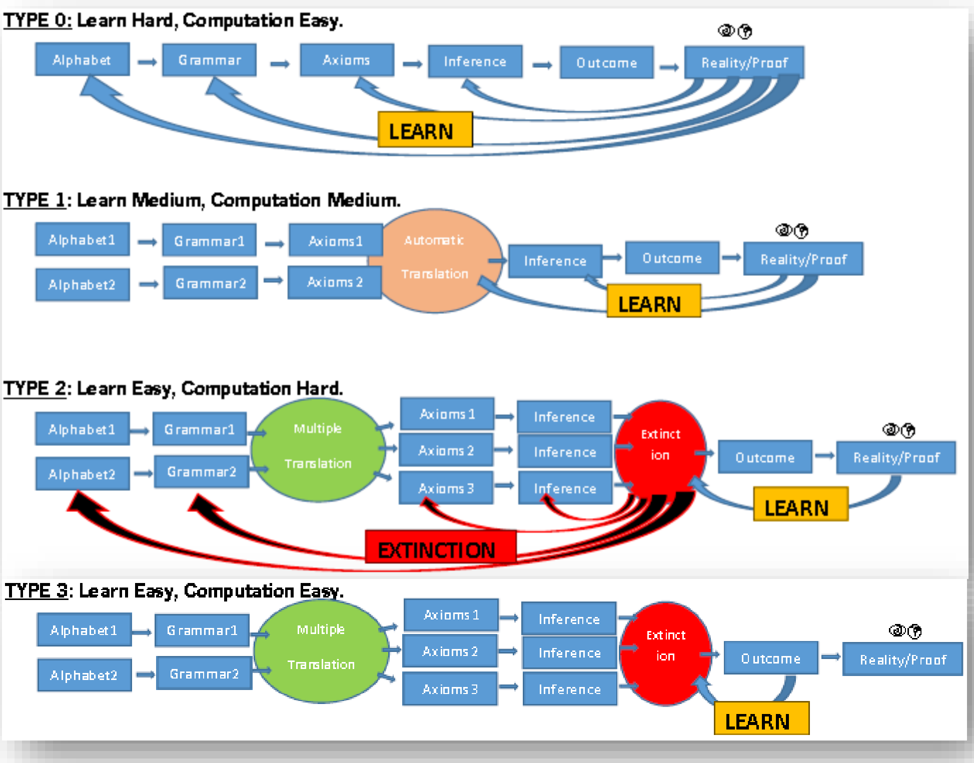

Figure 3.1.1. Relation between the axiomatic system from Alphabet to Output, and the extra structure of the connection relating the Information-based axiomatic system to the Consciousness Types 0-1-2 described in refs. (Shea, 2016)(Kahneman, 2011) and Consciousness Type 3 proposed in ref. (Lori, 2019).

In contemporary Neuroscience there are two well-known models of how Consciousness arises in biological entities, the Global Workspace (Dehaene, 2011) theory and the Information Integration (Tononi, 2016) theory. The Global Workspace theory proposes that the activation/ignition of the Global Workspace is the neuronal correlate of Consciousness, in this theory the different sensory stimuli compete for the activation/ignition of the Global Workspace. The ignition occurs at the frontal-parietal cortex when stimuli are strong enough for a sustained period, where, by strong enough it is meant that the addition of the stimuli across time reaches a certain threshold (the Global Workspace theory threshold). The Information Integration theory proposes that the maximization of Information Integration is the neuronal correlate of consciousness (here understood as the perceived apparent self-consciousness), but this theory could not compute where and when such maximization occurs. Recently, it was obtained that the two theories of Consciousness predict barely distinguishable results (Tagliazucchi, 2016), thus being essentially the same theory or simplifications of a more global theory that encompasses both theories. (Lori, 2019)

In the epiontic Consciousness theory proposed here, the *epiontic* nature of a system described by the random-causality axioms *o-iii* obtains state extinction from the maximization of the Information dissemination, plus, the implication that during the extinction transition the amplitude of the complex variable representing the relation between the neuronal ensemble and its environment needs to remain unchanged, which agrees with recent experimental data that the transition between unconscious and conscious states is represented simply by a phase (Haimovici, 2016). Thus, this theory explains the existence of a phase-only *envariance-like* relation between the neuronal ensemble systems, systems which hence can gain access to conscious states; and also the existence of neuronal ensemble environments which help/creates/enhances the preservation of the vector state representing the conscious decision. This envariance-like relation explained by this theory also helps/creates/enhances the corresponding extinction of the vector states representing the unconscious decisions. (Lori, 2019)

Because the random-causality axioms *o-iii* are valid for neuronal ensembles, it is thus possible for Darwinian processes in neuronal dynamics to eliminate alternative neuronal paths simply by the enforcement of the axioms *o-iii*, and so a corollary of this analysis is that the time-evolution of a conscious (hence a Consciousness Type 2 process) would be only phase-dependent. A counter-argument might be that in a different research (Eyherabide, 2009) it was possible to relate neuronal activity with effective transmission of Information about the system being represented, and it was obtained that the phase was not important for such a transmission but only the amount of action potentials in each packet and the temporal start of the packet mattered (Eyherabide, 2009). But this result was obtained for grasshoppers, a very Type 0 process animal, and so it has no implications for our result. Moreover, recent work has obtained that in processes associated to Consciousness, only the phase matters (Schurger, 2015). Thus, although going from Type 1 to Type 2 is a quantitative alteration, the Darwinian extinction is a quantitative alteration that very quickly becomes a winner-takes-all qualitative transition, and then Consciousness arises, as appearing to be un-caused to the Consciousness of the individual feeling it. (Lori, 2019)

A possible extension of the three Consciousness types 0-1-2 (Shea, 2016)(Kahneman 2011), would be a fourth type (Shea, 2016), Type 3. The Type 3 Consciousness was considered in the literature to be possible to exist, but extremely rare (Shea, 2016); whereas we propose here that it is associated to high level meditation/religious/contemplative states, which are known to be extremely hard to achieve, and so extremely rare in agreement with ref. (Shea, 2016). In the 4-state Logic more commonly used in Buddhism (Panikkar, 1989), not only an object can be negated, but also the "is" of that object can be negated by a NOT. But the denying of the "is" can, in our opinion, be best described as the denying of the entity which the "is" characterizes, a description of the 4-state Logic using Mind and Sensations can thus be (Lori, 2019):

a) NOT-Mind is NOT-Sensations (Type 0)
b) NOT-Mind is Sensations (Type1)
c) Mind is Sensations (Type 2)
d) Mind is NOT-Sensations (Type 3)

The Type 3 Consciousness bypasses both the use of external sensory data and the use of emotions-based self-appreciation relying on choices previously taken. Thus, Type 3 Consciousness rejects both the internal and the external extinction processes. The removal of the extinction processes neutralizes a great amount of neuronally-induced suffering associated to the requirements of eliminating many alphabet-to-outcome connections, and it bypasses the worldly imperfections by bypassing the need for external/societal confirmation through Reality/Proof. The Type 3 consciousness focusses on eliminating suffering by eliminating (or strongly reducing) the extinction process itself, thus obtaining high levels of happiness at the expense of the neglecting of one's capacity for choosing and for being realistic. The Type 3 of Consciousness can thus be a source of happiness and internal freedom, but also of great neglect and great cruelty; thus, accounting for both the positive and the negative characteristics of high-level spirituality. (Lori, 2019)

Joining the Consciousness types 0-1-2-3, it is possible to clarify the different types of Mind and Sensations that occur in the different types of Consciousness. A Sensation is a feed-forward translation into inferences which can have a contribution from Extinction processes if negative feelings are allowed; and cannot have negative feelings allowed if Extinction processes are not allowed. The Sensation is a Flow sensation if the Translation is immediately after the Axioms and there are no Extinction processes, and it is a Feel Sensation if the Translation occurs immediately before the Axioms and there is an Extinction process occurring immediately after the Inferences.

In the lack of negative feelings, one would feel a flow-like Sensation where one feels that all is going to turn-out fine. A Mind is a loop involving: Learning, Extinction, and Outcome. If Reality is allowed into the loop, we call it an Outer-world Mind loop, and if it does not, we call it an Inner-World Mind Loop. The types of Mind-less Learning are the Ground-based learning identical to Type 0 consciousness, and the Automatism Learning is the Learn of the appropriate Inference and the multiple-to-one Translation between axioms and Rule of Inference (see Fig. 3.1.1). The relation between the Types of Consciousness presented in Fig 3.1.1 and Fig. 3.1.2, together with the use of 4-state Logic (Panikkar, 1989) allows for the obtaining of a simple relation between Types of Consciousness and Sensations/Mind/Learning blocks (Lori, 2019):

a) Type 0 = Learn "Ground-Learning"
b) Type 1 = {Learn "Automatism"} + {Flow Sensation}
c) Type 2 = {Learn "Feel Sensation"} + {Outer-world Mind loop}
d) Type 3 = {"Feel Sensation"} + {Inner-world Mind loop}

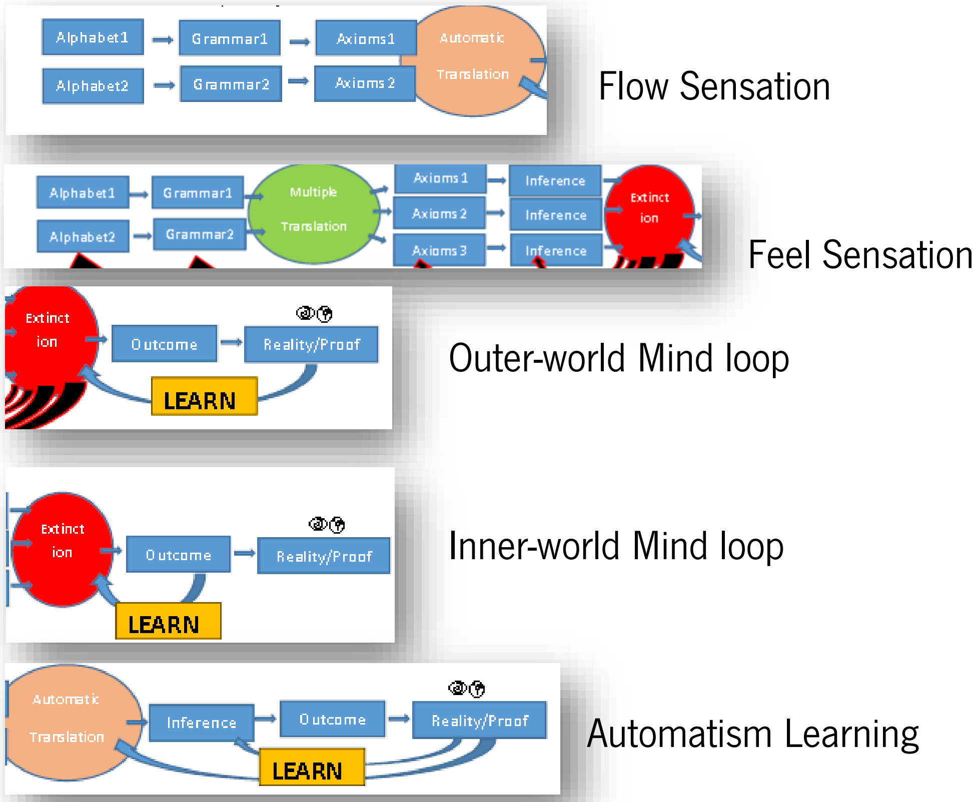

Fig. 3.1.2. Relation between axiomatic system (from Alphabet to Output), and the structure of the connection relating Information-based axiomatic system to Consciousness Type. (Lori, 2019)

3.1.3. Integrating objectivity and free-will using 3-axes approach

The development of the capacity to be self-conscious about one's future requires the development of abstract sceneries, and the capacity to decide the best option between different sceneries, the FWP is a person's own measurement of how much control one has over the choice being made between sceneries. Like many other human features, the FWP has grown throughout Darwinian evolution, and we will provide a small description of how we obtained that that evolution has three axes and that one of the axes is associated to the FWP. There are 3 aspects by which axiomatic systems can vary in a continuous (or discrete multi-valued) way between different options (see Table 3.1.1): 1) internal vs. external, 2) "complete+multi-alternatives" vs "consistent+single-alternative"; 3) "output-based proof-checking" vs. "input-based proof-checking". Those 3 options constitute a 3-axes system, which respectively can be called: space-axis, alternative-axis, and time-axis. The location relative to each of the three axes defines the structure of the axiomatic structure performance, by augmenting or diminishing the influence of certain aspects of the axiomatic structure. These three axes influence the psychological narrative similarly to the role feelings play in that same narrative; we will thus propose that these three axes are feeling prototypes. In other words, they are the aspects of the axiomatic system that will correspond to feelings in the brain. (Lori, 2019)

Human feelings have been associated to the body axes (Damasio, 2003)(Damasio, 2010), and the difference between the social decision-making approaches that are Kant-like (meaning here maxims-based) (Greene, 2004)) and those that are Hume-like (meaning here utilitarian-based) (Greene, 2004) have been associated to middle-lateral brain axis in ref. (Greene, 2004), plus the structure of the neuronal long-range connections (meaning the brain's white matter (WM)) has been associated to the three brain axes (Wedeen, 2012). Moreover, the supra-marginal gyrus is where mirror neurons exert the strongest influence by using the integration of somatosensory, visual, and auditory Information (Carlson, 2012). Plus, the angular gyrus is located superiorly and is associated with language, number processing, and spatial cognition, together with memory retrieval, attention, and theory of mind (Seghier, 2012); and it is known that theory of mind is strongly associated to self-consciousness (Frith, 1999).

The relation between body/brain axes and axiomatic systems has until recently (Lori, 2019) been foreign to Mathematics and CS, but it is relevant for the establishment of a link between axiomatic structures and human feelings. A relation between body axes, brain axes, and functional characteristics has been confirmed and/or assumed throughout the Neuroscience literature (Wedeen, 2012), and we describe a summary of such relations below (Lori, 2019) and in Fig. 3.1.3:

Axis1} ventral-center-dorsal axis ⇔ Inside→Outside

Axis2} left-center-right axis ⇔ Tone→Word

Axis3} posterior-center-anterior axis ⇔ Now→Then

The brain function locations and hemispheric preferences described above should not be considered as absolute, but rather as an assistant to the axiomatic structure representation of human decision-making. As can be seen in Fig. 3.1.1, the sum of the three axes above also provides an association that is mostly in agreement with the Neuroscience-known relation between brain function and brain area (see Fig. 3.1.3). We also use the evolution of the body and brain axes to relate the body axes, the brain axes, the axiomatic axes, the animal action-types, and the axiomatic aspects (see Fig. 3.1.2). (Lori, 2019)

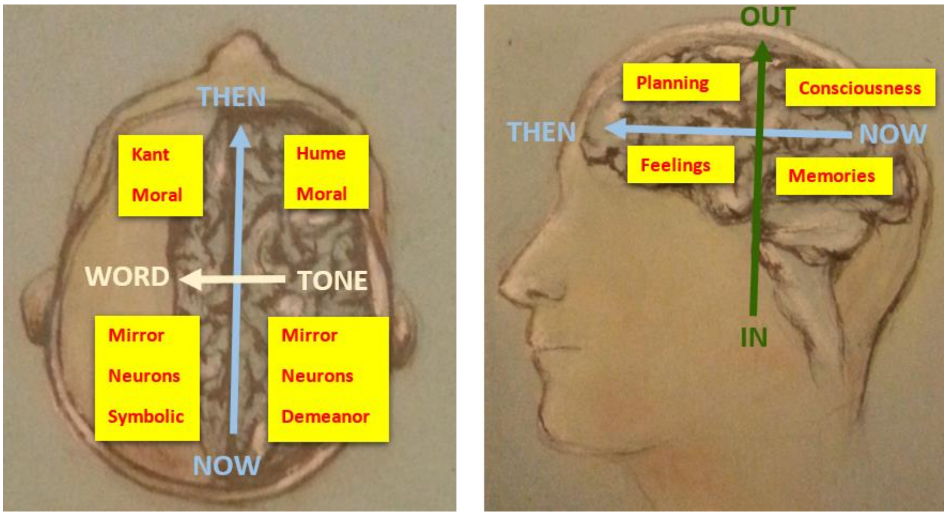

Figure 3.1.3. Simplified relation between brain 3-axes approach and brain function. On the left is a view from above (® Sandra Lori), and on the right a view from the left side (® Sandra Lori).

The first animals (meaning here structured multi-cellular organism) are believed to have been either a sponge (635 million years ago) or a comb jelly, but in any case, something sphere-like with a topology of simply "inside vs. outside" [1st animal evolution]. About 600 million years ago, before the Cambrian period, the arthropods started appearing and thus defined a medial-lateral axis of movement (with eyes eventually developing on each of the sides), thus assuming a flat disk-like shape with a "left-right" choosing axis [2nd animal evolution]. Around 550 million years ago the first predators appear as indicated by their predation marks, likely the flat worms. The need for hunting requires not only a choosing orientation but also a matching of the space and time concepts into the concept of trajectories.

Thus, animals developed the concept of time and adopted an arrow-like anterior-posterior axis marking its desired trajectory [3rd animal evolution]. The first gut that appeared remained mostly unchanged since the appearance of the Eukaryotes about 1700 million years ago [1st neuronal evolution], until when, about 800 million years ago a part of the gut started evolving, to then become a heart about 542 million years ago [2nd neuronal evolution]. The appearance of the brain occurred about 500 million years ago [3rd neuronal evolution]. The brain itself had three stages of evolution; the original hindbrain [1st brain evolution] gained a limbic system about 250 million years ago [2nd brain evolution], and then the cerebrum appeared about 200 million years ago [3rd brain evolution]. The relation between axiomatic system aspects, and body/brain development axes is proposed in Table 3.1.2 and Fig. 3.1.3.

The three different types of evolution and representation presented in Fig. 3.1.2 are justified using different types of arguments (e.g. mathematical, computational, neuroscientific, evolutionary), but for a more rigorous basis for the 3-aspects it is necessary to define an axiomatic representation general enough to account for all the phenomena described in Fig. 3.1.2., but with axiomatic expressions simple-enough to be able to be included in common speech. A major function of the brain is to execute Economics-like (Beinhocker, 2006) forecasts of costs and benefits using Bayesian inference rules (Anderson, 1994)(Montague, 2002)(Knill, 2004). For example, if a single form of neurotransmitter is postulated, then the corresponding economical system can reach a state of economical equilibrium (Montague, 2002). Moreover, it has been described how economical systems behave like Information-driven Darwinian systems (Beinhocker, 2006). In Section 4.2, a brief description is made about the importance of value attribution in the development of CS's future, and in that description Kant's perspective will again be relevant, and it will play the same role as in Fig. 3.1.3, which thus creates further evidence of this Thesis' self-consistency. (Lori, 2019)

Historically, in Psychology, there are only two major axes, the Eros and the Thanatos axes. The Eros is associated to the desire for pleasure, which can also be described as a "will to Pleasure" (Freud, 1990); and the Thanatos with the desire for conquest, which can also be described as a "will to Power" (Adler, 1927). Whereas, there were actually three Psychotherapy schools of Vienna, which left one of those schools, corresponding to a "will to Meaning" (Frankl, 2006), without an axis. We propose in Fig. 3.1.3. (Lori, 2019) and elsewhere in this Section, a 3-axes system, hence, to define a better connection between the approach proposed (Lori, 2019) in this Section and Psychology, it is preferable to propose a Choosing/free-will axis for Psychology. We proposed for that axis (Lori, 2019) the name of the Greek goddess of prosperity and randomness: Tyche. The 3-axes of Psychology thus becoming: Eros-Tyche-Thanatos. This 3-axes proposal is relevant, as since the proposal of the "will to Meaning", the mental health in Psychotherapy has been defined as a balance between these three axes of will, and this Section agrees with that. Moreover, as it will be described in Section 4.2.2, the use of the word "will" in defining the 3-axes of Psychology is not an accident, as the will is a key aspect of Schiller's attribution of objectiveness to Beauty (Moland, 2017), which in Section 4.2.2. is used to analyze the possibility of attributing an objectiveness to value, a key necessity for the validity of the CS approach (Neves, 2019) described in Section 2.4.

Table 3.1.2. Comparison of the axiomatic axes system with other axes systems. (Lori, 2019)

Animal Step	Evolution Novelty	Brain Axes	Body Axes	Action Type	Axiomatic Aspects	Psychiatry Disorder	Psychology Axes	Will Type
1st	Space	ventral-dorsal	inner vs. outer	Eating	Internal-External	Eat/Sleep	Eros	Pleasure
2nd	Alternative	middle-lateral	left vs. right	Choosin g	Complete-Consistent	Mood	Tyche	Meaning
3rd	Time	anterior-posterior	soon vs. late	Hunting	Input-Output	Anxiety	Thanatos	Power

For the Tyche feelings to be associated to an objective reality, it is needed that free-will in a certain objective sense exists. Thus, for Tyche feelings to be associable to objective reality, it must be possible to represent objective arbitrariness by using axiomatic systems. That is not an easy task, as axiomatic systems have been built to avoid arbitrariness through maintaining the logic validity of the axioms assumed to be valid. It has been proposed that independence of the present state of a system from the past located outside the system is necessary (Lori, 2009) and sufficient in realistic neuronal systems (Lori, 2010a) for the existence of free-will in those systems in a form that is compatible with the existent knowledge of the laws of nature. Thus, the Tyche feelings based on a FWP (see Table 3.1.3) do not contradict Reality. (Lori, 2019)

The number of different feelings considered in Damasio's model of feelings (Damasio, 2003) is quite thorough, thus, we will use both the grouping of feelings (Damasio, 2010) and Damasio's self-model perspective (Damasio, 2003), with some minor alterations. The feelings are the mind representations of present and past emotions, but in this work, the feeling and emotion terms will be used interchangeably. The feelings are divided by Damasio into three types (Damasio, 2003) and into four groups (Damasio, 2003). The three Damasio types of feelings are: Background emotions, Primary emotions and Social emotions. The four Damasio groups of feelings are constituted by four parts: Definer Emotion, Emotional-Competent-Stimulus (ECS), Consequences and Basis Emotions. Using the four Damasio groups (Damasio, 2003), we obtain the division below (Lori, 2019).

Group 1: Definer→ embarrassment, shame, guilt; ECS→ violations in personal space/purity; Consequences→ prevent continued aggression by others; Basis→ fear, submission.

Group 2: Definer→ contempt, indignation; ECS→ violation of cooperation/purity; Consequences→ enforcement of social norms by violation punishment; Basis→ disgust, anger.

Group 3: Definer→ sympathy, compassion; ECS→ another person in suffering/need; Consequences→ restoration of harmony in group; Basis→ attachment, sadness.

Group 4: Definer→ awe/wonder; elevation, gratitude, pride; ECS→ recognition in self/others of contribution to cooperation; Consequences→ reinforcement of cooperation; Basis→ happiness.

Using both the three types and the four groups, it is possible to use the success vs. frustration of the Eros-Tyche-Thanatos desires for the construction of Table 3.1.3, which includes all Background, Primary, and Social emotions. The two forms of separating the emotions, by types and/or by groups, has many coincident emotions. Nevertheless, there are four emotions (surprise, jealousy, envy, admiration) in the types, which are not mentioned in the groups; and four emotions (embarrassment, attachment, compassion, submissive) in the groups, which do not occur in the types. The surprise and embarrassment emotions can be considered to represent the same emotion, as can jealousy and attachment, and also sympathy and compassion, plus also envy and jealousy. Moreover, the feeling of admiration towards someone is very connected to feeling submissive towards that person. Thus, there is an agreement between the two forms of separating the emotions, that is, between separating by types and separating by groups. (Lori, 2019)

We will use the Groups 1-2-3 as representing emotions associated to, respectively, difficulties in: Eating, Hunting and Choosing, respectively. Whereas the fourth group is associated to the non-existence of those difficulties/frustrations, and thus a sense of balance for which we propose the use of the Greek word for Reason: Logos. The sadness emotion appears as a Basis emotion in both Groups 1 and 3, hence we consider that the association to the Group 1 is the most appropriate as sadness typically causes feelings of shame and guilt. We propose that although there is an Eating-Choosing-Hunting succession in Darwinian evolution, the satisfying occurrence of the positive feelings requires all three simultaneously. (Lori, 2009)

Damasio's levels of Consciousness (Damasio, 2003) are only explicitly differentiated up to the Extended Consciousness level (Damasio, 2003), and no further. In a previous work, some of us proposed (Lori, 2010a) that it is useful to divide the Extended Consciousness between three components: Personal-Consciousness based on one's memory about one's life, Historical-Consciousness about one's perceived interaction with the culture one feels to be a part of, and Universal-Consciousness about one's perceived interaction with the whole universe. Although a person is typically feeling as an "individual", what that individual-ness means depends on the level of Consciousness. At the Proto-self level are the Background emotions, at the Core Consciousness level are the Primary emotions, at the Personal Consciousness level are both the Primary and Social emotions, whereas at all upper Consciousness levels there are only Social emotions. The neuronal correlates of the highest Consciousness level (the Universal-Consciousness) are proposed here to be the sub-sections of the anatomical regions attributed to Extended Consciousness by Damasio, the more anterior portion of the temporal cortex (Grabowski, 2003), and the more anterior portions of the pre-frontal cortex (Bechara, 2005)(D'Argembeau, 2008). Whereas, Historical-Consciousness level areas are located between the Personal-Consciousness, and the Universal-Consciousness areas (see Table 3.1.3). (Lori, 2019)

Table 3.1.3. Relationship between the Eating-Choosing-Hunting axes, and feelings. (Lori, 2019)

Consciousness level ↓	**Frustration →** **Axis →** **Disorder →**	**Eating [1st Step]** **EROS [Group 2]** **Eat/Sleep**	**Choosing [2nd Step]** **TYCHE [Group 1]** **Mood**	**Hunting [3rd Step]** **THANATOS [Group 3]** **Anxiety**	**No Frustration** **LOGOS [Group 4]** **None**
Universal Consciousness		Guilt	Jealousy	Indignation	Wonder
Historical Consciousness		Shame	Envy	Contempt	Elevation
Personal Consciousness		Embarrassment	Bipolarity	Dispersiveness	Pride
Core Consciousness		Fear	Sadness	Anger	Happiness
Proto-Self		Submission	Attachment	Disgust	Enthusiasm

3.1.4. Experimental evidences for 3-axes approach

In Mathematics and CS, an axiomatic system is considered complete if it is applicable in all circumstances and consistent if it has no internal self-contradictions (Chaitin, 2006). Both consistence and completeness are forms of Kantian ethics reversibility, by reversibility meaning indifference to a change/swap of roles. In Kantian ethics, the universality of a rule implies that all deciding-agents necessarily acted according to that rule in all circumstances; and the failing of such universality can occur because of two types of reversibility failure: a) reversibility is not viable for the considered physical universe, b) reversibility contradicts the deciding-agent's intention. (Kant, 1993) The first type of Kantian reversibility failure in the axiom-based decision-process indicates a failure of axiomatic completeness, and is thus a failure in contextual-reversibility, which Kant called "perfect duties" (Kant, 1993); whereas the second type indicates a failure of axiomatic consistence, and it is thus a failure in formal-reversibility, which Kant called "imperfect duties". We thus recover Gilligan's concepts (Gilligan, 1985) in Psychology of "post-conventional formalism" and "post-conventional contextualism" by replacing "post-conventional" with "Kantian reversibility". Kant considers that "imperfect duties", as opposed to universal rules, can ethically be overcome by one's inclinations, e.g., by prefering pleasure rather than pain, satiety rather than hunger, health rather than sickness, happiness rather than misery, and so should not be included in civil legislation; whereas "perfect duties" cannot be ethically overturned by one's inclinations, and so can and should be included in civil legislation. (Lori, 2019)

Mythical hero stories are often focused in growing through increasing Consciousness levels. Moreover, although Campbell's study of the hero stories in multiple cultures (Campbell, 1972) is widely known (e.g. its use in George Lucas' Star Wars movies), a more recent work (Vogel, 2007) was able to found a more succinct structure for the Hero Story, which is composed by: A) Departure, B) Initiation, C) Return. These three parts, have the following components (Lori, 2019):

A) Departure: 1. Ordinary World, 2. Call to Adventure, 3. Refusal of the Call, 4. Meeting with Mentor; 5. Crossing threshold into Special World.
B) Initiation: 1. Tests with Allies and Enemies, 2. Approach to innermost Cave, 3. Going through Ordeal, 4. Receiving the Reward.
C) Return: 1. Traveling the Road back, 2. Hero's Resurrection, 3. Bringing back the Elixir.

We relate Consciousness Levels with the Hero Story by making the association (Lori, 2019):

A) Departure is a departure from Personal Consciousness.
B) Initiation is an initiation into a communal life and establishes the hero's Historical Consciousness.
C) Return is a return by the hero so as to bring a gift of Universal Consciousness which must be shared to be preserved.

The universal appeal of Shakespeare identifies him as someone that has deeply understood what is universal in human behavior. In his writings, it is possible to identify a "tragic equation" (Hughes, 1993) used throughout his plays. That "tragic equation" consists of an alteration of the Greek legend of Venus and Adonis by use of the writings of Seneca to replace Venus by Lucrece, and by the creation of a new type of Adonis. This new Adonis freely chooses a path of female-distancing and contemplation. In Shakespeare's "tragic equation", when the archetypical male encounters an actual female, he compares her to the extreme forms of female behavior; with the female doing likewise about the male. We have proposed (Lori, 2019), the joining of the two extreme forms of behavior in Shakespearean drama with the actual person, and so create the three-component archetypes for both the male and the female. The male archetype triplet is Collatine-Tarquin-Adonis, and the female archetype triplet is Venus-Persephone-Lucrece. (Lori, 2019)

In the history of human religion there are two major archetypes, that of the female Mother Earth, and that of the male Father Thunder. (Robbin, 1990)(Hughes, 1993) We hence propose that in Shakespeare's "tragic equation", we have "Mother Earth = Venus-Persephone-Lucrece" and "Father Thunder = Collatine-Tarquin-Adonis". Thus, for Shakespeare, any romantic relationship between a female and a male is projected into their minds, as being a relationship between Mother Earth and Father Thunder. Hence, all romantic relationships are always both transcendental and earthly, constituting a three-part structure for both the female and the male archetypes. The three parts being: Heavenly Male-Father Thunder, Earthly Female-Mother Earth, and their male or female human offspring connecting with both the Father Thunder and the Mother Earth. It is possible to see this structure as the result of the conflict in Shakespeare's time between Catholics and Puritans, with Adonis representing the Puritan Male-ideal and with Lucrece representing the Catholic Female-ideal (Hughes, 1993). Using Shakespeare's "tragic equation" (Hughes, 1993), it can be considered that for Shakespeare the mental health is the balance between the 3 archetypes, and that it is the difficulty of implementing this balance which constitutes the source of the difficulties in achieving and maintaining the state of mental health. (Lori, 2019)

The vision of contemporary Psychology goes beyond the prospect of a Manichean conflict between good and evil, towards the Shakespearean perspective where the evil is the stingy irrational search for the absolute power of either Nature or Reason. The mental health to Shakespeare is a balance between Catholicism\Nature\Female and Puritanism\Reason\Male, with a slight preference for the former (Hughes, 1993). We also propose here that a reason for the success of Shakespeare is in his discovery of the three Freudian identity types, Id-Ego-Superego, three centuries before they were proposed by Freud as the three parts of the Psyche (Freud, 1949). It should also be noted that such a discovery by Shakespeare might have been based on the approach to theatre developed by the Jesuits of that period (Wilson, 1997), and the Jesuit approach to spirituality has been known since Jung to have strong parallels to Psychotherapy (Becker, 2001). Those relations between Shakespeare, Freud, and Damasio Consciousness levels are expressed in Table 3.1.4. (Lori, 2019)

Table 3.1.4. Relation between Shakespeare, Freud, and Damasio Consciousness levels. (Lori, 2019)[5]

Consciousness Level	**Shakespearean Female Archetype**	**Shakespearean Male Archetype**	**Freud's Identity Types**
Universal	Venus	Adonis	Superego
Historical	Lucrece	Collatine	Ego
Personal	Persephone	Tarquim	Id

The entry of blood in the brain is regulated by the amount of neuronal activity, but there is both a seconds-long delay between neuronal activity and blood flow, and an excess of blood supply to the regions where the neuronal activity increases (Leopold, 2009). The magnetic field alterations caused by that excessive blood flow is what constitutes the fMRI signal. The fMRI data of ref. (Huth, 2016) obtained a cortical word-map presented in Fig. 3.1.4, for which the 3 principal components (PC) obtained using Principal Component Analysis (PCA) are (Lori, 2019):

PC1} locational/visual/tactile ⟹ emotional/communal (dorsal-ventral brain axis)

PC2} locational/visual/tactile ⟹ social/professional (medial-lateral brain axis)

PC3} locational/visual/tactile ⟹ mental/abstract (anterior-posterior brain axis)

There are several different approaches to Psychiatry based in different authors, such as Freud or Jung just to mention two classical examples. We chose to use the definitions used in what we consider to be a standard book in Psychiatry (Gerder, 2007). The Psychiatric pathologies can be divided between state (based in Table 3.1.2) and process (based in Table 3.1.1) pathologies, respectively. The 3 types of state pathologies are: a) mood disorders, which we consider to be social-role assessment issues; b)

[5] Structural causal modeling has been often used in Psychology, and the approach proposed here could be wrongly interpreted as a specific form of structural causal modeling, but it is a different approach, as it proposes specific archetypes as the source of the causal models.

anxiety, which we consider to be future-prediction issues, and c) eating/sleeping disorders which we consider to be body-awareness issues. (Lori, 2019)

The proposed relation above agrees in general with Fig. 3.1.3, and also obtain the results that Eating is about emotional satisfaction, that Choosing is about social rank, and that Hunting is about mental abstraction. This relation is obtained from the experimental data of ref. (Huth, 2016) and is represented in Fig. 3.1.4, thus being a further validation of the proposed 3-axes approach. (Lori, 2019)

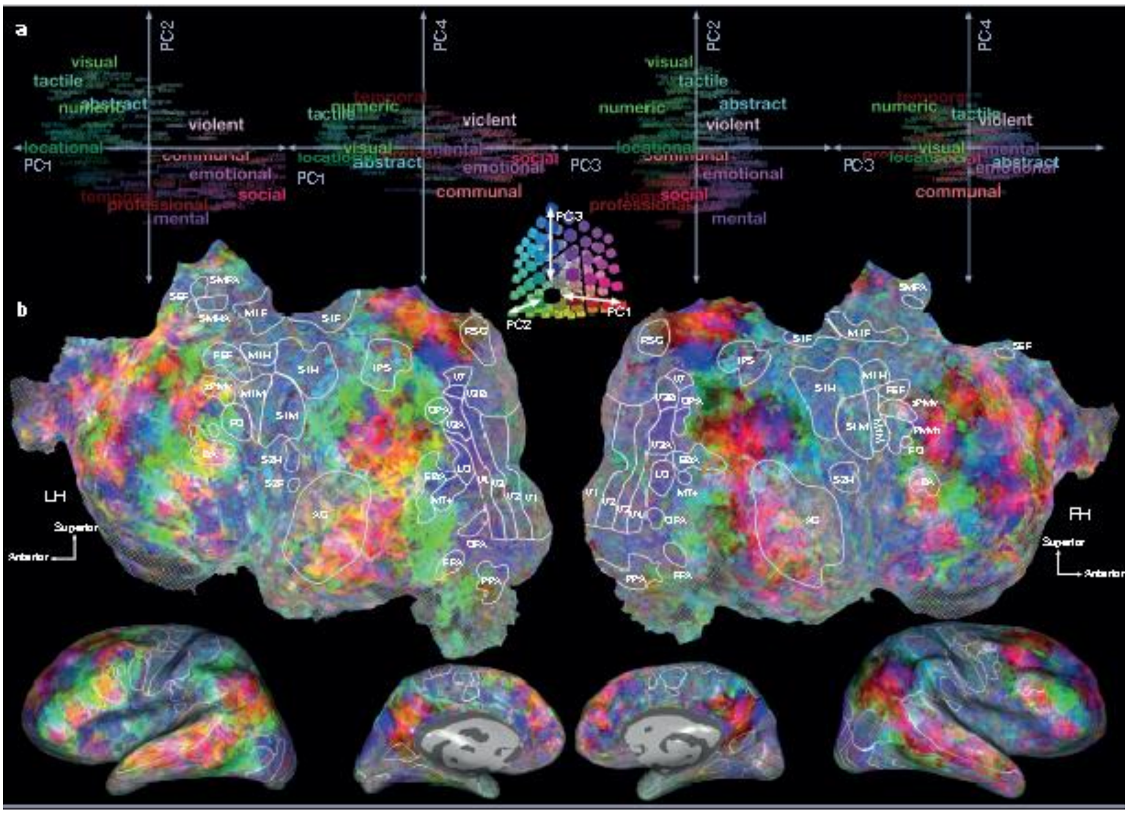

Figure 3.1.4. Cortical Word Map obtained by fMRI correlations. (Huth, 2016)

The mood disorders vary between depression and mania, with depression being associated to a lack of the appropriate amount of thinking needed to resolve the person's issues, whereas mania is associated to an excessive amount of thinking. Thus, mood disorders are mostly a problem in defining the correct amount of thinking choices available to the thought process, and so these disorders can be considered as being a Tyche-related pathology.

The anxiety disorders vary between autism and Williams-syndrome, with autism being associated to an excessive focus of attention and a dislike of social interactions, whereas Williams-syndrome is associated to an excessive liking of social interaction and a difficulty in focusing the attention. Thus, anxiety disorders are mostly a problem in defining the correct amount of focused attention versus the enjoyment of the dispersed nature of social interactions, thus these pathologies are about the search for a balance between individual space and social space, it can hence be considered as being a Thanatos-related pathology.

The eating/sleeping disorders can be expressed as overeating/oversleeping or undereating/undersleeping, with overeating/oversleeping being associated to body/tongue/skin intake/touch under-sensitivity, whereas undereating/undersleeping is associated to body/tongue/skin intake/touch over-sensitivity. Thus, eating/sleeping disorders are mostly a problem in defining the correct amount of body/tongue/skin intake/touch sensitivity, and so can be considered as being an Eros-related pathology. The psychiatric concept of elation is associated to adequate levels of self-confidence (meaning the Tyche axis of the person is doing well), arousal (meaning the Thanatos axis of the person is doing well), and well-being (meaning the Eros axis of the person is doing well) (see Table 3.1.2 and Table 3.1.3). (Lori, 2019)

The proto-self, Core Consciousness and Extended Consciousness (divided in both Table 3.1.5 and Table 3.1.4 into three Consciousness levels: Personal, Historical, Universal) have been proposed before (Damasio, 2003), and they are respectively related to the autonomic, somatic, and psycho aspects of the Psychiatric approach to pathology. The process pathology per excellence is schizophrenia, with hallucinations being one of its principal symptoms. The relation between schizophrenia, Psychology, and axiomatic systems is described in Table 3.1.5 (based in Table 3.1.1). The secondary delusions are a combination of vivid perceptions with primary delusions and, based in Table 3.1.5, they are hence a combination of proof-checking and axioms, and thus the secondary delusions appear to the person feeling them as being self-validated. The relations expressed in Table 3.1.5, will be helpful in clarifying the objective definition of mental-health to which we are aiming in this Section. (Lori, 2019)

Table 3.1.5. Relation between axiomatic systems in Mathematics and CS, narrative structure in Psychology, and the characteristics occurring in schizophrenia (from normal to pathological levels).

Axiomatic System	**Psychology Narrative**	**Schizophrenia [normal level]**	**Schizophrenia [mild level]**	**Schizophrenia [high level]**
Alphabet+Grammar	Setting	Sensory inputs	Sensory inputs	Sensory inputs
Proof-checking algorithm input	Initiating event	Images	Perceptions	Vivid Perceptions
Axioms	Internal response	Illusions	Hallucinations	Complex Hallucinations
Rules of inference	Goal + Actions	Controlled by Will	Non-Controlled by Will	Non-Controlled by Will
Inferred statements	Outcome	Valued Ideas	Delusions	Primary Delusions
Proof-checking algorithm output	Ending	Effect by Culture	Lack of Effect by Culture	Lack of Effect by Culture

The objective of this Section is to establish what is human mental health in an objective form, the proposed resume is that objective human mental health (Lori, 2019) is:

a) Wisdom to use the three forms of negative feelings to maximize the positive feelings.

b) Strength to develop and use the three aspects of Extended Consciousness (Personal, Historical, Universal).

c) Foresight to give more relevance to the higher Consciousness Levels.

The objective human mental health relation between the 3 axes approach and Psychiatry, obtains that when in a state of objective mental health, the person is: between too few thoughts and too many thoughts; between over-focused attention with under-enjoyment of social interactions, and under-focused attention with over-enjoyment of social interactions; and between overeating/oversleeping and undereating/undersleeping. The mental health being associated to a choosing of an intermediate path between two opposite perspectives is an overall accepted concept in both Philosophy and multiple religions (Flanagan, 2007)(Panikkar, 1989).

Thus, the mental health concept we obtained in this Section is not surprising in a religious or philosophical perspective (Flanagan, 2007)(Panikkar, 1989), but in here we have used experimental and cultural data to make clear that it is possible to objectively define what is mental health; objective because it is empirical data-based, multi-cultural, and can be described in a CS perspective as this approach is based in axiomatic systems. (Lori, 2019)

3.2. Quantum computing at sub-atomic scales and Moore's law future

Key points:

- This Section is the major conclusion of this Thesis, and it is major achievement.
- It is based in all other Sections of the Thesis, being in more direct relation to Section 2.1, Section 2.4, and Section 3.1; but is related to all of them.
- The result obtained is that between "Deep Learning in Imaging Neuroscience" and "Nuclear Physics in Quantum Computing", the most important contribution to the future of CS is obtained as being the first rather than the latter.
- Nevertheless, in the future of CS "Quantum Computing" is likely to be relevant in establishing the link between genetics and "Imaging Neuroscience".

The key issue for CS, in the near future, is to assess if Moore's law is to be maintained, or if instead a period of chip-size reduction stagnation will ensue (Technology, 2016). Moreover, it is wrong to assume a QC is always better than a CC, as there are many processes that can be done in a CC which cannot be done in a QC (Health, 2018). Until recently, Moore's law has guaranteed a systematic reduction of computation costs, as measured in bit/second/Dollar, but as chip miniaturization is reaching the atom-scale the limitations imposed by QM are starting to become relevant. The recent advances in QC's capacity (Arute et al., 2019) only confirm that QCs are better in simulating QM dynamics, which was already described as expectable in ref. (Health, 2018). The goal of this work is thus to determine if miniaturization is still the path towards CS progress, and hence the maintaining of Moore's law, or if instead a new path of lateralization is preferable. By lateralization meaning not only an integration between biological systems and computers, but also a new form of looking at the importance of computer ubiquitousness. (Lori, 2020)

As the scales being considered reduce in size, the applicable Physics also changes, going in the step-sequence: i. Newton's mechanics for the original mechanical computers, ii. Maxwell's electromagnetism for computers based in electric circuits, iii. Semi-classical QM for the contemporary CC, iv. QM for presently in development nanoscale QCs, v. Quantum Field (QF) theory of the Standard Model of Physics (SMP) for femtoscale QCs, vi. Quantum Gravity for black hole-like supercomputing devices. We are presently moving from step iii to step iv, whereas steps v and vi appear to us as "almost science-fiction". (Lori, 2020)

Despite the caveat that the speed and direction of evolutionary change has surprised us in the past and might be able to do so in the future, we conclude in this Section that step v is almost inconsequential for several reasons but mostly because of Pauli's Exclusion Principle, and step vi is completely unrealistic in the foreseeable future. This leaves us with step iii and step iv, but because of the difference between the classical and the quantum versions of the Hammersley-Clifford Theorem (HCT), it is obtained here that the QC will not be useful for the required lateralization because of two reasons: biological systems use classical Information transport rather than quantum, and QCs are very expensive because of the refrigeration requirements. (Lori, 2020)

The Physics relevant for steps v and vi is the QF theory of the SMP (Cottingham, 2007) which is the presently accepted Physics theory for both the atomic and sub-atomic scale, at least until the scale of the Grand Unified Theory (GUT) (about 10^{-31} m). The relation between QF's SMP, QM, and classical Physics, by classical Physics meaning Newton's mechanics/gravity and Maxwell's electromagnetism, is the following: 1) scale-range of the atoms/molecules which is a scale much smaller than the wavelength of most of the electromagnetic radiation reaching the Earth's surface and much larger than the wavelength of the nuclear force radiation, the electromagnetic radiation can thus be treated as a smooth classical field and the nuclear force's effect is to increase the density of the kinetic energy E of the nucleon's three quarks, which has as its main effect the increment of the nucleon's mass through the relation $m = \frac{E}{c^2}$, and hence in this case the approximations used in QM are valid; 2) scale-range much larger than the atoms/molecules, the wave-like characteristics of the atoms/molecules become irrelevant except during atomic/molecular impact where the wave-like characteristics allow for the outcome of the impact to be truly random (not just pseudo-random) (Zurek, 2003), thus QM converges to Brownian motion which is the basis for Statistical Mechanics (Klein, 2012); 3) then finally the Central Limit Theorem makes Statistical Mechanics apparently converge to classical Physics (Allahverdian, 2013). (Lori, 2020)

3.2.1. Quantum fields and the future Computing Power

According to the SMP, at a more fundamental level the universe is made of QFs. The QFs at different scales can be represented as a thermodynamic system, just as QM can (Peskin & Schroeder, 1995)(Snoke et al., 2012). Moreover, the description of the registration process in QM can also be applied to QF, provided that the time scales considered are much longer than the femtosecond, as for scales lower than the femtosecond/nanometer scale the QFs start to become time-reversible and hence are not representable by a thermodynamic equation, but rather by non-Markovian time-reversible evolution equations (Snoke et al., 2012). This is unsurprising, as below the femtosecond/nanometer scale the QFs start to lose the time-irreversibility caused by the impacts in Brownian motion, as that scale is below the Brownian-impact scale. Thus, all of Physics at temporal scales above the femtosecond/nanometer scale can be described using continuous Markov processes (CMPs). For classical Physics they are classical CMPs, and for quantum Physics they are quantum CMPs. (Lori, 2020)

The interactions of the QFs in the SMP are defined as being those that are compatible (Peskin & Schroeder, 1995) with the local Special Unitary *n*-dimensional (a.k.a. *SU(n)*) gauge invariance of the QFs fields where *n* is equal to 1, 2, or 3. The gauge invariance assumption means that the phase-transformation of the QF ψ_b by a *SU(n)* local gauge-transformation will not lead to alterations of the Physics of the system, but for this assumption to be valid there needs to exist the so-called *SU(n)* gauge-fields which will cancel the phase alteration of ψ_b with a gauge-alteration of their own. The local gauge-invariance of the SU(*n*) gauge-fields, together with local validity of Einstein's special relativity, imply that the Lagrangian densities of the SMP have one of the following forms: Klein-Gordon for zero spin QFs (such as the Higgs particle QF), Dirac for semi-integer spin QFs (such as the spin $\frac{1}{2}$ electron QF), Yang-Mills for non-zero integer spin QFs (such as the spin 1 photon QF) (Cottingham, 2007). (Lori, 2020)

One possibility for representing bits using QFs is to use the QF's spin, in this Section, we will make no distinction between bit and qubit as they both represent Information amount based on the probability of the occurrence of certain symbols within a finite range of possible symbols. The bits in CCs are typically represented through stable magnetic field states, with those magnetic fields being produced through the averaging across the spins of many individual particles. Hence, for us the QF's spin is the most realistic path towards miniaturization. For the case of an electron QF, the electron spin pointing down is represented as e↓ and we can assign it the bit state |0>, whereas the electron spin pointing up is represented as e↑ and we can assign it the bit state |1>. Likewise, for a neutron QF, the spin can be down, represented as n↓, or up, represented as n↑, which would then correspond to the bit states |0> and |1>, respectively. (Lori, 2020)

The establishment of a direct connection between spin states and bit states can be done because the existence of spin follows directly from the linear relation between energy and momentum with both being proportional to the derivative of the QF over spacetime coordinates, and hence is not at its core a relativistic phenomenon (Lévy-Leblond, 1967)(Hamdan, 2008), which implies that spin is a well-defined fundamental property of particles, and as such can be used as a bit representation for fermionic QFs. It is important that the QFs representing the bit are fermionic QFs, rather than bosonic QFs, so that to each spatial location there can be a single bit assigned to it. (Lori, 2020)

The range of a gauge force caused by a gauge-invariant SU(*n*) is inversely proportional to the mass of the force carrier, and so depending on the scale-range of the stored bits, different SU(*n*) gauge invariance forces will need to be considered. The range of the U(1)≡SU(1) electromagnetic force is infinite as its carrier, the photon, is massless, which implies that the electromagnetic force is relevant for all ranges; whereas the range of the SU(2) weak nuclear force is inversely proportional to the mass of the Z_0 particle, m_{Z_0}, and so it is about $10^{-18}\,\mathrm{m}$; and finally the longer range of the SU(3) strong nuclear force is at most inversely proportional to m_π which is the mass of the lightest quark doublet, the pion, and so it has a range of about $10^{-15}\,\mathrm{m}$. The SU(3) gauge force in the short range is carried by the massless gluons, but the existence of the quark confinement (Peskin & Schroeder, 1995) prevents the gluons from existing outside of either quark doublets (such as the pion) or quark triplets (such as the neutron). (Lori, 2020)

The scale of the CCs is in the hundred atoms scale, meaning about $10^{-8}\,\mathrm{m}$, and a temperature of about 70 °C. The highest Contemporary Maximum Information Processing Rate (CMIPR) is from about $10^{11}\,\frac{\mathrm{bit}}{\mathrm{s}}$ for an Ethernet network (Jain, 2016) or a Central Processing Unit (CPU) (Connatser, 2018), to about $10^{19}\,\frac{\mathrm{bit}}{\mathrm{s}}$ at a Temperature of 70 °C for a Summit super-computer (Oak, 2018). The Information contained in current QCs is at most a few bits in a volume of a few atoms, corresponding to a processing power for the IBM Q System One of about $0.7\cdot 10^{13}\,\frac{\mathrm{bit}}{\mathrm{s}}$ (Devoret, 2013)(Cross, 2018)(Loeffler, 2019)(Nersisyan, 2019), which is not yet competitive with the Summit

Super Computer in processing power, but with the caveat that the QC is a lot smaller than it. For Moore's law to continue being valid, it will be very useful for the miniaturization improvements to continue, but for such miniaturization to continue it is necessary to go beyond the 1 bit/atom Information content limit that is currently being reached. Even if Information is stored in the nucleus' spins rather than in the electron's spin, the difference is not very large as in both cases the spins of fermions tend to cancel each other at each nucleon energy-level because of the Pauli exclusion principle which prevents fermions from occupying the same quantum state. Hence, the Pauli exclusion principle implies that pairs of identical nucleons cancel each other's spin at each nuclear energy-level, and thus, at best, the total spin of the nucleus is equal to the number of nuclear-energy levels having a single nucleon. Hence, although there can be as much as 10 bit/atom in some especially prepared nuclei, that is not a large difference to the 1 bit/atom atomic Information storage that the electron's spin can already achieve. (Lori, 2020)

For the amount of bit/atom to increase, a possibility would be the use of neutronium (a.k.a. neutrium or neutrite) (Inglis-Arkell, 2012), which is basically a cluster of neutrons which would allow to put about 10^{15} neutrons in the volume of an atom, but neutronium is for now impossibly hard to keep stable, e.g. the best result yet for a stable neutronium was a 4-neutron state lasting about $10^{-21}\,\mathrm{s}$ (Bertulani & Zelevinsky, 2016). Moreover, although neutronium at near absolute zero is likely to form a degenerate gaseous Bose–Einstein condensate, that condensate would be composed of neutron pairs called dineutrons, which would have zero spin because of the Pauli exclusion principle. But, for high pressure and temperature, the Pauli exclusion principle makes the energy levels occupied by the neutrons become degenerate, which would allow for stable large particle number neutronium states. Unfortunately, the pressure and temperature required for a stable neutronium state are in the neutron star range, meaning temperatures of about $10^{6}\,\mathrm{K}$ (Lattimer, 2015) and pressures of about 10^{31} to $10^{34}\,\mathrm{Kg\,m^{-1}\,s^{-2}}$ (Ozel, 2016), whereas the highest pressure contemporary science has managed to create is about $10^{12}\,\mathrm{Kg\,m^{-1}\,s^{-2}}$ (Dubrovinsky, 2015) and hence we disregard the use of neutronium in the foreseeable future.

The limit of 1 bit/atom was experimentally reached in 2017 using Holmium atoms with the possibility of reaching working temperatures as high as -243 °C (Natterer, 2017). The DNA/RNA have about 0.7 bit/atom at 40 °C if the Holmium of ref. (Natterer, 2017) is used as an atom-size definer, which is quite close to 1 bit/atom. Thus, Biology has apparently not been able to go beyond the limit of about 1 bit/atom, either. (Lori, 2020)

The Pauli exclusion principle imposes limitations in the maximum Information storage and/or processing rate of Information transport by the spin of fermionic QFs, a more general limitation concerning Information transport (not just the spin-based Information transport) is the Bekenstein bound (Bekenstein 1981)(Bekenstein 2005) which requires that the Information contained in a spherical region of radius *R* cannot exceed that of a black hole of the same size which, in turn, is proportional to the surface area of the black hole, not to its volume. More specifically, if $\boldsymbol{D}$ is the diameter of the black hole, $\boldsymbol{I}$ is the total Information in the black hole, and $l_P = 1.62 \cdot 10^{-35}\,\mathrm{m/s}$ is Planck's length, then: $\boldsymbol{I} \leq \frac{\pi}{\ln 16}\left[\frac{\boldsymbol{D}}{l_P}\right]^2 \simeq 1.1\left[\frac{\boldsymbol{D}}{l_P}\right]^2$. This Information limit signifies that a black hole can store a tremendous amount of Information in a small volume, but there are a few important caveats. First, the smallest known black hole is called XTE J1650-500 and has about 5 times the mass of the sun occupying a sphere with a diameter of 24 Km. This is too heavy for a workable computer placed anywhere in our solar system, as for it to be safe to Earth's trajectory it would need to be located further away than Alpha Centauri. (Lori, 2020)

A different possibility are micro black holes (Hawking, 1971), which are theoretically possible but have not been experimentally detected yet, moreover the micro black holes have problems of their own as viable computers. Even if a micro black hole has a mass as large as the largest machine humanity has ever built, specifically the Large Hadron Collider which weighs about $2.8 \cdot 10^8\,Kg$, the corresponding Hawking Temperature is about $4.4 \cdot 10^{14}$ *K*, which is considerably higher than what contemporary technology can handle. If the temperature of the micro black hole is made low enough to be manageable by today's technology, such as that of the International Thermonuclear Experimental Reactor (ITER) project (ITER, 2006) which aims at fusion reaction temperatures of about 10^8 *K*, then the mass would need to be about $1.2 \cdot 10^{15}$ *Kg*, which is about five thousands larger that the Three Gorges Dam (Three, 2010), and over a million times larger than the largest QC-like machine that contemporary technology can build, the ITER (ITER, 2006). Thus, micro black holes are not viable computers in the foreseeable future. (Lori, 2020)

Moreover, although there has already been a lot of work concerning Information transport in relativistic thermodynamics (e.g., (Nakamura, 2006)), unfortunately there has been little attention paid to the Information transport's difference between zero spin (Nakamura, 2006) and non-zero spin particles. The relativistic QF theory of a zero spin Lagrangian density is the Klein-Gordon Lagrangian, whereas for the semi-integer spin particles (e.g. electrons and quarks) it is the Dirac Lagrangian, finally for integer non-zero spin particles it is the Yang-Mills Lagrangian (Peskin & Schroeder, 1995). The low velocity-limit of the Klein-Gordon Lagrangian is the well-known Schrödinger equation, but the low velocity limit of the Dirac equation is not the Schrödinger equation, but rather the Schrödinger equation with the extra Pauli matrices associated to the spin (Hamdan, 2008). Thus, the reason for existing spin is that particles can be represented by a wavefunction with phase terms having a covariant structure in accordance with Einstein's special relativity, and hence it is not valid to assume that spin is associated to the occurrence of relativistic speeds (Hamdan, 2008). (Lori, 2020)

We obtain here that the relativistic relation between the Information amount variation, dI, and the variation of energy density in the comoving frame, $d\epsilon$, is identical to that of the spin zero case except for the adding of an extra term which is dependent on the 4x4 Dirac gamma matrices γ^{μ}, the flat spacetime metric $\eta_{\mu\upsilon}$, the ensemble´s 4 velocity u^{υ}, the Boltzmann constant K, the temperature T, and the speed of light in vacuum c, through the expression: $\sum_{\mu,\upsilon=0}^{3}\gamma^{0}\gamma^{\mu}\eta_{\mu\upsilon}\left[\frac{u^{\upsilon}}{c}\right]$, which for velocities much lower than c becomes in average equal to 1. Thus, the relation between the variation of Information dI for a fixed rest-frame volume V_0 is: $dI=\left[\sum_{\mu,\upsilon=0}^{3}\gamma^{0}\gamma^{\mu}\eta_{\mu\upsilon}\left[\frac{u^{\upsilon}}{c}\right]\right]\cdot\left[\frac{V_0}{K\,T}\right]d\epsilon$, which is dependent on the chosen reference frame through the $\left[\frac{u_{\mu}}{c}\right]$ term. Moreover, if the spacetime is not flat (a very likely occurrence in the presence of micro black holes), then the flat spacetime metric tensor $\eta_{\mu\upsilon}$ must be replaced by an energy/momentum/stress-dependent general metric tensor $g_{\mu\upsilon}$ obtained from Einstein's GR (Wald, 1984), and thus (Lori, 2020):

$$dI=\left|\sum_{\mu,\upsilon=0}^{3}\gamma^{0}\gamma^{\mu}g_{\mu\upsilon}\left[\frac{u^{\upsilon}}{c}\right]\right|\left[\frac{V_0}{K\,T}\right]d\epsilon \qquad (3.2.1)$$

Hence, if micro black holes are used as computers, then the amount of Information being transmitted and/or received by the micro black holes is strongly affected by the presence and movement of the micro black holes, which is another reason why micro black holes are impractical as computation devices. In a 1959 lecture at Caltech, Feynman said that "there is plenty of room at the bottom". Whereas, in our opinion, we are reaching the end of the Information-workable room, long before we reach the room's bottom. But as miniaturization is reaching its limits, it is our opinion that lateralization is the direction from which the new source of Moore's law will come, and we discuss this in the next paragraphs below. For the more mathematically inclined, the calculation of Eq. 3.2.1 is deduced in the Mathematical Appendix at the end of this Section. (Lori, 2020)

3.2.2. From miniaturization to lateralization

If one cannot go down in the miniaturization scale, then the only possibility is to go side-ways, and in this sub-Section, we will describe what we mean by lateralization. By looking at a contemporary motherboard, there are computer chips which have an extremely fast rate of data processing, which are then connected through high conductance connections; with all these connected computer chips being cooled by fans and other heat dissipation devices. Nevertheless, when we look at the table where the computer is, often the only connection the computer has is through a wireless router to external devices (e.g. a printer).

This is not how Biology works, as in Biology there are mechanisms at multiple scales interacting with each other, hence what we propose by lateralization is that computer systems become more and more integrated at multiple scales. This has been proposed before (e.g. the "Brain scan: Bruno Michel" in ref. (Technology, 2016)), but the novelty in our approach is the suggestion that a lower-strength of miniaturization is capable of being a good improvement if a higher multi-path relational dynamic between data-processing units is achieved. The key points for achieving this higher multi-path relational dynamic between data-processing units requires thorough knowledge about two components of Information transport: a) how Information is being transmitted from the DNA/RNA to the cells as the genetic code appears to be able to have a strong influence in cell behavior (e.g. (Lorna, 2019)), and from the cells towards the external and internal behavior; b) how the general rules of Information representation differ between QM, Biology, and CS. (Lori, 2020)

The component a) is a major topic of Neuroscience, and advancements in that area are being done at multiple scales, but it is an area that is outside the scope of this Section. For the component b), a commonly used theory for Information representation in neuronal ensembles uses the negative minimum probability distribution functions (PDFs) approach (Anderson, 1994)(Knill, 2004), which by using the Weyl-Wigner transform (Wejl, 1927) implies that such a PDF can be transformed into a density matrix (as described in Section 3.1). In QM, a fermion that has been measured so as to be in a position eigenstate (meaning it is localized in a certain position as much as it is allowed by the Heisenberg uncertainty (Heisenberg, 1927)) has a density matrix that is diagonal when represented in the location-basis, moreover the elements in the diagonal are positive numbers that add up to one (implying that they can be understood as probabilities). In the wave-particle duality present in QM, the electron has in this case totally opted for particle-like characteristics. If the wave-like aspect of the electron becomes relevant, then off-diagonal elements of the density matrix in the location-basis start growing above zero, which implies that the Information amount associated to that location-basis is becoming reduced; likewise the density matrix in the momentum-basis would start to become more diagonal, and hence having a higher Information amount. The existence of off-diagonal elements in the location-basis density matrix for fermions is equivalent to the fermion's PDF no longer being a sharp gaussian-like PDF centered in its location, but rather becoming a PDF with negative minimum (Zurek, 2007). (Lori, 2020)

Thus, the density matrix corresponding to the negative minimum PDFs represented in the neurons is non-diagonal. This would imply that the classical CMP being implemented in the neurons has similarities to semi-classical approximations of QM, as they both obtain negative minimum PDFs, but it does not imply that neuronal dynamics are quantum, and we will see in the next paragraphs why they are not. (Lori, 2020)

There have been several efforts in CS for the inclusion of quantum algorithms in non-quantum environments: by generalizing the concept of Markov random walk to that of a quantum walk and then apply it to the modeling of judgments measured by rate scales (Wang, 2015); by applying the concept of "Information Vagueness" to the role of social hierarchy in organizational management improvement (Maia, 2019) in Section 2.4 (Neves, 2019); and by using the QD-based random-causality *o-iii* axioms to represent objective human mental health in Section 3.1 (Lori, 2019). Nevertheless, the goal of this Section is not to find interesting applications of quantum-like algorithms, but rather to find new forms of doing CS that allow for the keeping of Moore's law validity. We obtain here that the only path remaining for major CS improvements is lateralization, and so the use of quantum-like or Biology-like algorithms is only useful to us in as much as they can improve the capacity for lateralization. (Lori, 2020)

The process of building lateralized computer infrastructures is favored by the existence of desirable representation characteristics, and we will now compare the general representation characteristics of QC vs. CC-based representations. In classical Physics, the events can be typically separated between two types: the clearly discrete events where there are large regions of non-occurrence, and the clearly continuous events where the likelihood of occurrence is never zero. The clearly discrete events are typically represented by binomial random processes, whereas the clearly continuous events are typically represented by a Brownian motion random process. The binomial and Brownian processes can then typically be approximated by the Poisson and Wiener continuous processes, respectively. The Poisson and the Wiener process constitute the two major examples of classical CMPs, hence classical Physics' perspective of reality can always be approximated by CMP processes. Moreover, both Poisson and Wiener processes have always positive probabilities. Before getting into the quantum perspective, we find useful to notice that the mutual Information and the conditional mutual Information are defined in the same way for classical and quantum systems, which implies that the Markov property is also defined in the same way for both classical and quantum systems, as the Markov property is simply an affirmation of a constraint in the conditional mutual Information (Baez, 2012)(Poulin, 2012). (Lori, 2020)

In what concerns Information representation, the major difference between quantum and classical CMP is the difference between the classical and quantum versions of the Hammersley-Clifford Theorem (HCT). The classical version of the HCT (Hammersley & Clifford, 1971)(Clifford, 1990) being applicable to classical CMPs, and the quantum version of the HCT (Baez, 2012)(Poulin. 2012) being applicable to quantum CMPs. The classical HCT obtains that an always positive probability distribution satisfying the Markov property can always be represented by a random field satisfying a Gibbs measure (a.k.a. Gibbs random field) and vice-versa, hence implying that any positive probability distribution of a finite system can always be represented by the maximum entropy realization of a graph (meaning the Gibbs measure) and such realization is factorizable as a product of clique potentials. (Lori, 2020)

In short form, the classical HCT obtains that "locality is equivalent to factorization" (Ganchev, 2018). For the quantum HCT, the equivalence is valid in the Markov→Gibbs direction, but is not valid in the Gibbs→Markov direction unless the sub-Hamiltonians for each of the cliques of the graph commute with each other (Baez, 2012)(Poulin. 2012). This general commutative-ness between sub-Hamiltonians is a level of clique-independence that in general is physically unattainable. Hence, in the quantum HCT the Gibbs random fields can represent quantum probability fields that are not quantum CMPs, meaning that they are not physically realizable above the femtosecond/nanometer scale, as all the quantum Physics above the femtosecond/nanometer scale are quantum CMPs. Thus, the classical Gibbs random field has a space of possible arrangements which coincides with the space of possible arrangements of the classical CMPs, implying that if a biological entity uses a classical Gibbs random field to map the external reality, then that map would work for any type of classical CMP, meaning it always works in all classical Physics situations. Whereas, if a biological entity uses instead a quantum Gibbs random field to map external reality it would have a very large (possibly infinite) number of different possible representations for each physically occurring quantum CMP. (Lori, 2020)

The quantum approach is thus equivalent to having thousands of words representing the same object, meaning it would make the energetic cost of constructing a grammar with such words unbearable, unless the range of possible objects is very limited. Based in our analysis of the classical and quantum versions of the HCT, we obtain that Biology's Darwinian evolution would favor the use of the classical Gibbs random field as a form of representing classical reality (both internal and external), and that the use of quantum Gibbs random fields to represent quantum reality is too energetically expensive to be evolutionarily advantageous for biological systems. (Lori, 2020)

Recent works in Neuroscience have confirmed that the best fit to the in-vivo postsynaptic time histograms (PSTHs) obtained in non-human animals' cortex are cliques of neurons that represent the basic units of Information in the cortex (Reimann, 2017), and also that the neurons implement a classical diffusion event (describable by a classical CMP) that is capable of explaining in detail the experimental results for rats undergoing decision-making tasks (Pardo-Vazquez, 2019). Using the classical CMP perspective of the HCT, we propose here that what the rat's neurons are doing is to use the classical HCT to establish a one-to-one relation between the edge-interconnected cliques of neurons (where the edges are synaptic connections between neurons, and the nodes are neurons' cell bodies) with the physiological 3D areas constituting the vicinity of the neurons' cell bodies (which is where the classical diffusion/CPM occurs). Moreover, the experimentally found highest dimensionality of cliques obtained in statistically relevant quantities is a clique having 3-simplices (see Figure 2D (left) and Section 4.1.5 of ref. (Reimann, 2017)), meaning it is composed by 4 neurons, and hence the highest dimensionality of the diffusion process it can represent is 3D. (Lori, 2020)

Also, very high mean activity correlation was attained for connections belonging to 3-simpleces (Reimann, 2017), which using our HCT-based perspective implies that most of the brain's "thinking" occurs in 3D, including the "thinking about feelings". This is in strong agreement with Neuroscience work which indicates that: feelings have a strong parallelism to 3D space (Damasio, 2003)(Damasio, 2010); the brain's WM (meaning the brain's long-range neuronal connections) determined using dMRI has a 3-axes structure (Wedeen, 2012); the fMRI data of word-listening obtained a cortical word-map with the 3-axes structure determined using PCA (Huth, 2016); and several of these 3D-axes experimental data were integrated into a 3-axes approach for describing all mental processes, which helped describe the characteristics occurring in schizophrenia, from normal to pathological levels as described in Section 3.1 (Lori, 2019). (Lori, 2020)

We obtain in this Section that the future validity of Moore's law is unlikely to be based in further miniaturization, mostly because of Pauli's Exclusion Principle. Hence, it follows that lateralization is the most likely path for the maintaining of Moore's law validity; and moreover, the difference between the classical HCT and the quantum HCT implies that quantum-based representation of natural phenomena is largely over-representative in complex situations, which explains why Darwinian evolution in Biology "chose" the classical rather than the quantum approach to "reality representation". Our analysis and the "choice" made by biological evolution are, for us, strong indicators that the future CS developments will be made by lateralization-inducing architectures that almost exclusively use CCs. (Lori, 2020)

Contemporarily, there is already a strong tendency towards accepting that although QCs might be better at certain tasks than CCs, the capacity for clever algorithms to overcome the capacities of QCs is likely to remain (Bleicher, 2018). This tendency agrees well with the perspective we propose in this Section, with the slight caveat that we are of the opinion that QCs are likely to out-perform CCs when the physical system being represented is made of a small number of objects that can assume a very large number of possible states/values (e.g. the specification of a password). Also, rather than encryption, the focus of QCs has been in the modeling of quantum phenomena that cannot be modeled using classical CMPs, e.g. "modeling the interior of Black holes; calculate reaction rates, combustion and other effects" (Chhabra, 2019). Moreover, "There are lots of areas where quantum algorithms that show any improvement over classical areas do not exist" (Chhabra, 2019), which will imply that "the end user experience for an average user will not change" (Chhabra, 2019). (Lori, 2020)

Finally, although future high-level QCs might in the future be able to break public-key cryptography (PKC) systems, such as RSA and Diffie-Hellman (Martin, 2018), those QCs are unlikely to be able to break PKC systems developed in the NIST Post-Quantum Project (NIST, 2019)(Martin,2018). Some of the major Post-Quantum Cryptography (PQC) approaches that are candidates to winning the NIST Post-Quantum Project competition are (Microsoft, 2019) these: FrodoKEM uses a family of key-encapsulation mechanisms (KEMs) that are designed to be a conservative but practical PQC approach; SIKE uses arithmetic operations over finite fields; PICNIC uses a zero-knowledge proof approach; and qTESLA uses an improved decisional Ring Learning With Errors (R-LWE) approach. Thus, the lateralization computation proposed here can be correctly protected against hacking, even against hacking made by QCs, without needing to use QCs. (Lori, 2020)

Mathematical Appendix (Lori, 2020): The deduction of Eq. 3.2.1 describing the variation of Information amount in an ensemble of particles expressed in bits, dI, is described here. The dI is directly proportional to the entropy change dS through the relation $dI = \frac{1}{K \ln 2} dS$, where K is the Boltzmann constant. The relativistic equation for the Information amount change when Information is transported by spin 0 particles was obtained (Nakamura, 2006) to be: $dI = \left[\frac{V_0}{K \ln 2\, T}\right] d\epsilon - \left[\frac{\boldsymbol{P}}{K \ln 2\, T}\right] dV_0$, where V_0 is the rest-frame volume, T is the temperature, $d\epsilon$ is the variation of energy density in the comoving frame, and $\boldsymbol{P}$ is the pressure. This relativistic Information variation expression was obtained by generalizing the non relativistically-invariant thermal energy equation, $U = E - \frac{|\vec{p}|^2}{2 \cdot M}$ where E is the energy and $\vec{p}$ is the 3D linear momentum of the Information-carrying spin 0 particle of rest-mass M; to the relativistically-invariant thermal energy equation: $U=\sum_{\mu,\upsilon=0}^{3}\frac{1}{2\cdot M}\cdot p^{\upsilon}\cdot p^{\mu}\cdot\eta_{\mu\upsilon}$, where $\eta_{\mu\upsilon}$ is the flat spacetime metric, and $p^{\mu}\equiv\left\{-\frac{E}{c},\vec{p}\right\}$ is the spacetime tetravector linear momentum. This alteration is equivalent to a change from a Schrödinger equation to a Klein-Gordon equation, which is a valid relativistic generalization only for spin 0 particles, whereas for spin $\frac{1}{2}$ particles the relativistic generalization is to the Dirac equation. For the Dirac equation, the thermal energy equation is: $U=E-c\cdot\left[\gamma^{0}\sum_{j=1}^{3}\gamma^{j}[\vec{p}]_{j}\right]=\sum_{\mu,\upsilon=0}^{3}\gamma^{0}\gamma^{\mu}\eta_{\mu\upsilon}p^{\upsilon}c$, where γ^{μ} are the 4x4 Dirac gamma matrices. The difference, between spin 0 and spin $\frac{1}{2}$, for the relativistically-invariant expression for the thermal energy will not affect the dV_0 aspect of the dI Information variation (Nakamura, 2006), but it will affect its $d\epsilon$ part (Nakamura, 2006). If ${u_0}^{\upsilon}$ is the ensemble´s 4 velocity, and u^{υ} is the reference-frame 4-velocity, then by using ref. (Nakamura, 2006) it is obtained that the term multiplying the $d\epsilon$ part of the dI expression is actually: $dI=\left[\sum_{\mu,\upsilon,\varsigma,\zeta=0}^{3}\frac{\left[\frac{\partial U}{\partial p^{\upsilon}}\right]\cdot u^{\mu}\cdot\left[\frac{{u_0}^{\varsigma}}{c}\right]\cdot\left[\frac{{u_0}^{\zeta}}{c}\right]}{\sum_{\vartheta=0}^{3}{u_0}^{\vartheta}u^{\vartheta}}\eta_{\mu\varsigma}\eta_{\upsilon\zeta}\right]\cdot\left[\frac{V_0}{K\ln 2\,T}\right]d\epsilon$, which for the spin 0 case example described in ref. (Nakamura, 2006) has $\left[\frac{\partial U}{\partial p^{\upsilon}}\right]=\sum_{\vartheta=0}^{3}\eta_{\upsilon\vartheta}u^{\vartheta}$ which obtains $dI=\left[\frac{V_0}{K\ln 2\,T}\right]d\epsilon$ (Nakamura, 2006), and for the spin $\frac{1}{2}$ case has $\left[\frac{\partial U}{\partial p^{\upsilon}}\right]=\sum_{\mu,\upsilon=0}^{3}\eta_{\upsilon\mu}\gamma^{0}\gamma^{\mu}c$ which obtains the Information transport matrix $dI=\left[\sum_{\mu,\upsilon=0}^{3}\gamma^{0}\gamma^{\mu}\eta_{\mu\upsilon}\left[\frac{u^{\upsilon}}{c}\right]\right]\cdot\left[\frac{V_0}{K\ln 2\,T}\right]d\epsilon$. If ρ is the density matrix for the ensemble of spin $\frac{1}{2}$ particles, then using the "matrix generalization of the Shannon Information equation", the Information amount matrix of that ensemble is simply $-[\rho\ln\rho]$, whereas the classical Information stored in the systems is obtained through Von Neumann's trace, $-Tr[\rho\ln\rho]$ where Tr means trace, which is equivalent to a classical experimental measurement of the ensemble. Likewise, the relativistic expression for the change in the total Information stored in an ensemble of spin $\frac{1}{2}$ particles is: $\rho\left[\gamma^{0}\left[\sum_{\mu,\upsilon=0}^{3}\gamma^{\mu}\eta_{\mu\upsilon}\left[\frac{u^{\upsilon}}{c}\right]\right]\right]\cdot\left[\frac{V_0}{K\,T}\right]d\epsilon$, and the average amount of Information change that exists in such an ensemble permanently undergoing classical experimental measurements (a.k.a. mixed state) is: $\langle dI\rangle=Tr\left[\rho\left[\gamma^{0}\left[\sum_{\mu,\upsilon=0}^{3}\gamma^{\mu}\eta_{\mu\upsilon}\left[\frac{u^{\upsilon}}{c}\right]\right]\right]\cdot\left[\frac{V_0}{K\ln 2\,T}\right]d\epsilon\right]$, which for reference-frame velocities u^{υ} much lower than c is equivalent to $\langle dI\rangle=\left[\frac{V_0}{K\ln 2\,T}\right]d\epsilon$, meaning that for such low velocities $Tr\left[\rho\left[\gamma^{0}\left[\sum_{\mu,\upsilon=0}^{3}\gamma^{\mu}\eta_{\mu\upsilon}\left[\frac{u^{\upsilon}}{c}\right]\right]\right]\right]\approx 1$.

Chapter 4

Conclusion and Discussion

4.1. Conclusion of Thesis

Key points:

- We make here a resume of this Thesis, so as to highlight its contributions to CS.
- We also highlight how this Thesis clarifies the existence of different types of causality and how they apply to different aspects of CS.

The integration of the different Sections of this Thesis aims at showing these two points:

A. The present of CS is already an inter-disciplinary approach, often integrating collaborations with Psychology, Philosophy, Economy, and Physics. This inter-disciplinary approach often uses computational tools as a causal inference technology, but the maximization of computational tool's capacity for usefulness sometimes requires the development of new causal inference perspectives, and in such situations CS becomes a fundamental science rather than simply a tool for the representation of causal inference techniques developed by the other sciences (e.g., Mathematics, Physics, or Biology).

B. The future of CS is an unknown that only the future can clarify, but we propose here to make an educated guess of what that future might be. The future of CS will mostly be focused in “Deep Learning in Imaging Neuroscience” and “Nuclear Physics in Quantum Computing”, moreover the former will be more important than the latter, but the full development of the former will require the latter.

To confirm point **A** that computational tools are a valid approach to improving the causal inference of different technologies, meaning CS can be a fundamental science, we published the works of Section 2.2, Section 2.3, and Section 2.4; which constituted an application in Applied Statistics, Deep Learning, and Economics/Management. Whereas, in Section 2.1 the work presented indicated that CS can also allow for the creation of new perspectives of causal inference in the physical sciences. To further clarify the validity of point **A**, the types of causal inference existing in contemporary technology can be divided into three mostly independent types, viz.

- Deterministic;
- Statistical; and
- Quantum.

In contemporary CS, these three types of inferences are implemented in contemporary computational tools, but future CS will itself be the source of novel approaches to causal inference. The contemporary technology that correspond to each of these three types are expressed below, viz.

- Deterministic → Gravitation, Electromagnetism, Boolean-Logic, Classical Computer (CC);
- Statistical → Statistical Mechanics, Monte Carlo approaches, Information Theory;
- Quantum → Particle Collisions, Chemical reactions, Quantum Computer (QC).

In Table 4.1 is presented the relation between the work in this Thesis' Chapter 2 and Chapter 3, with both the causal inference approaches existent in contemporary technology and the novel approaches to causal inference that can be created by CS.

Table 4.1.1. Relation between works and causal inferences: The types of causal inference existing in contemporary technology can be divided into three types; viz.; Deterministic, Statistical, Quantum. In contemporary CS these three types of inferences are implemented, whereas future CS will develop novel approaches to causal inference.

Section	**Deterministic**	**Statistical**	**Quantum**	**Novel**
2.1	Yes	No	No	No
2.2	No	Yes	No	No
2.3	No	Yes	No	No
2.4	Yes	No	No	Yes
3.1	No	Yes	No	Yes
3.2	No	No	Yes	Yes

To confirm point **B**, the Information flow in biological systems is more important than the Information flow in quantum Physics. In Section 3.1 a new form of constructing axiom-based causal inference mechanisms was developed, with the help of which free-will can be quantified using axiom-based computing tools. In addition, a form of describing the flow of Information in the human mind has been developed in axiomatic causal inference, enabling that an objective definition of human mental health may be obtained; and Section 3.2 states that future developments in CS rests on the behavior of the flow of Information in biological systems rather than the flow of Information in quantum Physics used in Quantum Computing. Section 3.2 states that future advancements in CS does not lie in miniaturization from the atomic scale (the current application scale) to the core scale, but rather in the development of more integrated circuits in the micrometer to nanometer range to better mimic and interact with biological systems.

In Section 3.2, we analyzed both realistic and "almost-science fiction" approaches to developing better computer systems near the Bekenstein border, and it is not surprising that these approaches were not realistic. In addition, we used the difference between the classic and the quantum version of the HCT to explain why biological systems avoided the quantum calculation to represent the world, but instead chose the classic one. Finally, we analyzed examples of recent work that show future possibilities for integration between computers and biological systems. As a consequence of Section 3.1 and Section 3.2, we suggest that future developments in CS may be based more on biological integration than on Quantum Computation, but also that biological integration should reach the level of computer-gene interaction, then Quantum Computation likely to be required since the adequate scale of computer-gene interaction is the quantum scale.

4.2. Discussion of Work In-Progress

Key points:

- We discuss here two work-in-progress that follow directly from the Thesis but have not yet been published.
- The first work in-progress is in Neuroscience and is a direct consequence of Section 3.1.
- The second work in-progress is in Physics and is a direct consequence of Section 3.2.
- The two work-in-progress combined with the Thesis generalize the application of CS to the quantification of *value* and *Beauty*
- Further work is proposed to include the causal approaches described in the Thesis and the two work-in-progress in a new approach to CS, which we call *Statistical Philosophy*
- The *Statistical Philosophy* is here-proposed as a branch of the *Philosophy of Information*

The two major areas of this Thesis are "Deep Learning in Imaging Neuroscience" and "Nuclear Physics in Quantum Computing"; the former is in the "CS to Reality" direction, and the latter is in the "Realty to CS" direction. Hence, for the opposite direction to be considered in both works, it would be necessary to make a "Reality to CS" version of Section 3.1 and a "CS to Reality" version of Section 3.2; and this is respectively what the two work-in-progress are. Those two works, the first in Neuroscience and the latter in Physics, have been submitted for publication, but they have not yet been accepted in a peer-review journal. Moreover, their focuses are mostly outside CS, but still in strong interaction with CS. Those two work-in-progress are:

<u>Work in progress #1;</u> by Miguel Pais-Neves, Nicolás F. Lori, and colleagues

It is focused in Neuroscience and aims at complementing the work of Section 3.1 by attempting to determine the role Information and energy consumption play in the dynamic behavior of neuronal ensembles.

Work in progress #2; by Nicolás F. Lori, José Neves, and colleagues

It is focused in Physics and aims at complementing the work of Section 3.2 by attempting to determine the role CS can have in explaining certain features of the SMP and GR.

Both works in-progress will allow the relation between CS and Reality to go both ways, that is, they will both allow the establishment of a direct relation between CS and Reality where both the actual-Reality (meaning the Physical Universe) and our mental perception of a perceived-Reality (meaning the human Mind) can be put in a one-to-one relation with CS. This possibility elevates the theoretical aspects of CS to the status of a Philosophy.

In Plato`s Philosophy there are three *Transcendental* aspects of reality (a.k.a. Platonic Triad), viz.

- *Truth*
- *Beauty*
- *Good*

Contemporary Science fields, such as, Neuroscience, Psychology, and Psychiatry have clarified the relationship between the Actual Reality (i.e., the Physical Universe) and our mental perception of a Perceived Reality (i.e., the human mind). On the other hand, the role that computation can play in these areas may increase the need and / or capacity for the existence of computing tools that are able to deal with issues that have been in the past associated with Philosophy and its main branches, viz.

- Aesthetics
- Epistemology
- Ethics
- Logic
- Metaphysics

which deal with the questions, viz.

- What is Beauty?
- What is Truth?
- What is Good?
- Which axioms and conclusions are valid?
- What is one`s origin and end?

Although branches such as Logic and Metaphysics seem to be a very natural adaptation to contemporary computer tools, the other branches are not normally included in such devices; but in areas like healthcare, the relationship between Actual Reality and Perceived Reality breaks down when it comes to health, namely in Actual Health (the lack of physical harm) or Perceived Health (the lack of a feeling of discomfort). Therefore, when computer tools are used for health care, their applicability can be improved by including some taxonomies from the field of Philosophy, in which Beauty, Good and Truth are the most common. Undeniably, the two branches of Logic and Metaphysics fit well with the usual methods of today's computer tools once they implement a kind of axiomatic system that is in direct correspondence to Newtonian Axiomatic Systems (NAS) and Darwinian Axiomatic Systems (DAS), with a match into the system`s area of Deterministic Physics and Darwinian Biology (Lori, 2010a)(Lori, 2010b)(Lori, 2019) (see Section 3.1 and Table 4.1.1).

The Philosophy branches Aesthetics, Epistemology and Ethics look at different areas of human knowledge and depend, undoubtedly, on how these words are interpreted. For example, Truth may symbolize Experimental, Economic, and / or Personal truth. Depending on what the words *Truth*, *Beauty* and *Good* are thought to mean, the relationship to actual computer implementations may diverge. One`s perception is that the word *Truth* should only refer to the experimental value allocate to a strategy; and that *Good* should only relate to what improves patient health, while *Beauty* denotes the economic values corresponding to the staff`s salary. This last relationship between *Beauty* and *value* is possible above all because *Beauty* and Economic *value* are both physiologically (Montague, 2002) and culturally (Beinhocker,

2006) linked. Thus, the analysis in these final paragraphs also provides an assessment of the validity of the approach (Neves, 2009) described in Section 2.4.

In Kant's perspective there could be no objective definition, in principle, for *Beauty*, since the aesthetic experience of *Beauty* relates only to the subjective pleasure of the subject and not to a property of the object (Moland, 2017). In Schiller's viewpoint, *Beauty* can be defined objectively (Moland, 2017). Schiller's work uses the term *Beauty* and not *value*, but in our approach, they are inter-linked, and therefore the *Beauty-value* notation is used. The reason for keeping the *Beauty-value* notation is that it is possible to argue that the basis of all beauty feelings is the market value of neurotransmitters in the brain (Montague, 2002), and that the basis of all market values is the *Beauty* appreciation that people assign to the objects (Beinhocker, 2006), i.e., *Beauty* is the basis for *value* and vice versa. Therefore, and in accordance with Kant and Schiller, no finite *Beauty-value* can be assigned to a person, since each person is an archetypal of their freedom and is, consequently, a matter of their own (Moland, 2017). Thus, only countless *Beauty-value* can be assigned to people as people are both capable and entitled to freedom. As a result, Schiller ascribes the utmost *Beauty-value* to the objects that present the uppermost freedom, i.e., the objects that have the least usefulness and are therefore closer to a thing that exists for itself. While this definition of *Beauty* seems to be in direct contradiction with the definition of *value* in contemporary economy, which assigns *value* to knowledge, meaning "useful Information" (Beinhocker, 2006), and that we designed as *Truth*. Therefore, contemporary economics seems to place more value on *Truth* than *Beauty*, and people are prepared to spend large amounts of their wealth to improve their health, suggesting that *Good* is also worthwhile. In fact, there are three types of values, viz.,

- *Truth-value*;
- *Good-value*
- *Beauty-value*.

The infinite *value* that Kant and Schiller ascribe to man relates only to *Beauty*, and it is an ascription that characterizes Kant and Schiller's philosophical period, the romantic, which is a pre-Darwinian one. The development of Darwinism as a *Biological* (Smerlak, 2016), *Mathematical* (Chaitin, 2006), *Economic* (Beinhocker, 2006) and *Physical* (Zurek, 2009) concept raises new questions that may be assessed with the help of computing tools. In order to be able to judge these three types of values, we must be able to work with an "axiom-driven *value* calculation" for the *Truth-value*, e.g. NAS; and with an "environmentally-driven value calculation" for the *Good-value*, e.g. DAS; while a new form of calculation is required for the *Beauty-value*. This new form of adding up, which is suitable for calculating the *Beauty-value* of an object, is the partial Information-driven calculation given in (Neves, 2019) (see Section 2.4) and further developed in (Lori, 2019) (see Section 3.1), that presents the 3 axes of *Psychology*, viz.

- Thanatos
- Eros
- Tyche.

The relation between the 3-axes of Section 3.1 (Lori, 2019), the three factors of Section 2.4 (Neves, 2019), and the Plato's Transcendentals (a.k.a. Platonic Triad) of Philosophy are represented in Table 4.2.1 by integrating Fig. 3.1.3, Table 3.1.2, Table 3.1.3, and Fig. 3.1.4.

Table 4. 2.1. The relation between *value* and *Beauty* is described:

Plato	**Neves**	**Lori**
Truth	Initiative	Hunting/Power/Thanatos
Good	Empathy	Eating/Pleasure/Eros
Beauty	Self-Discipline	Choosing/Meaning/Tyche

This new form of calculation, appropriate for the calculation of the Beauty/value of an object, is the partial Information driven calculation (Neves, 2019) described in Section 2.4, and further developed (Lori, 2019) in Section 3.1, to allow for the conclusion of Section 3.2 that lateralization, not miniaturization, is the future of CS (Lori, 2020). The Information concept used here is that of *Shannon Information*, i.e., the logarithm of the inverse of the probability of occurrence of a symbol in an alphabet;

which is thus based on probability theory. This new form of calculation, the partial Information calculation, is a probabilistic one, without necessarily assuming that these probabilities are the result of a lack of discipline of the observer, but that the Information available is not sufficient to provide more than the probabilities.

A key question for this new form of partial Information-driven calculation named *Statistical Philosophy*, a here-proposed branch of the *Philosophy of Information*, is the importance of the role causality plays in the observed system. This is a central issue for *Statistical Philosophy*, since causality plays a direct role in the appropriate control of variables, which enables an appropriate statistical estimation of the probability of events. The correct way to use variable control depends on whether the variable ◊ acts as a *mediator*, *confounder* or *collider*. The role of the variable ◊ is defined by whether it is causality that will, viz., (Pearl, 2018)

- *go through*; → ◊ →; indicating a *mediator*
- *diverge*; ← ◊ →; indicating a *confounder*
- *converge*; → ◊ ←; indicating a *collider*

In order to use causality correctly in statistical analysis, it is necessary to carry out causal interventions in probabilistic inference using the MAKE operator, which corresponds to the occurrence of a causal effect (Pearl, 2018). The use of the MAKE enables the creation of a counterfactual statistical analysis, which enables the creation of the two upper levels of the causal inference above the correlation level, i.e., the interventional and counterfactual levels. The *correlative causality* resembles an act of *seeing*, meaning it identifies the likelihood of the simultaneous occurrence of events; the *intervention* an act of *doing*, meaning it identifies the likelihood that an effect resulted from a certain cause; and the *counterfactual* an act of *imagining*, meaning it identifies the likelihood that an effect that did not occur resulted from a certain cause not occurring (Pearl, 2018). Moreover, because of the conclusions in Section 3.2, the classical causality rules used in ref. (Pearl, 2018) will continue to be used in CS despite the recent appearance of QC (Arute, 2019), as according to Section 3.2, CC will continue to be the most relevant contributor to CS, and so the causality characteristics of quantum causality, such as the time-reversibility of the U(1) gauge invariance force, need not be considered.

This new form of calculation enables a *Statistical Philosophy* based on computational tools (Pearl, 2018). The counterfactual definition of causality was already available in the biblical dialogues of Abraham (Pearl, 2018), but was not used by Aristotle (Pearl, 2018); and it was not used by Hume in his work from 1739, but only appeared in Hume's work from 1748 (Pearl, 2018). In addition, it was Hume's analysis of ethics and causality that prompted Kant to develop his own thorough approach to ethics and causality (Wilson, 2018). This is relevant to the approach proposed here, since it is directly related to the distinction between Hume and Kant morals (Greene, 2004) (see Fig. 3.1.3); since Kant's ethics are based on duty (therefore associated with language), and Hume's are based in emotion (hence associated with tone of sound); moreover, "Kantian reversibility" (Kant, 1993) was described in Section 3.1 as being equivalent to Gilligan's concept of "post-conventional" (Gilligan, 1985), again centered in the issue of duty. Thus, it is a key issue the difference between Kant's view that *Beauty* is not objective and Schiller's view that *Beauty* can be objective (Moland, 2017).

The Kantian preference for a NAS approach implied that the causality rules can be axiomatically accepted but not empirically proven. Hume's 1739 approach opted for empirically based correlation-driven DAS validation of the causality rules, although such approach cannot resolve the induction problem (Henderson, 2019). It is Bayes' causal probability that enables the causality to be obviously derived from data. In fact, Bayes' causal probability can only infer correlative causality (Pearl, 2018), the first level of causal reasoning, as suggested by Hume's 1748 approach. However, the counterfactual algorithms currently implemented in today's computers use Bayesian networks (Pearl, 2018). In fact, the selection of the best possible counterfactual causality rules is already carried out in the big data analysis (Forney, 2017).

The goal of maximizing the *Truth*, *Beauty*, and the *Good* values seems to be the obvious answer to the health management problem raised here; but, just like in health management it seems impossible to have staff wages, equipment costs, and patient improvement maximized without going bankrupt. It will be shown here that when one tries to maximize *Truth-value*, *Beauty-value* and *Good-value* often leads to a kind of trilemma restriction that occurs in many forms (e.g. Fries' Trilemma (Fries, 2011)(Popper, 1959)). In this work the focus will be on the economic perspective, specifically in the "political trilemma" that confirms the paradox ''Democracy vs. national sovereignty vs. global economic integration'' (Rodrik, 2007)(Rodrik, 2011), and the impossible trinity that confirms the paradox ''independent monetary policy vs. fixed exchange rate vs. free movement of capital '', which has been confirmed by empirical studies (Boughton, 2003)(Obstfeld, 2005). The relationship between the three aspects of the ''political trilemma'' (Rodrik, 2007)(Rodrik, 2011), and the ''impossible trinity'' (Boughton, 2003)(Obstfeld, 2005) is straightforward; however, it is proposed here a form by which computational tools can be used in clarifying the balancing-characteristics of the "Impossible Trinity". Specifically, the attempt at an "independent monetary policy" is an attempt at establishing a NAS Truth-value using locally-defined consistent axioms, whereas a "free capital movement" is an attempt at establishing a DAS Good-value using globally-defined complete axioms. Yet, as it is known by the *Gödel Incompleteness* theorems, the axioms with a finite-amount of *Shannon Information* cannot simultaneously be *Complete* and *Consistent* (Chaitin, 2006), which can have implications in both *Brain Behavior* (Lori, 2010a)(Lori, 2019) and *Fundamental Physics* (Lori, 2010b).

The time evolution dynamics of *Darwinian* advancement is only partially predictable, not only because it is probabilistic, but also because the form of the aptitude-*Probability Distribution Function* (*PDF*) is only partially predictable, as the predictable part of the time evolution is only the aptitude of the newest types (Smerlak, 2016). The *Darwinian* evolutionary processes of *DAS*, i.e., the ''free movement of capital'' in the sense of *Good* value, are fundamentally unpredictable (Smerlak, 2016), whereas the Newtonian evolutionary processes of NAS, i.e., the ''independent monetary policy'' that means the *Truth* value, are fundamentally predictable (Chaitin, 2006); The balance between the NAS and the DAS, which represents the ''fixed exchange rate'' for the Beauty value, is therefore a weak balance between Predictability vs. Unpredictability, local influence vs. global influence, consistent axioms vs. complete axioms, between NAS vs. DAS. The calculation of this balance takes place in our brain when we evaluate the *value* of an action (Montague, 2002) and also the *value* of an object in the world economy (Beinhocker, 2006).

The choice of the clinical action that is more worthy, as it often occurs in health management, inevitably requires the projection of a three-dimensional value vector, i.e., [*Truth* value, *Beauty* value, *Good* value] into a one-dimensional worthiness-scalar. This projection is necessary, as the concept of best is necessarily one-dimensional. The various forms of projecting the value 3-vector to the one-dimensional worthiness-scalar form the *political / ethical / religious* decision that every person and every society makes. The *Statistical Philosophy* computational tools are unlikely to provide an unique answer to what is the best political, ethical or religious choice, but the *Statistical Philosophy* computational tools offer new and more thorough perspectives for the best possible assessment of what is the cause and what are the consequences of the political / ethical / religious decisions that occur.

The future developments in the fields of *Biomedicine*, *Neuro-informatics* or *Health Management* pose special requirements, which have led to the development of different approaches for calculating the associated value. We have found that the simple use of computing tools makes it difficult to estimate the value associated with a clinical act. However, these arithmetic tools are best used if they are integrated with philosophical perceptions, which have become clearer through recent developments in the fields of *Neuroscience*, *Economics*, *Physics* or *Mathematics*. Furthermore, the need to develop new computational tools for calculating the value-vector and its projection into a worthiness-scalar, will likely create new software industries based in future CS approaches.

The development of *Statistical Philosophy* is already occurring through the development of counterfactual-based algorithms, which have enthusiastically been used in AI and cognitive Neuroscience, but not in Philosophy (Pearl, 2018). Moreover, according to ref. (Pearl, 2018) the key approach for solving the “hard AI” problem is to resolve the free-will issue and for that it is essential to use causality rules; which is what we did in this Thesis (e.g. Section 3.1). Thus, this Thesis is likely to play a strong role in the future resolution of the “hard AI” problem.

Chapter 5

References

1. Adpakkala. (2017), November 10. Navigating the Sciences Jungle Around AI. In Opentech AI – Architecture, Ecosystem and Roadmap. Retrieved November 11, 2019, IN: https://opentechai.blog/2017/11/10/navigating-in-the-ai-sciences-jungle/
2. Adler, A. (1925). The Practice and Theory of Individual Psychology. Routledge & Kegan Paul.
3. Allahverdyan, A. E., Balian, R., Nieuwenhuizen, T. M. (2013). Understanding quantum measurement from the solution of dynamical models. Phys. Rep., pp. 525. 1-166.
4. Al-Rfou, R., Alain, G., Almahairi, A., et al. (2016). Theano: A Python framework for fast computation of mathematical expressions. IN: https://arxiv.org/pdf/1605.02688.pdf
5. Andersen, P. A. (2011). Handbook of Communication and Emotion: Research, Theory, Applications, and Contexts. Academic Press.
6. Anderson, C. H, Van Essen, D. (1994). Neurobiological Computational Systems. IN: Computational Inteligence Imitating Life, pp. 213-22, IEEE Press, New York, USA.
7. Arias, C. (2006). Enfoques teóricos sobre la, percepción que tienen las personas. Horizontes Pedagógicos. Volumen 8, No. 1.
8. Arute, F., Arya, K., Babbush, R., et al. (2019). Quantum supremacy using a programmable superconducting processor. Nature. Vol. 574, pp. 505-511.
9. Assaf, Y., Blumenfeld-Katzir, T., Yovel, Y., Basser, P.J. (2008). AxCaliber: A method for measuring axon diameter distribution from diffusion MRI. Magn Reson Med 59, pp. 1347–1354.
10. Baars, B. J. (2002). The conscious access hypothesis: origins and recent evidence. Trends Cogn. Sci. 6, pp. 47-52.
11. Baez, J. C. (2012). A Quantum Hammersley-Clifford Theorem. Azimuth. IN: https://johncarlosbaez.wordpress.com/2012/01/29/a-quantum-hammersley-clifford-theorem/

12. Ball, G., Aljabar, P., Arichi, T., Tusor, N., Cox, D., Merchant, N., Nongena, P., Hajnal, J. V., Edwards, A. D., Counsell, S. J. (2016). Machine-learning to characterise neonatal functional connectivity in the preterm brain. NeuroImage, 124, pp. 267–275.

13. Bandettini, P. (2009). What's new in neuroimaging methods? Annals of the New York Academy of Sciences, 14(4), pp. 260–293.

14. Bar, A. (2013). Brownian motion and the Central Limit Theorem.based on: Shang-Keng Ma, Statistical Mechanics, sections 12.2, 12.7 and the course's notes section 6.2.

15. Barkhof, F., Haller, S., Rombouts, S. A. (2014), Resting-state functional MR imaging: a new window to the brain. Radiology, 272(1), pp. 29-49.

16. Baumeister, R. F., Campbell, J. D., Krueger, J. I., Vohs, K. D. (2003). Does high self-esteem cause better performance, interpersonal success, happiness, or healthier lifestyles?. Psychological Science in the Public Interest 4, pp. 1–44.

17. Bechara, A., Damasio, A. R. (2005). The somatic marker hypothesis: a neural theory of economic decision. Games and Economic Behavior. 52, pp. 336-72.

18. Becker, K. L. (2001). Unlikely Companions: C.G. Jung on the Spiritual Exercises of Ignatius of Loyola: na Exposition and Critique Based on Jung's Lectures and Writings. Gracewing Publishing.

19. Behrens, T. E. J., Berg, H. J., Jbabdi, S., Rushworth, M. F. S., Woolrich, M. W. (2007). Probabilistic diffusion tractography with multiple fibre orientations: What can we gain? Neuroimage 34, pp. 144–155.

20. Beinhocker, E. D. (2006). The Origin of Wealth. Boston: Harvard Business School Press.

21. Bekenstein, J. D. (1981). Universal upper bound on the entropy-to-energy ratio for bounded systems. Phys. Rev. D 23, pp. 287-298.

22. Bekenstein, J. D. (2005). How does the Entropy/Information Bound Work? Foundations of Phys. 35, Issue 11, pp. 1805-1823.

23. Bennett, M., Dennett, D., Hacker, P., Searle, J. (2007). Neuroscience & Philosophy. Columbia University Press.

24. Bertulani, C. A., Zelevinsky, V. (2016). Four neutrons together momentarily. Nature. 532 (7600). pp. 448–449.

25. Bleicher, A. (2018). Quantum Algorithms Struggle Against Old Foe: Clever Computers. FROM: The Future of Quantum Computing. Quanta Magazine. IN: https://www.quantamagazine.org/quantum-computers-struggle-against-classical-algorithms-20180201/

26. Boughton, J. M. (2003). On the Origins of the Fleming-Mundell Model. IMF Econ Rev 50, pp. 1-9.

27. Buffelli, M., Burgess, R. W., Feng, G., Lobe, C. G., Lichtman, J. W., Sanes, J. R. (2003). Genetic evidence that relative synaptic efficacy biases the outcome of synaptic competition. Nature 424, pp. 430-434.

28. Biswal, B., Yetkin, F. Z., Haughton, V. M., Hyde, J. S. (1995j). Functional connectivity in the motor cortex of resting human brain using echo-planar MRI. Magnetic Resonance in Medicine, 34(4), pp. 537–41.

29. Boubela, R. N., Kalcher, K., Huf, W., Našel, C., Moser, E. (2015). Big Data Approaches for the Analysis of Large-Scale fMRI Data Using Apache Spark and GPU Processing: A Demonstration on Resting-State fMRI Data from the Human Connectome Project. Front Neurosci, 9, p. 492

30. Bourilkov, D. (2001). Hint for axial-vector contact interactions in the data on e+e-→e+e-(γ) at center-of-mass energies 192–208 GeV. Phys. Rev. D 64, 071701R.

31. Brovelli, M., Ding, A., Ledberg, Y., Chen, R., Nakamura, Bressler, S. (2004). Beta oscillations in a large-scale sensorimotor cortical network: Directional influences revealed by Granger causality. Proc. Natl. Acad. Sci. USA v. 101, p. 9849.

32. Byun, H. Y., Lu, J. J., Mayberg, H. S., Günay, C. (2014). Classification of Resting State fMRI Datasets Using Dynamic Network Clusters. Modern Artificial Intelligence for Health Analytics, 14, pp. 2–6.

33. Campbell, J. (1972). The Hero With a Thousand Faces. Princeton University Press.

34. Carlson, N. R. (2012). Physiology of Behavior (11th Edition). Pearson.

35. Chaitin, G. J. (2006). Meta Math!: The Quest for Omega, New York, Vintage Books.

36. Chandra, T., Toueg, S. (1996). Unreliable failure detectors for reliable distributed systems. Journal of the ACM, 43(2), March, pp. 225– 267.

37. Chhabra, S. K. (2019). Quantum Computers Are Imminent But Will Not Replace Classical Computers. Business World. IN: http://www.businessworld.in/article/Quantum-Computers-Are-Imminent-But-Will-Not-Replace-Classical-Computers/26-11-2017-132515/

38. Ciesielski, K. (1997). Set Theory for the Working Mathematician. Cambridge University Press. p. 4. ISBN 0-521-59441-3. Retrieved 12 August 2015.

39. Clifford, P. (1990). Markov random fields in statistics. FROM: Disorder in Physical Systems: A volume in honour of John M. Hammersley. Grimmett, G. R., Welsh, D. J. A. (eds.). Oxford University Press. Pp. 12-32. IN: http://www.statslab.cam.ac.uk/~grg/books/hammfest/3-pdc.ps

40. Commision, F. C. I. (2011). The Financial Crisis Inquiry Report, Authorized Edition: Final Report of the National Commision on the Causes of the Financialo and Economic Crisisis in the United States. 1st Edition. BN Publishing.

41. Connatser, M. (2018). AMD's new 2990WX is now the world's fastest CPU, with some caveats. Notebook Check, 2018/08/14.

42. Connectedreams.com. (2016), September 15. Beginner's Guide to Computer Science. In Connectedreams' Resources. Retrieved November 11, 2019, IN: https://medium.com/readers-writers-digest/beginners-guide-to-computer-science-engineering-361ae1682f5c

43. Continuum Analytics. (2016). Anaconda Software Distribution. Retrieved December 6, 2017, IN: https://docs.anaconda.com/anaconda/faq#how-do-i-cite-anaconda-in-an-academic-paper

44. Conturo, T. E., Lori, N. F., Cull, T. S., Akbudak, E., Snyder, A. Z., Shimony, J. S., McKinstry, R. C., Burton, H., Raichle, M. E. (1999). Tracking neuronal fiber pathways in the living human brain. Proc Natl Acad Sci U S A 96, pp. 10422–10427.

45. Cottingham, W. N., and Greenwood, D. A. (2007). Standard Model Lagrangian (including neutrino mass terms). FROM: An Introduction to the Standard Model of Particle Physics, 2nd Edition., Cambridge University Press, Cambridge. {Extracted by J.A. Shifflett from Particle Data Group tables at pdg.lbl.gov, 2 Feb 2015.}

46. Craddock, R. C., Tungaraza, R. L., Milham, M. P. (2015). Connectomics and new approaches for analyzing human brain functional connectivity. Gigascience, 4, p. 13.

47. Crick, F. C., Koch, C. (2005). What is the function of the claustrum? Philos Trans R Soc Lond B Biol Sci 360, pp. 1271–1279.

48. Cross, A. W., Bishop, L. S., Sheldon, S., Nation, P. D., Gambetta, J. M. (2018). Validating quantum computers using randomized model circuits. IN: https://arxiv.org/pdf/1811.12926.pdf

49. Damasio, A. R. (2000). The Feeling of What Happens. New York: Harvest Books.

50. Damasio, A. R. (2003). Looking for Spinoza. New York: Harcourt.

51. Damasio, A. R. (2010). Self Comes to Mind. New York: Pantheon.

52. Dani, A., Huang, B., Bergan, J., Dulac, C., Zhuang, X. (2010). Superresolution Imaging of Chemical Synapses in the Brain. Neuron 68, pp. 843–856.

53. D'Argembeau, A., Xue, G., Lu, Z.-L., Van der Linden, M., Bechara, A. (2008). Neural correlates of envisioning emotional events in the near and far future. NeuroImage, 40, pp. 398–407.

54. Dehaene, S, Changeux, J.-P. (2004). Neural mechanisms for access to consciousness. In: Gazzaniga M, editor. The cognitive neurosciences. 3rd edn. MIT Press; Cambridge, MA.

55. Dehaene, S., Changeux, J.-P. (2011). Experimental and Theoretical Approaches to Conscious Processing. Neuron, Volume 70, Issue 2, pp. 200–227.

56. Dennett, D. C. (2003). Freedom Evolves. Viking Books. New York.

57. Dennis, E. L., Thompson, P. M. (2014). Functional brain connectivity using fMRI in aging and Alzheimer's disease. Neuropsychology Review, 24(1), pp. 49–62.

58. Desikan, R. S., Ségonne, F., Fischl, B., Quinn, B. T., Dickerson, B. C., Blacker, D., Buckner, R. L., Dale, A. M., Maguire, R. P., Hyman, B. T., Albert, M. S., Killiany, R. J. (2006). An automated labeling system for subdividing the human cerebral cortex on MRI scans into gyral based regions of interest. Neuroimage. 2006 Jul 1;31(3), pp. 968-980.

59. Devoret, M. H., Schoelkopf. R. J. (2013). Superconducting Circuits for Quantum Information: An Outlook. Science. 339(6124), pp. 1169-1174.

60. Dubrovinsky, L., Dubrovinskaia, N., Bykova, E., Bykov, M., Prakapenka, V., Prescher, C., Glazyrin, K., Liermann, H.-P., Hanfland, M., Ekholm, M., Feng, Q., Pourovskii, L. V., Katsnelson, M. I., Wills, J. M., Abrikosov, I. A. (2015). The most incompressible metal osmium at static pressures above 750 GPa. Nature. 525, pp. 226–229.

61. Edelman, G. (1987). Neural Darwinism: The Theory of Neuronal Group Selection. Basic Books. New York.

62. Eigenfactor.org. (2014). Mapping Science. University of Washington In Eigenfactor.org. Retrieved November 11, 2019. IN: http://www.eigenfactor.org/map/maps.php

63. Einstein, A., Rosen, N. (1935). The Particle Problem in the General Theory of Relativity. Physical Review 48, pp. 73-77.

64. Ekert, A., Knight, P. L. (1995). Entangled quantum systems and the schmidt decomposition. American Journal of Physics 65(5), pp. 415–423.

65. Eyherabide, H. G., Rokem, A., Herz, A. V. M., Samengo, I. (2009). Bursts generate a non-reducible spike-pattern code. Frontiers in Neuroscience. Volume 3, Issue 1, 8-14.

66. Finn, E. S., Shen, X., Scheinost, D., Rosenberg, M. D., Huang, J., Chun, M. M., Papademetris, X., Constable, R. T. (2015). Functional connectome fingerprinting: Identifying individuals using patterns of brain connectivity. Nature Neuroscience, 18(11), pp. 1664–1671.

67. Fischer, D. S. (2011). Leading the dog of selection by its mutational nose. PNAS, vol. 108, n° 7, pp. 2633-2634.

68. Fischer, M. J., Lynch, N. A., Paterson, M. S. (1985). Impossibility of distributed consensus with one faulty process. Journal of the ACM, 32 (2), pp. 374–382.

69. Fischl, B., Van Der Kouwe, A., Destrieux, C., Halgren, E., Ségonne, F., Salat, D. H., Busa, E., Seidman, L. J., Goldstein, J., Kennedy, D., Caviness, V., Makris, N., Rosen, B., Dale, A. M. (2004). Automatically Parcellating the Human Cerebral Cortex. Cerebral Cortex, 14(1), pp. 11–22.

70. Flanagan, O. (2007). The Really Hard Problem: Meaning in a Material World. MIT Press.

71. Forney, A., Pearl, J., Bareinboim, E. (2017). Counterfactual datafusion for online reinforcement learners. Proceedings of the 34th International Conference on Machine Learning. Proceedings of Machine Learning Research 70, pp. 1156-1164.

72. Frankl, V. (2006). Man's Search for Meaning. Beacon Press.

73. Freud, S. (1949). The Ego and the Id. Hogarth Press.

74. Freud, S. (1990). The Psychopathology of Everyday Life. W. W. Norton & Company.

75. Fries, J. F. (2011). Neue oder anthropologische Kritik der Vernunft. Nabu Press.

76. Frith, U., Happé, F. (1999). Theory of Mind and Self-Consciousness: What Is It Like to Be Autistic?. Mind & Language 14, pp. 82–89.

77. Functional Magnetic Resonance Imaging (FMRI). (2009). In Encyclopedia of Neuroscience. Berlin, Heidelberg: Springer Berlin Heidelberg, pp. 1652–1652.

78. Friston, K. J. (1994). Functional and effective connectivity in neuroimaging: A synthesis. Human Brain Mapping, 2(1–2), pp. 56–78.

79. Galves, A., Löcherbach, E. (2013). Infinite Systems of Interacting Chains with Memory of Variable Length — A Stochastic Model for Biological Neural Nets. Journal of Statistical Physics, vol. 151, n. 5, Jun, pp. 896-921.

80. Ganchev, A. (2018). About Markov, Gibbs, ..., Gauge Theory...Finance. Quantum Theory and Symmetries with Lie Theory and Its Applications in Physics: Volume 1. Dobrev, V. (ed.). p. 404. Springer Proceedings in Mathematics & Statistics. Springer-Verlag.

81. Gerder, M., Harrison, P., Cohen, P. (2007). Shorter Oxford Textbook of Psychiatry. Oxford University Press.

82. Gilligan, C. (1985). In a Different Voice: Psychological Theory and Women's development. Harvard University Press.

83. Gonçalves, O. F., Machado, P. P. P. (2000). Emotions, narrative and change. European Journal of Psychotherapy & Counselling, 3:3, pp. 349 – 360.

84. Gorgolewski, K., Burns, C. D., Madison, C., Clark, D., Halchenko, Y. O., Waskom, M. L., Gosh, S. S. (2011). Nipype: a flexible, a lightweight and extensible neuroimaging data processing framework in python. Frontiers in Neuroinformatics, 5. 13.

85. Grabowski, T. J., Damasio, H., Tranel, D., Cooper, G. E., Ponto, L. L. B., Watkins, G. L., Hichwa, R. D. (2003). Residual naming after damage to the left temporal pole: a PET activation study. NeuroImage, 19 (3), pp. 846-860.

86. Greene, J. D, Nystrom, L. E., Engell, A. D., Darley, J. M., Cohen, J. D. (2004). The neural bases of cognitive conflict and control in moral judgment. Neuron 44 (2), pp. 389-400.

87. Greenspan, H., Van Ginneken, B., Summers, R. M. (2016). Guest Editorial Deep Learning in Medical Imaging : Overview and Future Promise of an Exciting New Technique. IEEE Transactions on Medical Imaging, 35(5), pp. 1153–1159.

88. Gusnard, D. A., Raichle, M. E., Raichle, M. E. (2001). Searching for a baseline: functional imaging and the resting human brain. Nature Reviews. Neuroscience, 2(10), pp. 685–94.

89. Haimovici, A., Balenzuela, P., Tagliazucchi, E. (2016). Dynamical signatures of structural connectivity damage to a model of the brain posed at criticality. Brain Connectivity. Dec;6(10), pp. 759-771.

90. Hallotschek, O. (2011). The noisy edge of traveling waves. PNAS, vol. 108, n° 5, pp. 1783-1787.

91. Haslam, S. (2004). Psychology in Organizations – The Social Identity Approach. SAGE Publications, London

92. Hassan, M. T., Luu, T. T., Moulet, A., Raskazovskaya, O., Zhokhov, P., Garg, Karpowicz, N., Zheltikov, A. M., Pervak, V., Krausz, F., Goulielmakis, E. (2016). Optical attosecond pulses and tracking the nonlinear response of bound electrons. Nature 530, pp. 66–70

93. Hammersley, J. M., Clifford, P. (1971). Markov fields on finite graphs and lattices IN: http://www.jstor.org/stable/2317621

94. Hamdan, N., Chamaa, A., Lopez-Bonilla, J. (2008). On the Relativistic Concept of the Dirac's Electron Spin. Latin American Journal of physics Education. 2(1), pp. 120-136.

95. Haug, H., Koch, S. W. (2004). Quantum Theory of the Optical and Electronic Properties of Semiconductors. World Scientific.

96. Hawking, S. W. (1971). Gravitationally collapsed objects of very low mass. Monthly Notices of the Royal Astronomical Society. 152, pp. 75-78.

97. Hawrylycz, M. J., Lein, E. S., Guillozet-Bongaarts, A. L., Shen, E. H., Ng, L., et al. (2012). An anatomically comprehensive atlas of the adult human brain transcriptome. Nature 489, pp. 391–399.

98. Health, N. (2018). Quantum Computing: Seven truths you need to know. TechRepublic. IN: https://www.techrepublic.com/article/quantum-computing-seven-truths-you-need-to-know/

99. Henderson, L. (2019). The Problem of Induction. The Stanford Encyclopedia of Philosophy (Winter 2019 Edition), Edward N. Zalta (ed.). IN: https://plato.stanford.edu/archives/win2019/entries/induction-problem/

100. Hill, S. L., Wang, Y., Riachi, I., Schürmann, F., Markram, H. (2012). Statistical connectivity provides a sufficient foundation for specific functional connectivity in neocortical neural microcircuits. Proc Natl Acad Sci U S A 109: E2885–94.

101. Hodgkin, A. L., Huxley, A. F. (1952). A quantitative description of membrane current and its application to conduction and excitation in nerve. The Journal of Physiology 117 (4), pp. 500–544.

102. Hogg, M., Abrams, D. (1998). Social Identifications – A Social Psychology of Intergroup Relations and Group Processes. Routledge, New York

103. Hughes, T. (1993). Shakespeare and the Goddess of Complete Being. Faber & Faber.

104. Huth, A. G., de Heer, W. A., Griffiths, T. L., Theunissen, F. E., Gallant, J. L. (2016). Natural speech reveals the semantic maps that tile human cerebral cortex. Nature. 2016 April 28; 532(7600), pp. 453–458.

105. Ibañez, A., Zimerman, M., Sedeño, L, Lori, N., Rapacioli, M., Cardona, J., Suarez, D., Herrera, E., García, A., Manes, F. (2018). Early bilateral and massive compromise of the frontal lobes. NeuroImage: Clinical. Volume 18, pp. 543-552.

106. Inglis-Arkell, E. (2012). Neutrium: The Most Neutral Hypothetical State of Matter. Io9.com. Retrieved 2013-02-11. https://io9.gizmodo.com/neutrium-the-most-neutral-hypothetical-state-of-matter-5899961

107. ITER Project. (2006). EFDA, European Fusion Development Agreement. IN: https://web.archive.org/web/20060824071609/http://www.efda.org/the_iter_project/index.htm

108. Jain, P. C. (2016). Recent trends in next generation terabit Ethernet and gigabit wireless local area network. 2016 International Conference on Signal Processing and Communication (ICSC), Noida, pp. 106-110.

109. Jung, W. H., Prehn, K., Fang, Z., Korczykowski, M., Kable, J. W., Rao, H., Robertson, D. C. (2016). Moral competence and brain connectivity: A resting-state fMRI study. NeuroImage, 141, pp. 408–415.

110. Kahneman, D. (2011). Thinking, Fast and Slow. Farrar, Straus, and Giroux.

111. Kant, I. (1993). Grounding for the Metaphysics of Morals. Translated by James W. Ellington (3rd ed.). Hackett, pp. 30-43.

112. Klein, U. (2012). What is the limit $\hbar \to 0$ of quantum theory?. American Journal of Physics. Vol. 80, Issue 11, pp. 1009-16.

113. Knill, D. C., Pouget, A. (2004). The Bayesian brain: the role of uncertainty in neural coding and computation. TRENDS in Neurosciences Vol.27 No. 12 December, pp. 712-719.

114. Koksma, J. F., Prokopec, T., Schmidt, M. G. (2010). Decoherence in an Interacting Quantum Field Theory: The Vacuum Case. Phys. Rev. D. 81.065030.

115. Lane, R. D., Wager, T. D. (2009). Introduction to a Special Issue of Neuroimage on Brain-Body Medicine. NeuroImage, 47(3), pp. 781–784.

116. Lattimer, J. M. (2015). Introduction to neutron stars. American Institute of Physics Conference Series. AIP Conference Proceedings. 1645 (1), pp. 61–78.

117. LeCun, Y., Bengio, Y., Hinton, G. (2015). Deep learning. Nature, 521(7553), pp. 436–444.

118. Leopold, D. (2009). Pre-emptive blood flow. Nature 457, pp. 387–388.

119. Lévy-Leblond, J.M. (1967). Nonrelativistic Particles and Wave Equations. Commun. math. Phys. 6, pp. 286-311.

120. Loeffler, J. (2019). IBM Reveals Major Performance Gain For IBM Q System One. 05/03/2019. Interesting Engineering. IN: https://interestingengineering.com/ibm-reveals-major-performance-gain-for-ibm-q-system-one

121. Lichtman, J. W., Pfister, H., Shavit, N. (2014). The big data challenges of connectomics. Nat Neurosci, 17(11), pp. 1448-1454.

122. Lori, N. F., Akbudak, E., Shimony, J .S., Cull, T. S., Snyder, A.Z., Guillory, R. K., Conturo, T. E. (2002). Diffusion tensor fiber tracking of human brain connectivity: aquisition methods, reliability analysis and biological results. NMR Biomed 15, pp. 494-515.

123. Lori, N. F. (2009). Relation between Contemporary Physics and Free-will: an Application of Quantum Existentialism. Mind and Matter, vol.7 issue 1, pp. 111-129.

124. Lori, N. F., Jesus, P. R. (2010a). Matter and Selfhood in Kant's Physics: A Contemporary Reappraisal. Relations of the Self. Edmundo Balsemão Pires, Burkhard Nonnenmacher, and Stefan Büttner von Stülpnagel (ed.). Imprensa da Universidade de Coimbra., pp. 207-226.

125. Lori, N. F., Blin A. (2010b). Application of Quantum Darwinism to Cosmic Inflation: an example of the limits imposed in Aristotelian logic by information-based approach to Gödel's incompleteness, in: Foundations of Science, Special issue on the First International Conference on the Evolution and Development of the Universe, pp. 160-168.

126. Lori, N. F., Travasso, R. D. M., Blin, A. H. (2010c). Use of a Darwinian perspective of quantum mechanics to an analysis of science's contemporary description of the transition from pre-life to life. Revista Portuguesa de Filosofia, 66, pp. 3-4.

127. Lori, N. F. (2011). Brownian Motion: from Quantum Decoherence to Diffusion MRI medical imaging. In: Brownian Motion: Theory, Modelling and Applications. Editors: R. C. Earnshaw and E. M. Riley, Nova Science Publishers, pp. 291-304.

128. Lori, N. F., Ibañez, A., Lavrador, R., Fonseca, L., Santos, C., Travasso, R., Pereira, A., Rossetti, R., Sousa, N., Alves, V. (2016). Processing Time Reduction: an application in living human high-resolution diffusion magnetic resonance imaging data. Journal of Medical Systems. 40(11), 243.

129. Lori, N. F., Alves, V. (2017). Wormhole approach to control in distributed computing has direct relation to physics. CONTROLO 2016. Proceedings of the 12th Portuguese Conference on Automatic Control. Lecture Notes in Electrical Engineering (LNEE), volume 402. Springer-Verlag. pp. 105-117.

130. Lori, N. F., Ramalhosa, I., Marques, P., Alves, V. (2018). Deep Learning Based Pipeline for Fingerprinting Using Brain Functional MRI Connectivity Data. Procedia Computer Science. Volume 141, Pages 539-544.

131. Lori, N. F., Samit, E., Picciochi, G., Jesus, P. (2019). Free-will Perception in Human Mental Health: an Axiomatic Formalization. FROM: Automata's inner movie: Science and philosophy of mind. Chapter VIII, Curado, M., Gouveia, S. S. (eds.). Vernon Press. pp. 139-172.

132. Lori, N. F., Neves, J., Blin, A. H., Alves, V. (2020). Some considerations on quantum computing at sub-atomic scales and its impact in the future of Moore's law. Quantum Information & Computation. Rinton Press. [IN PRESS]

133. Lorna, A. F., Thompson, R. E., Zhao, S, Lepack, A. E., Lyu, Y., Bhanu, N. V., Zhang, B., Loh, Y.-H. E., Ramakrishnan, A., Vadodaria, K. C., Heard, K. J., Erikson, G., Nakadai, T., Bastle, R. M., Lukasak, B. J., Zebroski, H., Alenina, N., Bader, M., Berton, O., Roeder, R. G., Molina, H., Gage, F. H., Shen, L., Garcia, B. A., Li, H., Muir, T. W., Maze, I. (2109). Histone serotonylation is a permissive modification that enhances TFIID binding to H3K4me3. Nature. 567, pp. 535–539.

134. Luhtanen, R., Crocker, J. (1992). A collective self-esteem scale: Self-evaluation of one's social identity. Personality and Social Psychology Bulletin 18, pp. 302–318

135. Maximo, J. O., Cadena, E. J., & Kana, R. K. (2014). The implications of brain connectivity in the neuropsychology of autism. Neuropsychology Review, 24(1), pp. 16–31.

136. Magalhães, R., Marques, P., Soares, J., Alves, V., Sousa, N. (2015). The Impact of Normalization and Segmentation on Resting-State Brain Networks. Brain Connectivity, 5(3), pp. 166–176.

137. Maia, N., Neves, M., Barbosa, A., Carrulo, B., Araújo, N., Fernandes, A., Ribeiro, J., Vincente, H., Neves, J. (2019). Social Role in Organizational Management Understanding People Behavior and Motivations.

138. Martin, K. (2018). Waiting for quantum computing: Why encryption has nothing to worry about. Tech Beacon. IN: https://techbeacon.com/security/waiting-quantum-computing-why-encryption-has-nothing-worry-about

139. Massachusetts Institute of Technology. (2013). You can't get entangled without a wormhole: Physicist finds entanglement instantly gives rise to a wormhole. ScienceDaily. ScienceDaily, 5 December.

140. Marder, E. (2015). Understanding brains: details, intuition, and big data. PLoS Biol, 13(5): p. e1002147.

141. McClelland, D. (1973). Testing for Competence Rather Than Intelligence. American Psychologist 28, pp. 1–14.

142. Microsoft Research. (2019). IN: https://www.microsoft.com/en-us/research/project/post-quantum-cryptography/

143. Milne, M. L., Conradi, M. S. (2009). Multi-exponential signal decay from diffusion in a single compartment. J Magn Reson 197, pp. 87– 90.

144. Moland, L. L. (2017). Friedrik Schiller. The Stanford Encyclopedia of Philosophy (Summer 2018 Edition). Zalta, E. N. (ed.). IN: https://plato.stanford.edu/archives/sum2017/entries/schiller/

145. Montague, P. R., Berns, G. S. (2002). Neural economics and the biological substrates of valuation. Neuron, 36, pp. 265-284.

146. Nakamura, T. K. (2006). Covariant thermodynamics of an object with finite volume. Physics Letters A. 352(3). 27 March, pp. 175-177

147. Natterer, F. D., Natterer, Fabian, D., Yang, K., Paul, W., Willke, P., Choi, T., Greber, T., Heinrich, A. J., Lutz, C. P. (2017). Reading and writing single-atom magnets. Nature, 543, pp. 226-228.

148. Nersisyan, A., Poletto, S., Alidoust, N., Manenti, R., Renzas, R., Bui, C.-V., Vu, K., Whyland, T., Mohan, Y., Sete, E. A., Stanwyck, S., Bestwick, A., Reagor, M. (2019). Manufacturing low dissipation superconducting quantum processors. IN: https://arxiv.org/abs/1901.08042

149. Neves, J. (1984). A logic interpreter to handle time and negation in logic databases. In: Muller, R., Pottmyer, J. (eds.) Proceedings of the 1984 annual conference of the ACM on the 5th Generation Challenge, ACM, New York. pp. 50–54.

150. Neves, J., Maia, N., Marreiros, G., Neves, M., Fernandes, A., Ribeiro, J., Araújo, I., Araújo, N., Ávidos, L., Ferraz, F., Capita, A., Lori, N., Alves, V., Vicente, H. (2019). Entropy and Organizational Performance. In: Pérez García, H., Sánchez González, L., Castejón Limas, M., Quintián Pardo, H., Corchado Rodríguez, E. (eds) Hybrid Artificial Intelligent Systems. HAIS 2019. Lecture Notes in Computer Science, vol 11734. Springer, Cham.

151. NIST Post-Quantum Project. (2019), IN: https://csrc.nist.gov/projects/post-quantum-cryptography

152. Nowak, M. A., Ohtsuki, H. (2008). Prevolutionary dynamics and the origin of evolution, PNAS, 105, 14924.

153. NVIDIA Developer. (n.d.-ai). (2017). Retrieved October 12, 2017. IN: https://developer.nvidia.com/

154. Oak Ridge National Laboratory. (2018). IN: https://www.olcf.ornl.gov/2018/06/08/genomics-code-exceeds-exaops-on-summit-supercomputer/

155. Obstfeld, M., Shambaugh, J. C., Taylor, A. M. (2005). The Trilemma in History: Tradeoffs Among Exchange Rates, Monetary Policies, and Capital Mobility. Review of Economics and Statistics 87 (3), pp. 423-438.

156. Ogawa, S., Lee, T. M., Kay, A. R., Tank, D. W. (1990). Brain magnetic resonance imaging with contrast dependent on blood oxygenation. Proceedings of the National Academy of Sciences of the United States of America, 87(24), pp. 9868–9872.

157. Ozel, F., Freire, P (2016). Masses, Radii, and the Equation of State of Neutron Stars. Annu. Rev. Astron. Astrophys. 54 (1), pp. 401–440.

158. Panikkar, R. V. (1989). The Silence of God: The answer of the Buddha. Orbis Books, New York.

159. Pardo-Vazquez, J. L., Castiñeiras-de Saa, J. R., Valente, M., Damião, I., Costa, T., Vicente, M. I., Mendonça, A. G., Mainen, Z. F., Renart, A. (2019). The mechanistic foundation of Weber's law. Nature Neuroscience. 22, pp. 1493–1502.

160. Pearl, J., Mackenzie, D. (2018). The Book of Why: The New science of Cause and Effect. Basic Books.

161. Peskin, M. E., Schroeder, D. V. (1995). An Introduction to Quantum Field Theory (Frontiers in Physics), First Edition. Westview Press.

162. Popper, K. R. (1959). The logic of scientific discovery. Basic Books.

163. Poulin, D. (2012). Quantum graphical models and belief propagation. Sydney Quantum Information Theory Workshop: Coogee 2012. IN: https://cnls.lanl.gov/CQIT/poulin.pdf

164. Prinz, W. (1996). Freiheit oder Wissenschaft. em M. VON CRANACH – FOPPA, K. (eds.), Freiheit des Entscheidens und Handeln. Ein Problem der nomologischen Psychologie.

165. Raffelt, D., Tournier, J.D., Rose, S., Ridgway G.R., Henderson, R., Crozier, S., Salvado, O., Connelly, A. (2012). Apparent Fibre Density: A novel measure for the analysis of diffusion-weighted magnetic resonance images. Neuroimage 59, pp. 3976–3994.

166. Rentz, S. (2012). Your Guide to Medical Imaging Equipment. Block Imaging. IN: https://info.blockimaging.com/bid/87030/3t-mri-vs-1-5t-mri

167. Reardon S. (2017). A giant neuron found wrapped around entire mouse brain. Nature 543, 24 February, pp. 14–15.

168. Reimann, M. W., Nolte, M., Scolamiero, M., Turner, K., Perin, R., Chindemi, G., Dłotko, P., Levi, R., Hess, K., Markram, H. (2017). Cliques of Neurons Bound into Cavities Provide a Missing Link between Structure and Function. Front. Comput. Neurosci. 11:48.

169. Robbin, T. (1990). Skinny Legs and All. Bantam Books.

170. Rodrik, D. (2007). The inescapable trilemma of the world economy. Dani Rodrik's weblog. (27 June 2007), IN: https://rodrik.typepad.com/dani_rodriks_weblog/2007/06/the-inescapable.html

171. Rodrik, D. (2011). The Globalization Paradox: Democracy and the Future of the World Economy. W.W. Norton.

172. Rosenberg, M. (1965). Society and the adolescent self-image. Princeton University Press, Princeton.

173. Rouzine, I. M., Wakeley, J., Coffin, J. M. (2003). The solitary wave of asexual evolution. PNAS USA 100 no. 2, (Jan), pp. 587-592.

174. Sakurai, J. J. (1994). Modern Quantum mechanics. AddisonWesley.

175. Salazar, N. (1986). Psicología Social. México: Trillas.

176. Salazar, N., Doston, S., Bressler, C. Gray. (2012). Content-Specific Fronto-Parietal Synchronization During Visual Working Memory. Science, Vol. 338, pp. 1097-1100.

177. Schiller, F. (2003). Kallias, or Concerning Beauty: Letters to Gottfried Körner. IN: Bernstein, J. M. (ed.), Classic and Romantic German Aesthetics. Cambrdge University Press. pp. 145—83.

178. Schurger, A., Sarigiannidis, I., Naccache, L., Sitt, J. D., Dehaene, S. (2015). Cortical activity is more stable when sensory stimuli are consciously perceived. Proc Natl Acad Sci U S A 112(16): E2083-92.

179. Sedeño, L., Piguet, O., Abrevaya, S. G., Garcia-Cordero, I., Baez, S., de la Fuente, L. A., Reyes, P., Tu, S., Mogilner, S., Lori, N., Landin-Romero, R., Matallana, D., Slachevsky, A., Torralva, T., Chialvo, D., Kumfor, F., Garcia, A. M,. Manes, F., Hodges, J., Ibañez, A. (2017). Tackling variability: A multicenter study to provide a gold-standard network approach for frontotemporal dementia. Human Brain Mapping. 38(8), Aug, pp. 3804-3822.

180. Seghier, M. L. (2012). The angular gyrus: multiple functison and multiple subdivisions. Neuroscientist 19, pp. 43–61.

181. Sharp, D. J., Scott, G., Leech, R. (2014). Network dysfunction after traumatic brain injury. Nat Rev Neurol, 10(3), pp. 156-66.

182. Shea, N., Firth, C. D. (2016). Dual-process theories and consciousness: the case for 'Type Zero' cognition. Neuroscience of Consciousness, pp. 1-10.

183. Shen, X., Tokoglu, F., Papademetris, X., Constable, R. T. (2013). Groupwise whole-brain parcellation from resting-state fMRI data for network node identification. NeuroImage, 82, pp. 403–415.

184. Smerlak, M., Youssef, A. (2016). Limiting fitness distributions in evolutionary dynamics. arXiv:1511.00296v2 [q-bio.PE] 16 Feb 2016.

185. Smith, S. M. (2012). The future of FMRI connectivity. NeuroImage, 62(2), 1257–1266.

186. Snoke, D. W., Liu, Gangqing; Girvin, S. M. (2012). The basis of the Second Law of thermodynamics in quantum field theory. Annals of Physics 327, pp. 1825–1851.

187. Sonner. J. (2013). Holographic Schwinger Effect and the Geometry of Entanglement. Physical Review Letters; 111 (21), pp. 211603-211607.

188. Soon, CH. S., Baas, M. Haynes, J-D. (2008). Unconscious determinants of free decisions in the human brain. Nature Neuroscience 11.

189. Stanford Encyclopedia of Philosophy. (2010a). In: https://plato.stanford.edu/entries/freewill/

190. Stanford Encyclopedia of Philosophy. (2010b). In: https://plato.stanford.edu/entries/freewill/

191. Suzuki, K., Yan, P., Wang, F., Shen, D. (2012). Machine learning in medical imaging. International Journal of Biomedical Imaging, 2012, pp. 2012–2014.

192. Swanson, L. R. (2016). The Predictive Processing Paradigm Has Roots in Kant. Front. Syst. Neurosci., 10 October 2016.

193. Tagliazucchi, E., Chialvo, D. R., Siniatchkin, M., Amico, E., Brichant. J. F., Bonhomme, V., Noirhomme, Q., Laufs, H., Laureys, S. (2016). Large-scale signatures of unconsciousness are consistent with a departure from critical dynamics. Journal of the Royal Society/Interface, Jan;13(114):20151027.

194. Tajfel, H. (1981). Human Groups and Social Categories – Studies in Social Psychology. Cambridge University Press, Cambridge.

195. Tajfel, H., Turner, J. C. (1986) The social Identity Theory of Inter-Group Behavior. In: Worchel S., Austin, W.G. (eds.) Psychology of Inter-Group Relations, , Nelson-Hall Publishers Chicago. pp. 7–24.

196. Technology Quarterly. (2016). After Moore's Law: Double, double, toil and trouble. The Economist. IN: https://www.economist.com/technology-quarterly/2016-03-12/after-moores-law

197. Three Gorges Dam Project – Quick Facts. (2010). IN: www.ibiblio.org/chinesehistory/contents/07spe/specrep01.html#Quick%20Facts. Archived from the original on November 25, 2010. Retrieved November 23, 2010.

198. Tononi, G., Boly, M., Massimini, M., Koch, C. (2016). Integrated information theory: from consciousness to its physical substrate. Nature Reviews Neuroscience 17, pp. 450–461.

199. Torgerson, C. M., Irimia, A., Goh, S., Van Horn, J. D. (2015). The DTI connectivity of the human claustrum. Human Brain Mapping, 36, pp. 827- 838.

200. Tuch, D. S., Reese, T. G., Wiegell, M. R., Wedeen, V. J. (2003). Diffusion MRI of Complex Neural Architecture. Neuron 40, pp. 885–895.

201. Tuch, D. S. (2004). Q-ball imaging. Magn Reson Med 52, pp. 1358–1372.

202. Tzourio-Mazoyer, N., Landeau, B., Papathanassiou, D., Crivello, F., Etard, O., Delcroix, N., Mazoyer, B., Joliot, M. (2002). Automated Anatomical Labeling of Activations in SPM Using a Macroscopic Anatomical Parcellation of the MNI MRI Single-Subject Brain. NeuroImage, 15(1), pp. 273–289.

203. UALT-University of Arkansas at Little Rock. (2019). Department of Computer Science's FAQ's Freshmen Student Questions. Retrieved November 11 2019. IN: https://ualr.edu/computerscience/prospective-students/frequently-asked-questions/#u3

204. U.C.L.A. (n.d.) (2012). LONI Image Data Archive (IDA). Accessed 16 November 2012. IN: https://ida.loni.ucla.edu/login.jsp.

205. Van Rossum, G., Drake, F. L. (2006). Python Reference Manual. October, 22, pp. 9117–9129.

206. Veríssimo, P. E. (2006). Travelling through Wormholes: a new look at Distributed Systems Models. ACM SIGACT News Distributed Computing Column 21, vol. 37, no. 1, pp. 66-81.

207. Vogel, C. (2007). The Writer's Journey: Mythic Structure For Writers. Michael Wiese Productions.

208. Wald, R. (1984). General Relativity. Chicago University Press.

209. Wang, R., Benner, T., Sorensen, A. G., Wedeen, V. J. (2007). Diffusion Toolkit : A Software Package for Diffusion Imaging Data Processing and Tractography. Proc Intl Soc Mag Reson Med 15: 3720.

210. Wang, Z., Busemeyer, J. R. (2015). Comparing quantum versus Markov random walk models of judgments measured by rating scales. Phil. Trans. R. Soc. A, 374: 201550098.

211. Wang, P., Ge, R., Xiao, X., Cai, Y., Wang, G., Zhou, F. (2016). Rectified-Linear-Unit-Based Deep Learning for Biomedical Multi-label Data. Interdisciplinary Sciences: Computational Life Sciences.

212. Wedeen, V. J., Wang, R. P., Schmahmann, J. D., Benner, T., Tseng, W. Y. I., Dai, G., Pandya, D. N., Hagmann, P., D'Arceuil, H., de Crespigny, A. J. (2008). Diffusion spectrum magnetic resonance imaging (DSI) tractography of crossing fibers. Neuroimage 41, pp. 1267–1277.

213. Wedeen, V.J., Rosene, D.L., Wang, R., Dai, G., Mortazavi. F., Hagmann, P., Kaas, J. H., Tseng, W.-Y. I. (2012). The geometric structure of the brain fiber pathways. Science. 335, pp. 1628–1634.

214. Wegner, D. M. (2002). The Illusion of Conscious Will, MIT Press, Cambridge.

215. Weyl, H. (1927). Quantenmechanik und Gruppentheorie. Zeitschrift für Physik. 46, pp. 1–46.

216. Wilson, E. E., and Denis, L. (2018). Kant and Hume on Morality. The Stanford Encyclopedia of Philosophy (Summer 2018 Edition). Zalta, E. N. (ed.). IN: https://plato.stanford.edu/archives/sum2018/entries/kant-hume-morality/.

217. Wilson, R. (1997). Shakespeare and the Jesuits: New connections supporting the theory of the lost Catholic years in Lancashire. Times Literary Supl., pp. 11-13.

218. Wenterodt, T., Herwig, H. (2014). The Entropic Potential Concept: A New Way to Look at Energy Transfer Operations. Entropy 16, pp. 2071–2084.

219. Wikipedia contributors. (2019), October 7. Hierarchy of the sciences. In Wikipedia, The Free Encyclopedia. Retrieved November 11, 2019, LICENSE: https://creativecommons.org/licenses/by-sa/3.0/legalcode, IN: https://en.wikipedia.org/w/index.php?title=Hierarchy_of_the_sciences&oldid=920031096

220. Worbe, Y. (2015). Neuroimaging signature of neuropsychiatric disorders. Curr Opin Neurol, 28(4), pp. 358-64.

221. Yoris, A., Abrevaya, S., Esteves, S., Salamone, P., Lori, N., Martorell, M., Legaz, A., Alifano, F., Petroni, A., Sánchez, R., Sedeño, L., García, A. M., Ibáñez, A. (2017). Multilevel convergence of interoceptive impairments in hypertension: New evidence of disrupted body-brain interactions. Human Brain Mapping, 39(4), Apr, pp. 1563-1581.

222. Zhang, Y., Brady, M., Smith, S. (2001). Segmentation of brain MR images through a hidden Markov random field model and the expectation-maximization algorithm. IEEE Trans Med Imaging 20, pp. 45–57.

223. Zhou, J., Seeley, W. W. (2014). Network dysfunction in Alzheimer's disease and frontotemporal dementia: implications for psychiatry. Biol Psychiatry, 75(7), pp. 565-73.

224. Zurek, W. H. (2005). Probabilities from entanglement, Born’s rule pk = $/\psi_k/^2$ from envariance. Physical Review A 71, 052105.

225. Zurek, W. H. (2007). Relative states and the environment: Einselection, envariance, quantum darwinism, and existential interpretation. arXiv: 0707.2832v1.

226. Zurek, W. H. (2009). Quantum Darwinism. Nature Physics 5, pp. 181–188.